1225-0767(ISSN Print)
2287-6715(ISSN Online)
한국연구재단 우수등재학술지

Journal of Ocean Engineering and Technology

Vol. 37, No. 5 (Serial Number 174)

October 2023

한국해양공학회지

KSOE

www.joet.org

KSOE The Korean Society of Ocean Engineers

Journal of Ocean Engineering and Technology
한국해양공학회지
Vol. 37 No. 5
(Serial Number 174)
October 31, 2023
www.JOET.org

Published on October 31, 2023
Published by The Korean Society of Ocean Engineers (KSOE)
Room 1302, 13, Jungang-daero 180beon-gil, Dong-gu, Busan, 48821, Korea
TEL: +82-51-759-0656 FAX: +82-51-759-0657 E-mail: ksoehj@ksoe.or.kr URL: http://www.ksoe.or.kr
Printed by Hanrimwon Co., Ltd., Seoul, Korea E-mail: hanrim@hanrimwon.co.kr
ISSN(print) 1225-0767 **ISSN(online)** 2287-6715

This journal was supported by the Korean Federation of Science and Technology Societies (KOFST) grant funded by the Korean government.

Journal of Ocean Engineering and Technology
한국해양공학회지

CONTENTS

Volume 37, Number 5 October, 2023

<Original Research Articles>

GENERAL INFORMATION

The **"Journal of Ocean Engineering and Technology" (JOET)** was launched in 1987 and is published bimonthly in February, April, June, August, October, and December each year by "The Korean Society of Ocean Engineers (KSOE)." Its ISO abbreviation is "J. Ocean Eng. Technol." JOET publishes original research articles, technical articles, and review articles on all aspects of ocean engineering, including experimental, theoretical, numerical, and field observations. All manuscripts undergo peer-review by two or more reviewers.

The scope of JOET encompasses the following research areas:

- Ships and offshore engineering:
  Design of ships and offshore structures; Resistance and propulsion; Seakeeping and maneuvering; Experimental and computational fluid dynamics; Ocean wave mechanics; Fatigue strength; Plasticity; Optimization and reliability; Arctic technology and extreme mechanics; Noise, vibration, and acoustics; Concrete engineering; Thermodynamics and heat transfer; Hydraulics and pneumatics; Autonomous and unmanned ship; Greenship technology; Digital twin of ships and offshore structures; Marine materials

- Coastal engineering:
  Coastal, port, and harbor structures; Waves transformation; Coastal and estuary hydrodynamics; Sediment transport and morphological change; Subsea geotechnics; Coastal groundwater management; Prevention or mitigation of coastal disaster; Coastal zone development and management; Shore protection technique; Coastal environmental process; Beach safety

- Ocean energy engineering:
  Offshore wind turbines; Wave energy platforms; Tidal current energy platforms; Floating photovoltaic energy platform; Small modular reactor; Combined energy platforms

- Marine robot engineering:
  Robot sensor system; Autonomous navigation; Robot equipment; Marine robot control; Environment mapping and exploration; Underwater communication and networking; Design of marine robots

 It is indexed in databases such as the Korean Citation Index (KCI), Google Scholar, Science Central, Korea Science, and the Directory of Open Access Journals (DOAJ). JOET offers PDF or XML versions for free on its website (https://www.joet.org). For business matters, authors need to contact KSOE Secretariat by email or phone (e-mail: ksoehj@ksoe.or.kr or Tel: +82 51 759 0656). Correspondences for publication matters can be asked via email to the Editor-in-Chief (e-mail: heroeswise2@gmail.com).

Journal of Ocean Engineering and Technology 37(5), 181-189, October, 2023
https://doi.org/10.26748/KSOE.2023.014
pISSN 1225-0767
eISSN 2287-6715

Original Research Article

Impact of Hull Condition and Propeller Surface Maintenance on Fuel Efficiency of Ocean-Going Vessels

Tien Anh Tran[1,2] and Do Kyun Kim[3]

[1]Assistant Professor, Faculty of Marine Engineering, Vietnam Maritime University, Haiphong, Vietnam
[2]Visiting Researcher, Research Institute of Marine Systems Engineering, Seoul National University, Seoul, Korea
[3]Associate Professor, Department of Naval Architecture and Ocean Engineering, Seoul National University, Seoul, Korea

KEYWORDS: Energy efficiency of ships, Fuel consumption, Ship hull condition, Marine propeller roughness, Navigation environment condition

ABSTRACT: *The fuel consumption of marine diesel engines holds paramount importance in contemporary maritime transportation and shapes energy efficiency strategies of ocean-going vessels. Nonetheless, a noticeable gap in knowledge prevails concerning the influence of ship hull conditions and propeller roughness on fuel consumption. This study bridges this gap by utilizing artificial intelligence techniques in Matlab, particularly convolutional neural networks (CNNs) to comprehensively investigate these factors. We propose a time-series prediction model that was built on numerical simulations and aimed at forecasting ship hull and propeller conditions. The model's accuracy was validated through a meticulous comparison of predictions with actual ship-hull and propeller conditions. Furthermore, we executed a comparative analysis juxtaposing predictive outcomes with navigational environmental factors encompassing wind speed, wave height, and ship loading conditions by the fuzzy clustering method. This research's significance lies in its pivotal role as a foundation for fostering a more intricate understanding of energy consumption within the realm of maritime transport.*

1. Introduction

Reducing fuel consumption and exhaust-gas emission from ships is a critical issue to comply with the stringent regulations of the International Maritime Organization (IMO) nowadays. The global maritime transportation industry is developing and is showing that it is an important environment for increasing the income of each nation in the world. Based on the United Nationals Conference on Trade and Development (UNCTAD, 2017), shipping transportation has been seaborne during the last four decades. But greenhouse gas emissions are a problem that many countries seek to solve. Significantly, the IMO (2009) gave a forecast of increased carbon dioxide (CO_2) emissions by 50% to 250% by 2050. General studies on measures taken have investigated the main topics that are directly related to the energy consumption of ships, as shown in Fig. 1.

The same challenges hen investigating a ship's energy efficiency management and navigation condition are investigated when considering the fuel consumption of marine diesel engines. A prediction model of fuel consumption for inland river ships was established with Long-Short-Term-Memory (LSTM) in China (Yuan et al., 2021). Tran (2021) investigated the uncertain parameters of navigation conditions based on a hybrid multi-criteria decision-making system. Işikli et al. (2020) estimated the fuel consumption in maritime transportation through the response surface methodology when considering the navigation condition. Tillig et al. (2020) reduced the negative factors from environmental conditions to reduce fuel consumption with wind-assisted propulsion vessels.

The marine fouling phenomenon degrades the ship hull condition during the operation process. Therefore, more needless fuel-oil consumption by marine diesel engines is needed to maintain the voyage speed and the cargo handling plan. This is the reason why there are many different studies to try to calculate and predict the total resistance and the added resistance due to changing the ship hull condition and the marine surface propeller. A full-scale model of a ship was designed to predict the antifouling coating of the ship hull through the roughness and fouling conditions (Schultz, 2007). Then, the ship's owner could have a large amount of control over the energy efficiency, which was investigated with the ship hull condition and

Received 24 May 2023, revised 10 August 2023, accepted 24 August 2023
Corresponding author Do Kyun Kim: +82-2-880-7129, do.kim@snu.ac.kr

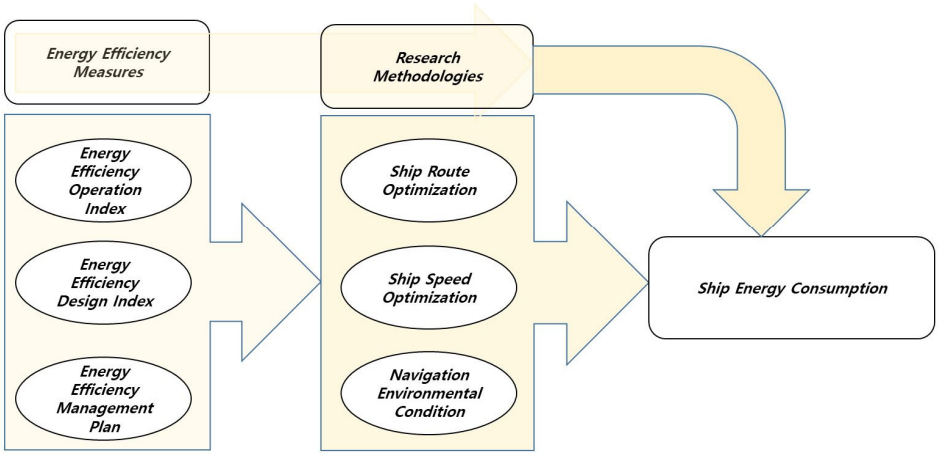

Fig. 1 Study trend of energy consumption based on energy efficiency measures by IMO

biofouling during the ship operation process. Marine biofouling is a critical issue related to increasing ship resistance, leading to more fuel consumption. Moreover, it is the main factor that causes increasing amounts of greenhouse gas emissions and harmful non-indigenous species (Demirel et al., 2017).

Estimations of the external environmental condition of a ship could be determined accurately through a numerical simulation method like computational fluid dynamics (CFD) or finite element analysis (FEA). However, these methods are determined and calculated based on only theoretical equations established from experimental work and a designed ship model from a towing tank in a laboratory of universities or /research institutes. Therefore, the accuracy of the collected results is not high compared with the actual sea condition. Additionally, the ship model is entirely built in calm water conditions. This differentiates the initial model from the computation and simulation results in a hydrodynamic environment. This drawback was indicated and confirmed by Kuroda et al. (2017) when calculating a ship's total resistance and added resistance in wave sea conditions and irregular wave height from the actual sea during an operational process. In this study, the prediction of ship-hull and marine propeller conditions was investigated through artificial intelligence (AI) based on deep learning techniques. The collected results are presented and indicate more advantage in predicting uncertain factors like the ship hull condition and marine propeller's impact on the fuel consumption of ships.

2. Literature Review

The fuel consumption of a ship's main diesel engine is a critical issue in maritime transportation nowadays. There are many uncertain factors that influence a ship's fuel consumption during voyage time. There are some recent research results that have addressed some external factors surrounding ships that impact the fuel oil consumption as well as the ship performance. Bialystocki and Konovessis (2016) estimated the fuel oil consumption through a speed curve, ship draft and displacement, weather force and direction, and hull and propeller roughness. However, this research did not investigate the ship hull condition and propeller roughness clearly from the initial condition of the ship.

Moreover, various studies have given monitoring methods for ship fuel consumption through a cyber-physical system (CPS) (Shi et al., 2020). The real-time modelling of ship fuel consumption was established through the relationship between the fuel consumption and effective power of the main diesel engine versus the ship speed (Yin et al., 2017). Moreover, a statistical method to monitor the fuel consumption of the main diesel engine has been investigated (Bocchetti et al., 2015). In particular, fuel oil consumption monitoring is important to improve the energy efficiency of the ship operation process (Trodden et al., 2015). Therefore, ship energy-efficiency management was reviewed to decrease exhaust gas emissions in maritime transportation (Jimenez et al., 2022). The transpacific crossing technique was studied to monitor the real-time energy consumption of container vessels to reduce greenhouse gas emissions (Yeh et al., 2022; Doulgeris et al., 2020).

Adland et al. (2018) studied the effect of periodic ship hull conditions on fuel oil consumption for tanker vessels. Moreover, the ship hull condition and marine propeller were the investigated factors in selecting a ship docking period by Koboević et al. (2019). The initial studies have given some fundamental knowledge on the ship hull condition and marine propeller's influence on the ship fuel consumption. The interaction between the ship hull condition, marine propeller, and diesel engines in regular waves was studied by simulating and verifying it through experimental work (Ghaemi and Zeraatgar, 2021). However, both factors have still not been investigated and researched in monitoring ship fuel-oil consumption and naval architecture.

The above studies also indicated clearly that the influences of the external surface of the ship decide the fuel consumption of marine diesel engines. However, the studies have not investigated the ship hull condition, marine propeller, navigation environment condition, and ship loading condition. The previous studies have only approached calm water conditions. In reality, calm water and the experimental conditions in the laboratory differ from the actual navigation

conditions of ships. To overcome the existing issues above, this research was conducted to address two factors that influence the ship fuel consumption during the ship operation process. The collected results were evaluated and verified with the collected parameters from a specific ocean-going vessel of a shipping transportation company in Vietnam.

3. Proposed Methodologies

Several researchers have presented the usage of numerical computing, a test model, or simplified CFD. However, there are still challenges in predicting the hydrodynamic parameters of a ship, such as the added resistance, ship performance, ship hull condition, marine propeller fouling, and many others in a natural ocean environment (Shigunov et al. 2018). Therefore, the data-driven prediction model paid attention to recent times through its collected results with high accuracy compared with the actual condition in the operational environment of a ship.

In the framework of this research (Fig. 2), the steps of this study were investigated by collecting a database of typical vessels. Then, a predictive model was built based on the specific database. The validation of the proposed model was analyzed through experimental work on a certain vessel. Two cases were investigated in this research based on a convolution neural network (CNN) model. The proposed algorithms determine the ship hull (Fig. 3) and marine propeller conditions (Fig. 4) based on the collected database and ship age (T) during the ship operation process. The performance of the CNN model is presented by determining the coefficient R^2. If this coefficient is more than 0.9, the proposed model can be finalized through the algorithms in Figs. 3-4. The time of ship use influences the quality of the ship's surface along with the temperature of the external navigation environment and sea water temperature. These parameters affect the external surface roughness of the ship.

3.1 Convolutional Neural Network (CNN)

A CNN is a type of deep learning neural network that works excellently for pattern recognition. It is analogous to an artificial neural network (ANN), which comprises neurons in a self-optimization platform and updates the weights of the neurons based on the back propagation (BP) algorithm. The advantageous feature of CNN is that it is able to extract the regional features and develop the private benefit through dealing with complicated tasks. Additionally, it has a high accuracy level in image recognition. But a traditional ANN cannot solve the complicated characteristics of different databases.

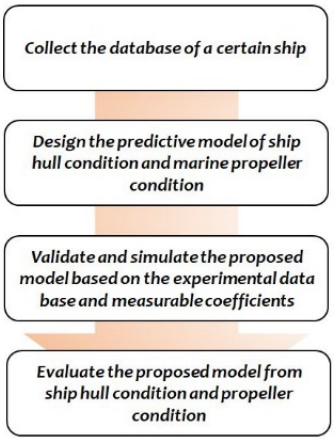

Fig. 2 The research framework for determining the effect of fuel consumption

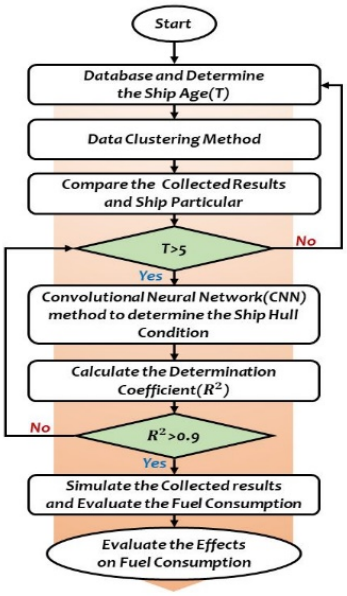

Fig. 3 Case 1: The ship hull condition

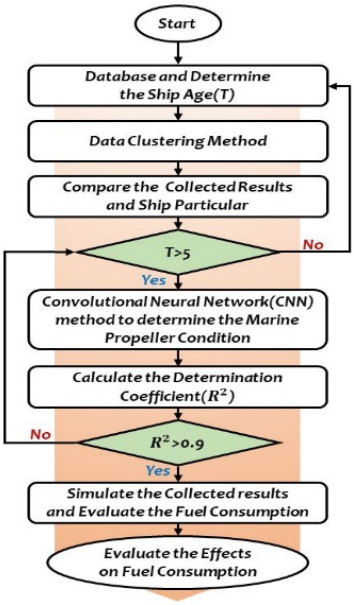

Fig. 4 Case 2: Marine propeller condition

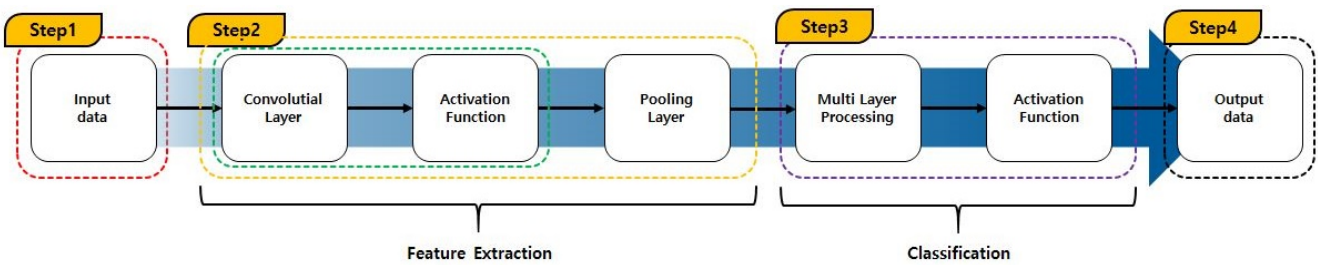

Fig. 5 The basic structure of a CNN

This has explained that the complicated features and the non-linear relationship of inputs make the challenges of traditional ANN models. However, a CNN model could address the abovementioned weak points of a traditional ANN.

The CNN architecture depicted in Fig. 5 comprises feature extraction and classification stages. Initially, the convolutional layer recognizes features from a database. The output layer is then derived using activation functions, introducing non-linearity into the feature learning module. This process is iterated M times before transitioning to the pooling layer, effectively reducing dimensionality in the CNN model and cutting computation costs. A "convolution-act-pool" sequence is executed N times, and ultimately, the output layer connects to a dense multilayer perceptron with K layers.

The mean square error (MSE) at each point is defined in Eq. (1):

$$MSE = \frac{1}{n}\sum_{i=0}^{n-1}(y_i - \hat{y}_i)^2 \tag{1}$$

where y_i is the actual dimensional value, $\hat{y}_i$ is the predicted value at each point, and n is the number of datasets for the training process. The root mean square error (RMSE) is defined in Eq. (2) as follows:

$$RMSE = \sqrt{\frac{1}{n}\sum_{i=1}^{n}(y_i - \hat{y}_i)^2} \tag{2}$$

The coefficient of determination (R^2) is defined in Eq. (3) below.

$$R^2 = 1 - \frac{\sum_{i=0}^{n-1}(y_i - \hat{y}_i)^2}{\sum_{i=0}^{n-1}(y_i - \bar{y}_i)^2} \tag{3}$$

3.2 Fuzzy Clustering Method

The fuzzy clustering method is useful for classifying a database during data processing in machine learning (Zadeh, 1965). This method divides the raw database into different clusters based on the same characteristics in the same group. In this research, a cluster was employed the same as the layers to support the predicted model through the proposed methodologies. Therefore, the object of the study was calculated through the fuzzy clustering algorithm to determine the minimum distance between the center layer and the nearest layer (Fig. 6).

The fuzzy clustering method has two processes, as illustrated in Fig. 6: calculating and determining the center cluster (layer) and the assignment of points of other clusters (layers) determined through the Euclidian distance (Δ) between the center cluster and a layer. In Fig. 6, the loop of determining the nearest distance between the center cluster is presented between the center clusters, and its iteration converges.

Additionally, the membership function is a specific coefficient in fuzzy set theory, with which the fuzzy clustering method was used and developed. The specific values of the membership function are in a range of [0, 1]. The definition of the fuzzification parameter (m) is

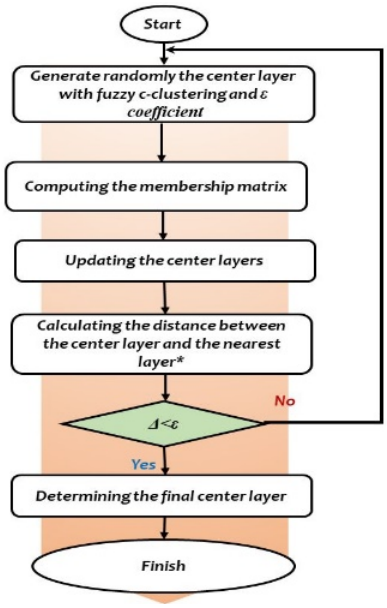

Fig. 6 Scheme of fuzzy clustering algorithm (where *Δ=*Maximum* $(|U^{(t+1)}) - U^{(t)})|)$)

employed to determine the range of value [1, n] in the fuzzy clustering algorithm. Determination of the fuzziness degree was conducted at each cluster (layer). The equation of the membership function is presented in Eq. (4) below.

$$\mu_{j(x_i)} = \left[\frac{1}{d_{ij}}\right]^{\frac{1}{m-1}} \Big/ \sum_{k=1}^{p}\left[\frac{1}{d_{ki}}\right]^{\frac{1}{m-1}} \tag{4}$$

An explanation of each specific parameter in Eq. (4) is provided as follows: $\mu_{j(x_i)}$ stands for the membership (x_i) belonging to the jth cluster; d_{ji} stands for the distance of x_i belonging to the cluster c_j; m stands for the fuzzification of the fuzzy clustering algorithm; p stands for the specific cluster number of the fuzzy clustering algorithm; and d_{ki} stands for the distance x_i belonging to the cluster c_k. The new center cluster (layer) is computed according to Eq. (5) with the same membership function:

$$c_j = \sum_i x_i(\mu_j(x_i))^m \Big/ \sum_i(\mu_j(x_i))^m \tag{5}$$

where c_j stands for the centre at the jth cluster; x_i stands for the ith point of the cluster; μ_j stands for the membership function; and m stands for the fuzzification value. In this research, the algorithm programming of the fuzzy clustering method was done through the MATLAB platform. The following parts present the collected results of the quantitative values combined with classified clusters (layers).

4. Case Study: Bulk Carrier

To verify the collected results, a specific ship was used in this research. A certain large-size bulk carrier was selected to evaluate

(a) (b)

Fig. 7 Target ship: (a) overall vessel and (b) main engine (Tran, 2021)

Table 1 The specifications of M/V NSU KEYSTONE (Tran, 2021)

Overall vessel		
1	IMO number	9641883
2	MMSI[1)]	431977000
3	GT	107217
4	DWT	207684
5	Draught	10.9 m
6	Speed recorded (Max/ Average)	11.2/8.4 (Nautical mile per hour)
7	Year built	2013
8	Length × Breadth (*L*×*B*)	299.94 m × 50 m
Engine and propeller		
9	Type of engine	MITSUI MAN B&W 6S70ME-C8.2;
10	Type of propeller	4 bladed solid type (Ni-Al-Br)

[1)] MMSI: Maritime mobile service identity

and validate the proposed methodologies. This ship is a specific type of ship that is being operated widely in the world nowadays under management of the ship owner from a Japanese shipping transportation company. The specific parameters of this bulk carrier are presented in Table 1. Currently, this kind of ship is operating in international ocean areas. Moreover, the bulk carrier selected in this study is a typical modern vessel used in a shipping transportation company in Vietnam. The overall vessel and the main diesel engine are provided in Fig. 7.

In the main propulsion plant system of this vessel, the power plant is supplied sufficiently with indicators and monitoring devices at the main switch board for the main engine and diesel generator onboard the vessel. The collected operation parameters, including the fuel oil consumption and the navigation environment conditions [wind speed (m/s) and wave height (m)] were recorded and indicated. To study energy efficiency management, the onboard data acquisition system is very important to collect the operational parameters used in this research. The operation processing database was recorded at a certain voyage number that the ship master and the vessel's chief engineer have managed. The voyage data recorder (VDR) collects this data. Moreover, a flow meter monitors the system energy consumption during the operation. This flow meter is equipped with both a suction and the discharging pipe system for the fuel-supplying pump in the vessel's engine room. They monitor and present the fuel consumption level of the main engine during the ship operation process. The navigation environment condition is an essential factor influencing the ship's fuel consumption during the operation, so the wind speed (m/s) and the wave height (m) were recorded by devices in the boong department of the ship. The collected parameters are presented in the following parts.

5. Results and Discussion

The ship's energy efficiency system is the main topic in this research investigating an operational database and energy consumption model based on data processing and ocean engineering. A deep learning technique was studied and applied in this study. The raw database was treated and refined through computer science and data science techniques to deal with energy consumption in the maritime transportation industry. The data-processing flowchart is presented in Fig. 8. The data feature extraction was done through a modern informative clustering system and a deep learning technique. The combination of these modern methods was able to deal with problems related directly to ocean engineering. The fuel consumption and the operational condition of the ship are the objectives of the study.

The dataset was based on the collected database from the sea-trial database of a vessel. This database was collected from a target ship built in 2013 at the Saijo Shipyard of Imabari Shipbuilding Co., Ltd.,

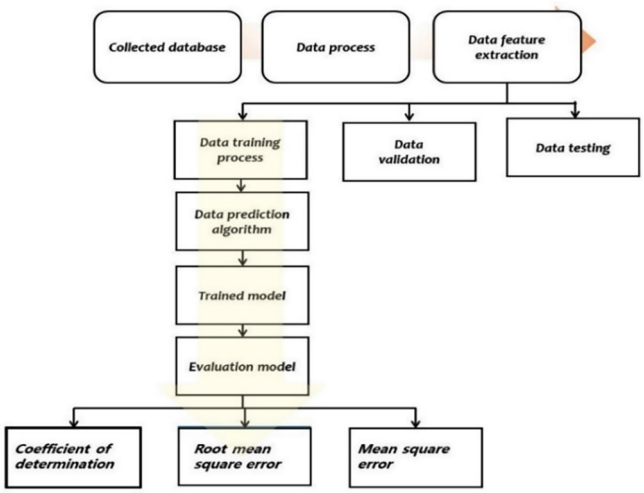

Fig. 8 Flow chart of data analysis based on machine learning

in Japan. There were 520 samples of training data in this study. The dataset of the vessel was split for training (80 percent) and validation (20 percent). The correlation between the fuel consumption and the hull and propeller condition was validated through cross-validation of the trained model. This technique is suitable for a limited dataset as well as data feature extraction. The collected database was verified through the current status of the ship. The ship hull condition and the marine propeller were investigated through the effects of parameters on the fuel consumption of the main engine along with the navigation environment condition at each voyage of the ship.

A deep learning technique was employed in this research based on a CNN model. This technique is helpful to predict uncertain factors and changeable values under the navigation environment condition. The maritime navigation environment condition is always changeable in different ocean areas. This is the main reason that the fuzzy set theory was studied and developed through clustering the uncertain database into different clusters/layers based on the feature extraction database.

The prediction model of the ship hull condition and the marine propeller was designed through a CNN model, which is an advanced machine learning technique to predict uncertain parameters that are variable and changeable during the operation of a ship. Additionally, determining input parameters is important to decide the appropriate degree level of the proposed prediction model for two factors (ship hull condition and marine propeller). Through the onboard vessel operation process, the ship operation condition decides and influences the investigated parameters related directly to the ship hull and marine propeller conditions. These parameters influence fuel consumption, the navigation environment condition, and marine engineering. The predictive model is presented in Fig. 9.

The input parameters of the CNN model include the time of the test (X1), the ship speed (X2, unit: knots), the shaft speed (X3, unit: rpm), the temperature of the sea water environment (X4, unit: ^{o}C), and the temperature of the atmosphere environment (X5, unit: ^{o}C). These parameters directly influence the ship hull and marine propeller condition, which were the investigated factors in this research. The output parameters of the model are the surface roughness image of the ship hull (Y1) and the surface roughness image of the marine propeller (Y2). These parameters are the main factors influencing the residual surface status of the ship hull and the marine propeller. To verify the proposed model accurately, images of the ship hull condition and marine propeller of the target ship were recorded and are presented in Fig. 10. The ship was scheduled to come to the dock by a shipping plan due to the proposed work by the transportation company. The ship position was recorded and supervised by an assigned person and engineers at the building shipyard. For this research, the target ship came to Fujian Huadong Shipyard in Fujian Province, China.

The collected database was evaluated and validated based on the Matlab platform before selecting the number of clusters. The fuzzy clustering method enables the evaluation of the collected results from one layer to five layers. The weight of each layer is illustrated in Fig. 11. Based on the collected results, the number of layers in the three groups with the highest proportional value was 61% from the initial database, which was used in the predicted model.

From the proposed model, the predicted and actual values of the ship hull condition and the marine propeller are presented in Figs. 12 and 13. The depth of the residual surface (mm) was predicted and validated with the actual values when the target ship was at Fujian Huadong Shipyard, China. This was based on the proposed algorithms in the two cases shown in Figs. 3 and 4 above in the section about the proposed methodologies.

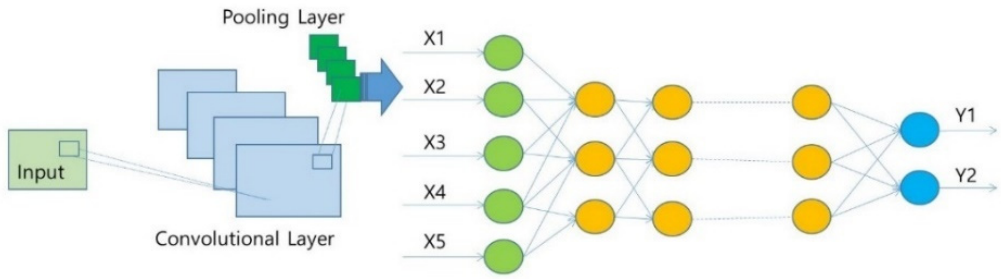

Fig. 9 CNN model

(a) (b) (c) (d)

Fig. 10 Actual surface condition of ship hull and marine propeller before/after coming to dock: (a) ship hull (before), (b) propeller (before), (c) ship hull (after), and (d) propeller (after)

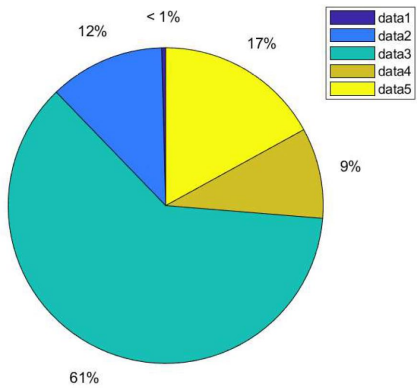

Fig. 11 The weight of the data extraction group influencing the predicted results

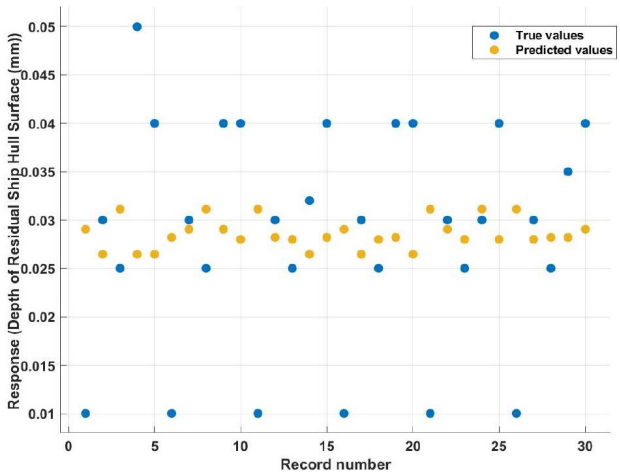

Fig. 12 Depth of residual ship hull surface from CNN model (mm)

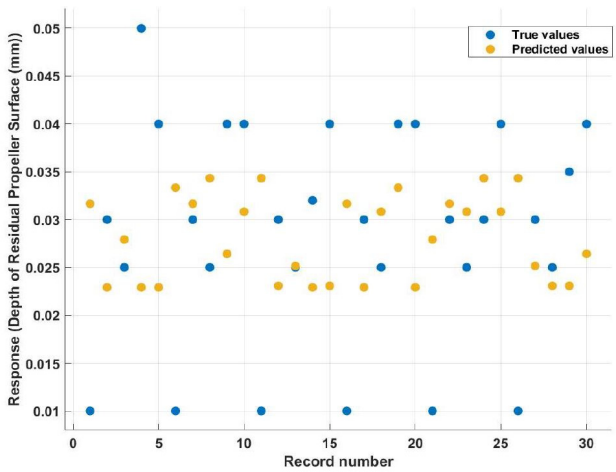

Fig. 13 Depth of residual marine propeller surface from CNN model (mm)

The proposed model collected good results with a coefficient of determination $R^2 > 0.94$)for both the ship hull condition and the marine propeller. The RMSE was also reasonably low with 0.0120 and 0.0139 for the ship hull surface roughness and the marine propeller surface roughness, respectively. Additionally, the mean absolute error in both cases was acceptably small, with 0.0097 and 0.0115 corresponding to the ship hull condition and marine propeller conditions, respectively (Table 2).

Additionally, the marine environment condition also influences fuel consumption along with the ship hull condition and the marine propeller. The actual navigation operation condition and the ship hull condition influence the ship's energy consumption. The actual operation process was presented through certain voyages. The details of each investigated voyage were provided and verified by the ship master and the chief engineer of the ship.

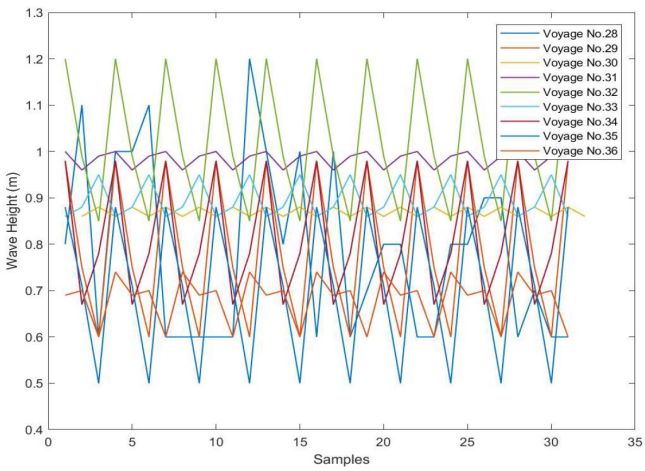

Fig. 14 The actual wave height (m) parameter of a certain bulk carrier

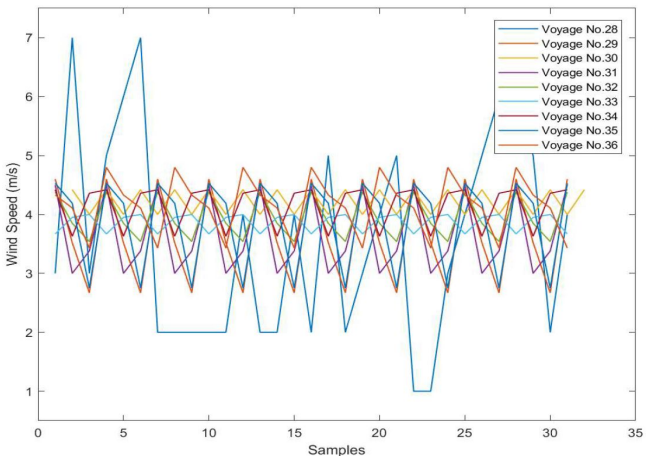

Fig. 15 The actual wind speed (m/s) of a certain bulk carrier

Table 2 The validated results from the proposed CNN models

Case 1: Ship hull surface condition			Case 2: Marine propeller surface condition		
1	Coefficient of determination (R^2)	0.98	1	Coefficient of determination (R^2)	0.94
2	Root mean square error (RMSE)	0.0120	2	Root mean square error (RMSE)	0.0139
3	Mean absolute error (MAE)	0.0097	3	Mean absolute error (MAE)	0.0115

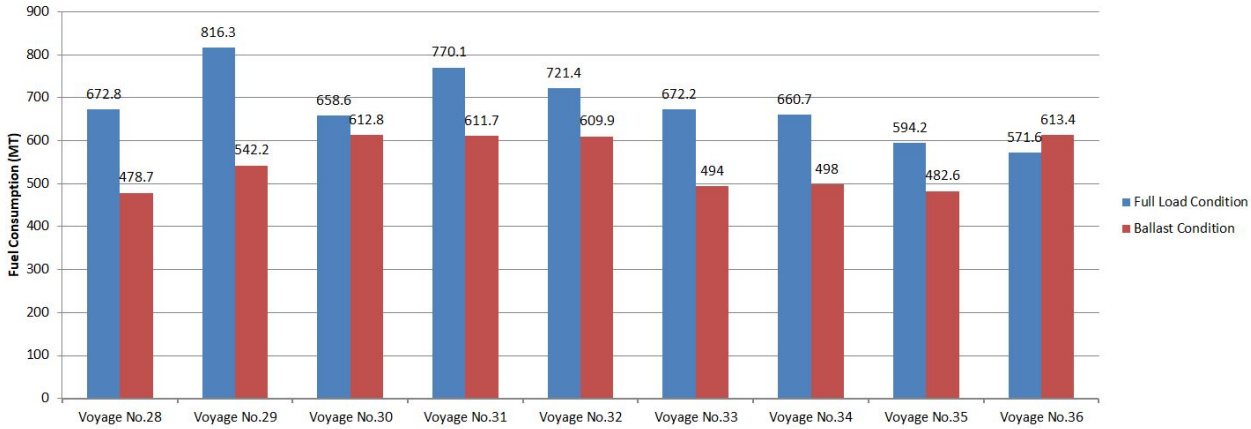

Fig. 16 The actual fuel consumption of a certain bulk carrier

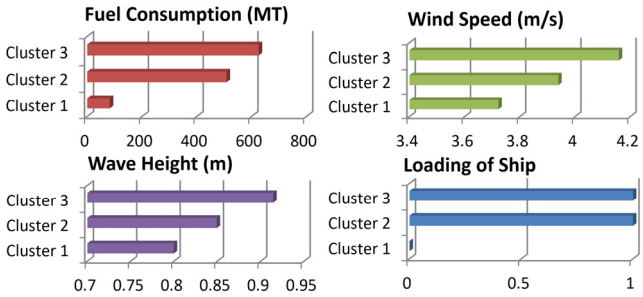

Fig. 17 Data classification based on clusters impacting fuel consumption

The wind speed (m/s) and the wave height (m) are presented in Figs. 14–16. In the collected results, the rough sea condition in voyages No. 28 and No. 32 led to high fuel consumption of the vessel along with higher depth of the residual surface of the ship hull and marine propeller (mm) at values of 0.04–0.05 mm. Voyage No. 35 had a calm water condition with the minimum wave height (m) and wind speed (m/s). The fuel consumption in this voyage was low, corresponding to a depth of the residual surface of 0.01 mm.

The same database cluster/layer considering the ship loading condition (full load condition/ballast condition) is presented in Fig. 17. From the collected results in Fig. 11, three clusters were selected with specific values in each group. The collected results were expressed through the optimization algorithm in Fig. 6. The same characteristics of a parameter were classified into a cluster with the nearest Euclidean distance compared with the center layer. The hyper-parameters were arranged into the same group with an identical feature through this optimization algorithm.

In the first layer/cluster, the engine's fuel consumption was lowest and under 100 t in the investigated voyage corresponding to the calm sea condition along with the ship loading condition (ballast condition). The wave height was under 0.8 m, and the wind speed was about 3.7 m/s. In contrast, the rough sea condition made the fuel consumption the highest at the third cluster/layer at about 600 t. The navigation environment condition was also heavy with a full load condition, wind speed above 4.1 m/s, and wave height above 0.9 m.

Concluding Remarks

Evaluating fuel consumption is vital for effective ship operation and management. External factors, such as environmental conditions and ship load, influence fuel consumption and energy efficiency. This study systematically assessed these conditions with an emphasis on navigational environment factors, ship load, hull, and propeller conditions. The aim was to improve understanding of variables impacting ships' fuel consumption, thereby enhancing energy efficiency management. Key contributions of this study include the following:

(1) The proposed methodology utilizes fuzzy set theory within an informatic system and employs machine learning clustering to refine data from actual ship operations.

(2) We applied a CNN model to predict the residual surface depth for both ship hull and marine propeller conditions. This approach aided in examining impacts on energy consumption, navigation conditions, and ship loading. The model's effectiveness was underscored by an R^2 value exceeding 0.94 in both cases.

(3) Enhanced accuracy in calculating ship fuel consumption benefits ship owners and operators. The results demonstrate that combining informatics theory, machine learning, and deep learning (CNN) effectively addresses complex challenges in maritime transportation and ocean engineering.

Conflict of Interest

Do Kyun Kim serves as an editorial board member of the Journal of Ocean Engineering and Technology, but he had no role in the decision to publish this article. No potential conflict of interest relevant to this article was reported.

Funding

This work was supported under the framework of the international cooperation program managed by the National Research Foundation of Korea (NRF-2022K2A9A1A09087779).

References

Adland, R., Cariou, P., Jia, H., & Wolff, F. -C. (2018). The energy efficiency effects of periodic ship hull cleaning. *Journal of Cleaner Production, 178*, 1−13. https://doi.org/10.1016/j.jclepro.2017.12.247

Bialystocki, N., & Konovessis, D. (2016). On the estimation of ship's fuel consumption and speed curve: A statistical approach. *Journal of Ocean Engineering and Science, 1*(2), 157-166. https://doi.org/10.1016/j.joes.2016.02.001

Bocchetti, D., Lepore, A., Palumbo, B., & Vitiello, L. (2015). A statistical approach to ship fuel consumption monitoring. *Journal of Ship Research, 59*(3), 162−171. https://doi.org/10.5957/jsr.2015.59.3.162

Doulgeris, S., Zacharof, D. N., Toumasatos, Z., Kolokotronis, D., & Samaras, Z. (2020). Real world fuel consumption prediction via a combined experimental and modeling technique. *Science of the Total Environment, 734*, 139254. https://doi.org/10.1016/j.scitotenv.2020.139254

Demirel, Y. K., Turan, O., & Incecik, A. (2017). Predicting the effect of biofouling on ship resistance using CFD. *Applied Ocean Research 62*, 100−118. https://doi.org/10.1016/j.apor.2016.12.003

Ghaemi, M. H., & Zeraatgar, H. (2021). Analysis of hull, propeller and engine interaction in regular waves by a combination of experiment and simulation. *Journal of Marine Science and Technology, 26*, 257−272. https://doi.org/10.1007/s00773-020-00734-5

International Maritime Organization (IMO). (2009). *Second IMO GHG Study 2009*. International Maritime Organization, 4 Albert Embankment, London SE1 7SR. https://wwwcdn.imo.org/localresources/en/OurWork/Environment/Documents/SecondIMOGHGStudy2009.pdf

Işikli, E., Aydin, N., Bilgili, L., & Toprak, A. (2020). Estimating fuel consumption in maritime transport. *Journal of Cleaner Production, 275*, 124142;. https://doi.org/10.1016/j.jclepro.2020.124142

Jimenez, V. J., Kim, H., & Munim, Z. H. (2022). A review of ship energy efficiency research and directions towards emission reduction in the maritime industry. *Journal of Cleaner Production, 366*, 132888. https://doi.org/10.1016/j.jclepro.2022.132888

Koboević, Z., Bebić, D., & Kurtela, Z. (2019), New approach to monitoring hull condition of ships as objective for selecting optimal docking period. *Ships and Offshore Structures, 14*(1), 95−103. https://doi.org/10.1080/17445302.2018.1481631

Kuroda, M., Takagi, K., Tsujimoto, M., & Fujisawa, J. (2017). Measurement of added resistance in irregular waves and estimation of the long-period components. *Journal of the Japan Society of Naval Architects and Ocean Engineers 24*, 181−188. https://doi.org/10.2534/jjasnaoe.24.181

Shi, Y., Xue, S., Zhang, X., & Huang, T. (2020). Data-aware monitoring method for fuel economy in ship-based CPS. *IET Cyber-physical Systems: Theory & Application, 5*(3), 245−252. https://doi.org/10.1049/iet-cps.2019.0080

Shigunov, V., Moctar, O., Papanilolaou, A., Potthoff, R., & Liu, S. (2018). International benchmark study on numerical simulation methods for prediction of manoeuvrability of ships in waves. *Ocean Engineering, 165*, 365−385. https://doi.org/10.1016/j.oceaneng.2018.07.031

Schultz, M. P. (2007). Effects of coating roughness and biofouling on ship resistance and powering. Biofouling, 23, 331−341. https://doi.org/10.1080/08927010701461974

Tran, T. A. (2021). Effects of the uncertain factors impacting on the fuel oil consumption of sea ocean-going vessels based on the hybrid multi criteria decision making method. *Ocean Engineering 239*, 109885. https://doi.org/10.1016/j.oceaneng.2021.109885

Trodden, D. G., Murphy, A. J., Pazouki, M., & Sargeant, J. (2015). Fuel usage data analysis for efficient shipping operations. *Ocean Engineering, 110*(Part B), 75−84. https://doi.org/10.1016/j.oceaneng.2015.09.028

Tillig, F., Ringsberg, J., Psaraftis, H., & Zis, T. (2020). Reduced environmental impact of marine transport through speed reduction and wind assisted propulsion, *Transportation Research Part D: Transport and Environment, 83*, 102380. https://doi.org/10.1016/j.trd.2020.102380

United Nationals Conference on Trade and Development (UNCTAD). (2017). *Review of Maritime Transport 2017*. Geneva, Switzerland.

Yin, Q., Ding, Z., Ding, K., & Liu, G. (2017). Design of a real-time ship fuel consumption monitoring system with self-checking function. In *2017 4th International Conference on Transportation Information and Safety (ICTIS),* 735−738. https://doi.org/10.1109/ICTIS.2017.8047849

Yeh, C. K., Lin, C., Shen, H., Cheruiyot, N. K., Nguyen, D., & Chang, C. (2022). Real-time energy consumption and air pollution emission during the transpacific crossing of a container ship. *Scientific Reports, 12*, 15272. https://doi.org/10.1038/s41598-022-19605-7

Yuan, Z., Liu, J., Zhang, Q., Liu, Y., Yuan, Y., & Li, Z. (2021). Prediction and optimization of fuel consumption for inland ships considering real-time status and environmental factors. *Ocean Engineering, 221*, 108530. https://doi.org/10.1016/j.oceaneng.2020.108530

Zadeh, L. A. (1965). Fuzzy set. *Information and Control 8*(3), 338−353. https://doi.org/10.1016/S0019-9958(65)90241-X

Author ORCIDs

Author name	ORCID
Tran, Tien Anh	0000-0002-2231-2764
Kim, Do Kyun	0000-0001-5735-4625

Journal of Ocean Engineering and Technology 37(5), 190-197, October, 2023
https://doi.org/10.26748/KSOE.2023.011
pISSN 1225-0767
eISSN 2287-6715

Original Research Article

A Study for Digital Transformation Based on Collaboration Master Plan for Shipbuilding & Marine Engineering Industry

Seung-Uk So[1], Myeong-Ki Han[2], Young-Hun Kim[3] and Jun-Soo Park[3]

[1]*Vice president, Hanwha Ocean Digital Co., Ltd., Geoje-si, Korea*
[2]*General manager, Hanwha Ocean Digital Co., Ltd., Geoje-si, Korea*
[3]*Professor, Dept. of Naval Arch. and Ocean System Eng. Kyungnam University, Changwon, Korea*

KEYWORDS: Digital transformation, Small, medium, and large companies collaboration, Value chain, Master plan

ABSTRACT: *In the shipbuilding and marine industry, digital transformation activities are promoted primarily by large shipyards. However, bottlenecks are observed across value chains, and digital transformation effects are reducing because of the cost and technical challenges encountered by supplies. In this study, we proposed a win-win cooperation model for large, small, and medium-sized companies using digital transformation based on the characteristics of the shipbuilding and marine industry through case studies. We investigated the digital transformation progress in German and Korean small and medium-sized enterprises (SMEs). In addition, we identified information-sharing methods and management challenges encountered in enterprise resource planning and manufacturing execution systems in the collaboration process of pipes, panels, blocks, etc. of SMEs that are suppliers of a Korean shipyard, and clarified communication by building a platform based on a common format between shipyards and suppliers. Further, we proposed a standard model of a digital transformation system for enhancing the collaboration between large companies and suppliers and proposed a basic plan including strategies to efficiently and effectively build a digital transformation system based on the standard model.*

1. Introduction

In the era of the Fourth Industrial Revolution, companies are actively involved in digital transformation as an innovative strategy to secure competitiveness and achieve growth. The International Data Corporation (IDC) defines digital transformation as a continuous process of adapting to or driving disruptive changes in customers and markets (the external ecosystem) by using digital capabilities to create new business models, products, and services. AT Kearney defines digital transformation as an enterprise activity that proactively responds to changes in the business environment triggered by digital technologies such as mobile, cloud, big data, artificial intelligence (AI), and IoT(Internet of Things), aiming to significantly enhance the competitiveness of existing businesses or pursue new growth through innovation. According to IBM, it is a strategy that involves the integration of digital and physical elements to transform business models and establish new directions within industries.

One significant aspect of digital transformation is the increasing importance of collaboration networks within companies and among various partners within the value chain. Digital transformation enables the establishment of organic collaboration networks among raw material suppliers, component providers, service providers, and research institutions within the value chain, facilitating seamless data exchange. The integration of comprehensive and organic production processes through networking among companies in the value chain can lead to improved productivity through supply chain synchronization, efficient resource utilization, reduced production lead times, and accelerated innovation cycles (Oh and Kim, 2022).

The shipbuilding and marine engineering industry, particularly Engineering to Order (ETO) industries, is a representative example where various tasks such as design, material procurement, sourcing, and production are performed simultaneously once an order is received from a client The processes in this industry are complex and have different levels of difficulty, with multiple companies collaborating cooperatively at each stage of the process.

Therefore, the Korean shipbuilding and marine engineering industry, primarily led by large corporations, is vigorously promoting digital transformation as a core strategy to enhance productivity,

Received 26 April 2023, revised 22 September 2023, accepted 13 October 2023
Corresponding author Young-Hun Kim: +82-55-249-2686, younghun@kyungnam.ac.kr

reduce costs, and focus on core business activities. Many digital transformation initiatives are planned and executed in the areas of Smart Factory/Yard and Smart Ship, with a primary focus on large corporations, aiming to enhance the competitiveness of the shipbuilding and marine engineering industry. However, for more than 50% of partner companies, including suppliers, in the shipbuilding and marine engineering value chain, the implementation of digital transformation strategies is challenging because of the complexity of internal operations and a lack of digital transformation experts. This implies that the technological interfaces related to digital transformation initiatives pursued by large corporations are not sufficiently established, limiting the effectiveness of digital transformation initiatives within large corporations and, consequently, the overall impact of digital transformation across the shipbuilding and marine engineering value chain.

In this study, we analyzed the overall progress of digital transformation and reviewed digital transformation cases from the perspective of cooperation between large, medium, and small-sized enterprises to propose a master plan for cooperative digital transformation for the Korean shipbuilding and marine engineering industry. This plan is expected to foster consensus on collaborative value chain development based on digital transformation in the shipbuilding and marine engineering industry. To this end, we analyzed the current collaboration status between large corporations and partner companies and explored methods to establish an efficient and structured collaborative ecosystem by leveraging digital transformation technologies. Moreover, to facilitate this endeavor, we planned and executed strategies to secure momentum within related internal and external organizations, focusing on a large shipbuilding company “HO Company” (formerly known as “D Company”). Specifically, the responsibilities of the shipbuilding company include providing support for enhancing competitiveness, such as procurement and outsourced production, improving its collaboration systems, and sharing data with partner companies. Partner companies are tasked with enhancing competitiveness by establishing and advancing digital transformation-based systems, such as suitable smart factory systems. These efforts enable the exchange of production and manufacturing information between the shipbuilding company and partner companies using digital transformation technologies. Moreover, to activate the ecosystem within the shipbuilding and marine engineering sector, government agencies should increase financial support by allocating budgets for the development of smart factory systems based on digital transformation, an area where the direct intervention of shipbuilders is restricted to maintaining fairness. Furthermore, by fostering specialized information and communications technology (ICT) companies with in-depth knowledge of the shipbuilding and marine engineering sector and expertise in digital transformation technologies, they will provide technical interface support for digital transformation and develop solutions to bridge the technological gap between large corporations and partner companies. This approach is expected to enhance the overall competitiveness of the entire South Korean shipbuilding and marine engineering value chain using digital transformation.

2. Preliminary Research on Digital Transformation

2.1 Analysis of the Digital Transformation Concept

With the widespread adoption of the government-led Fourth Industrial Revolution, several companies are embracing digital transformation. Previous studies have primarily focused on defining the concept and meaning of digital transformation based on the prevailing trends at the time.

Martin (2008) defined digital transformation from the perspective of ’the use of digital technology by individuals. Specifically, it refers to the ultimate stage of digital literacy, which includes the technical ability to effectively utilize digital tools and perceptual skills to determine when to use them. Furthermore, it enables innovation and creativity in advanced levels of digital usage. However, as the adoption of digital technology is an organizational decision, digital transformation is generally considered an organizational concept rather than an individual concept.

White (2012) defined digital transformation as a concept that emerges when individuals, organizations, and societies adopt new digital technologies. It also encompasses changes in business models resulting from the use of digital technology.

Kreutzer (2014) defined digital transformation as the process of changing customers’ interaction with the market in response to the rapidly changing market conditions and business models. The author emphasized that adapting to such changes is essential for survival in a competitive environment.

Westerman et al. (2014) stated that digital transformation includes the use of technology to expand the scope of a company's business. It also involves changes within the corporate culture and processes of an organization as a result of the broader societal and individual changes caused by the adoption of digital technology. From a strategic business perspective, digital transformation also encompasses changes in business models.

According to Schwab (2017), digital transformation involves adopting Fourth Industrial Revolution digital technologies into a company's business model. It has four major effects including meeting customer expectations, improving products, promoting collaborative innovation, and transforming organizational structures. Schwab emphasized that in an era where customers are increasingly central to the economy, enhancing customer service has become the primary goal for companies, and digital capabilities can enhance both physical products and services.

Morakanyane et al. (2017) argued that the literature between 2011 and 2016 lacks consensus regarding the definition of digital transformation. Moreover, they provided a conceptual framework for digital transformation by analyzing the characteristics of commonly used terms.

Udovita (2020) described the process of digitalization using the

terms, “digitization” and “digitalization.”. The former refers to the conversion of analog technology, information, and products into digital formats, and the latter refers to creating new revenue and socio-economic value through changes in business models or processes using digital opportunities.

Digital transformation is defined as a restructuring that arises from changes in individuals and society resulting from digitalization. A thorough review of the literature reveals that digital transformation emphasizes changes and innovations resulting from the evolving trends in digital technology, particularly in the realms of business and IT. To optimize the advantages of digital transformation, concepts and definitions that have attracted global attention since 2010 should be investigated and implemented.

Essentially, digital transformation optimizes IT infrastructure, enhances customer-centric business models, increases service value, and promotes external collaboration using innovative digital technologies. Such changes encompass personal, organizational, and societal transformations in the pursuit of efficient internal operations.

According to Vial (2019), digital transformation is a more advanced concept than IT-based transformation and requires continuous evolution through the active use of emerging technologies. Digital transformation has significant implications for organizations as they adapt to changes in the business environment, consumer behavior, and internal innovation. With the increasing demand for mobile devices among consumers, companies can enhance customer experiences by developing mobile applications that strengthen customer communication, data collection, and analysis. Adaptation to these real-time changes can be considered as a form of digital transformation (Lee et al., 2022).

Bonnet et al. (2020) emphasized the importance of becoming digital masters for companies to drive digital innovation. A digital master refers to an individual who possesses both digital and leadership capabilities, enabling organizations to improve business elements and drive change. In recent years, the development of advanced technologies such as IoT and AI has made digital innovation increasingly complex. Therefore, although leadership skills are crucial, digital capabilities are emerging as a new essential element.

2.2 Research on Digital Transformation in German SMEs

Studies on German Small and Medium-sized Enterprises (SMEs) have reported that approximately 80% of the surveyed companies identified optimizing production processes through inter-company networking as a primary goal. Leveraging digital transformation ensures the sharing and utilization of production process data between companies, enabling swift identification and improvement of weaknesses in the value chain. Furthermore, the enhancement of production and services has emerged as a core value for digital transformation. Notably, digital transformation can lead to the optimization of existing production processes while fostering the development of new products and services. However, networking-associated costs are an obstacle to its promotion, with companies displaying a lack of trust in the expected benefits of high-cost networking.

Furthermore, digital transformation initiatives emphasize the growing significance of data security through enhanced inter-company networking within and beyond the value chain. According to Oh and Kim (2022), during the planning and pilot phases of digital transformation, factors such as a shortage of relevant personnel, inadequate legislation, and internal resistance posed significant challenges for companies. Nevertheless, cybersecurity has emerged as a critical concern in subsequent stages of application and digital transformation. Therefore, the presence and maturity of industries that can provide security solutions are crucial for effective digital transformation.

2.3 Research on the Digital Transformation Process in Mid-sized Manufacturing Companies

Digital transformation comprises the use of digital technology to enhance operations, improve productivity, create innovative business models, and enhance customer experiences as a strategic management approach. According to the IDC, 89% of companies consider digital transformation a crucial managerial priority, with an expected market growth rate of 23% by 2025. This underscores the importance of digital transformation as a response to competition and a means to achieve business success and sustainability. However, McKinsey reported that 70% of digital innovation initiatives fail because of various factors such as resistance to change, inadequate leadership, poorly designed processes, lack of inter-departmental collaboration, and a shortage of digital skills. One of the core elements highlighted by the Boston Consulting Group is the importance of "people" in achieving effective digital transformation, emphasizing a member-centric perspective and the integration of data and processes. Digital transformation is not a static change but a dynamic process requiring internal and external transformations. IDC predicted that by 2022, 65% of the global GDP will be digitized, with approximately $2 trillion invested in technology and services in this domain.

Digital transformation is a long-term and continuous process that requires well-defined objectives, efficient resource allocation, and a specific execution plan for effective implementation. Hence, active support and leadership from the management team are essential to drive digital transformation. This strategy encompasses a wide range of tasks, including improving operational efficiency through the use of digital technology, strengthening operations, renewing customer experiences, and developing new business. For effective digital transformation, CEOs need to possess technological expertise, prioritize digital trends, and drive innovation. Therefore, exceptional technological insight and drive from the leadership team are necessary, and the success of digital transformation hinges on a company-wide strategy and systematic implementation. Digital transformation has been considered a strategic concept since the late 2000s for enhancing value across various business functions, from production to services, by addressing vulnerabilities in the value chain based on the analysis

results of existing studies (Kim, 2022).

3. Status of ICT-Based Collaboration in Medium and Small-Sized Enterprises

Since 2008, South Korean shipbuilding companies have been developing and maintaining collaboration systems to share information related to procurement and external production with their partner companies. Furthermore, they have supported their partners in establishing smart factories through government-funded projects. Fig. 1 shows the collaboration system development and support for HO Company, a prominent shipbuilding company in South Korea, highlighting the gradual progression of system development for collaboration support among major shipbuilding companies.

To facilitate seamless collaboration between shipbuilders and their partner companies, information regarding drawings, materials, schedules, transportation, and regular updates on the progress of mutual processes is shared. For partner companies without their systems, shipbuilders utilize Excel-based data for sharing collaboration information. However, partners with their systems are required to separately access and register collaboration data. Fig. 2 shows the service framework for establishing collaboration between shipbuilders and partner companies. Information sharing within the shipbuilding industry is primarily based on Excel, with plans and execution information shared between parent companies and partner companies. Some partner companies equipped with enterprise resource planning/manufacturing execution system (ERP/MES) consider collaboration from a system perspective.

In the shipbuilding industry, information sharing between shipbuilders and SMBs is predominantly important. But it is difficult to standardize ICT systems between shipbuilders and partner companies. So Excel-based information sharing is mostly done owing to the characteristics of the industry.

Consequently, partner companies cannot easily adopt ICT-based systems. As presented in Table 1, which provides an overview of the current state of partner companies in the shipbuilding and maritime

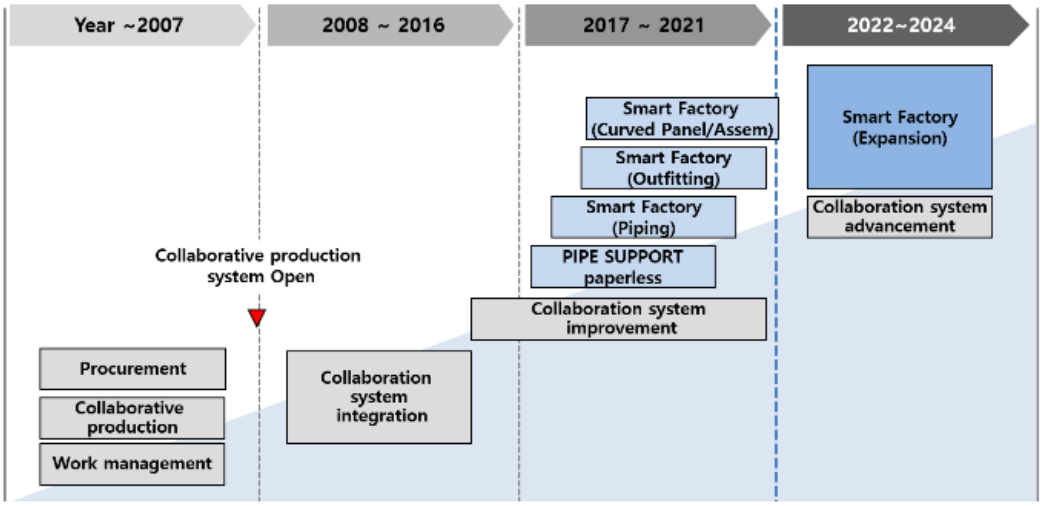

Fig. 1 Implementation of collaboration ICT system

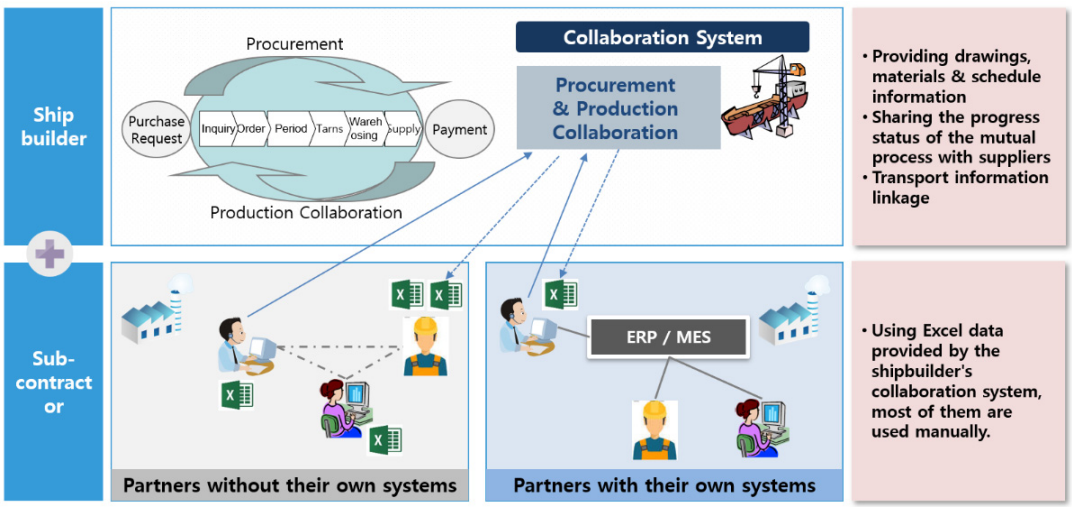

Fig. 2 Collaboration service in the shipbuilding and marine Biz.

Table 1 Shipbuilding partners by region/field & ICT status

Current status of subcontractor's number					
City	Hull	Machi.	Outfit'g	Elec.	sum
Busan	19	36	260	54	398
Gyeongsangnam-do	22	32	357	29	440
Ulsan	11	18	86	17	39
Junnam	20	2	81	1	104
Others	7	13	110	64	258
SUM	79	101	894	165	1,239

Current status of subcontractor's number				
Region	Sum (company)	ICT sys.	manual	Rate of Holding ICT sys.
Gyeongsangnam-do & Busan	185	58	127	31%

industry by region and function, the possession rate of information systems such as ERP/MES among partner companies in the Gyeongsangnam-do and Busan regions is low at 31%. The absence of these information systems poses constraints on smooth collaboration and information exchange, ultimately impacting the competitiveness of large shipbuilders at the top of the value chain. To address this issue, shipbuilders and partner companies need to collaborate to establish efficient and effective ICT systems for symbiotic collaboration.

Therefore, shipbuilders and partner companies manage symbiotic collaboration using collaboration systems provided by shipbuilders, along with Excel-based tools, as shown in Fig. 3. However, the absence of their information systems poses significant limitations in achieving smooth collaboration and information exchange.

Similarly, the majority of partner companies in the shipbuilding and maritime industry significantly rely on Excel for business management. Even when developing systems, efficient implementation can be challenging, potentially resulting in reduced utility because of a lack of skilled personnel and significant manual work related to tasks and operations. Nonetheless, high-quality information systems are crucial as they serve as the foundation for digital transformation.

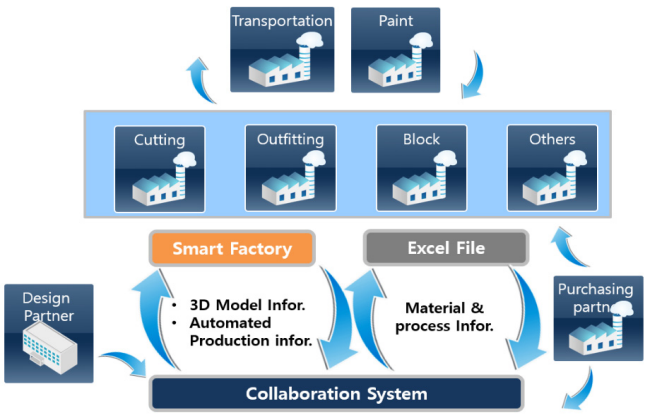

Fig. 3 Current status of cooperation between companies

Table 2 Business specifications of partner companies

Kind	Job Issues
Pipe	Many manual tasks are required to generate individual PIECE drawing files and connect them to PIECE information by receiving production POR drawings from the customer and SCAN of the drawings
Valve	Standard BOM is managed because of the numerous mass products of various varieties, and the appropriate inventory of STOCK items must be maintained and managed because of numerous emergency orders.
Equipment	Owing to the production of order-based products, BOM is often reorganized except for standard products. Therefore production BOM management is required
Steel Out.	Many work instructions and purchase orders are provided because of numerous tasks in the form of in-house outsourcing, inventory management, storage location, and material warehousing of manufactured products

Furthermore, to address limitations related to source data sharing due to national infrastructure constraints, advanced security systems should be implemented, along with support for enhancing the ease of source data sharing through information systems for design and production information. Table 2 presents an overview of the characteristics of the field of each business partner, emphasizing areas that require significant manual work and information management.

4. Fundamental Plan for Digital Transformation-based Collaborative Cooperation

A strategic approach emphasizes developing a standardized open digital foundation system to support process innovation for various partners, instead of crafting a system exclusively for a specific partner. Notably, field experts should be involved when conducting practical process innovatory consultation. Additionally, shipbuilding companies must establish 3D model-based design/production information delivery systems to expand ongoing digital transformations to external production. Then, partner companies can leverage this system and information to minimize vulnerabilities in the shipbuilding and maritime industries, enhance productivity, and reduce costs. Shipbuilding and partner companies should build a technology interface system and automate all processes except those requiring personnel. Fig. 4 shows the direction for establishing a collaborative system for digital transformation. This system should be constructed on a platform that enables data exchange between shipbuilding and partner companies through a common format, rather than integrating data separately for each shipbuilder and its partners. For partner companies without ICT expertise, cloud-based system services should be provided. Notably, the leadership of this system should be implemented in coordination with government-supported projects, rather than being solely initiated by a specific shipbuilder.

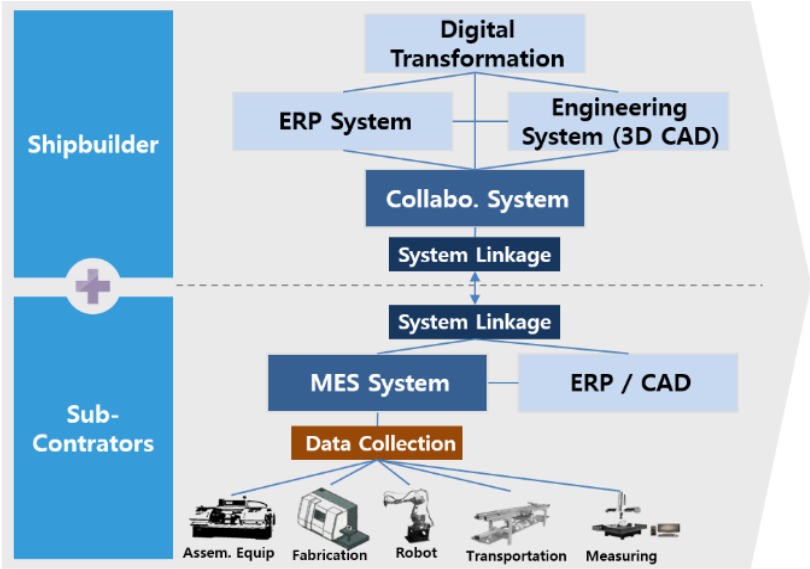

Fig. 4 Partner collaboration system implementation architecture

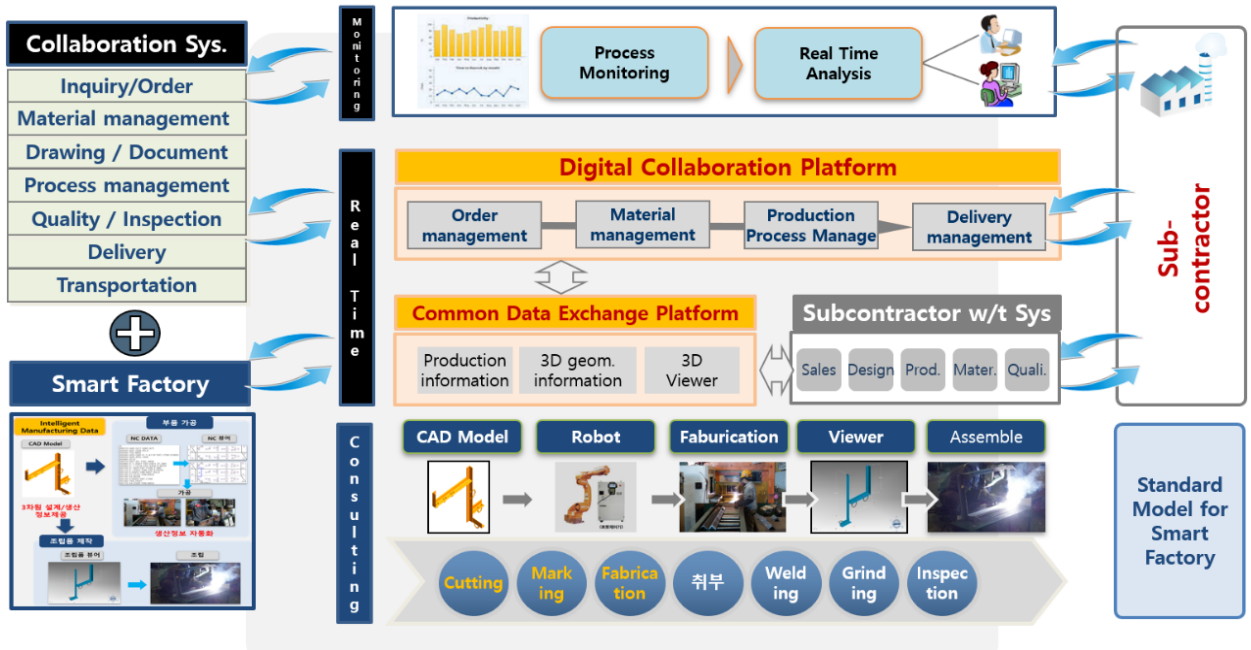

Fig. 5 Collaboration framework

The framework presented in Fig. 5 summarizes the necessary tasks for promoting collaborative cooperation, including the development of a digital transformation-based collaboration platform, the development of a common data exchange platform between shipbuilders and partner companies, and digital transformation consulting, based on digital transformation. These efforts should be based on the smart factory standard model integrated with the collaborative systems in shipbuilding companies.

The priority for advancing tasks related to collaborative cooperation based on digital transformation is shown in Fig. 6, considering both urgency and feasibility. Depending on the tasks, government agencies and shipbuilding companies should take the lead in their implementation. Furthermore, specific tasks and roadmaps for digital

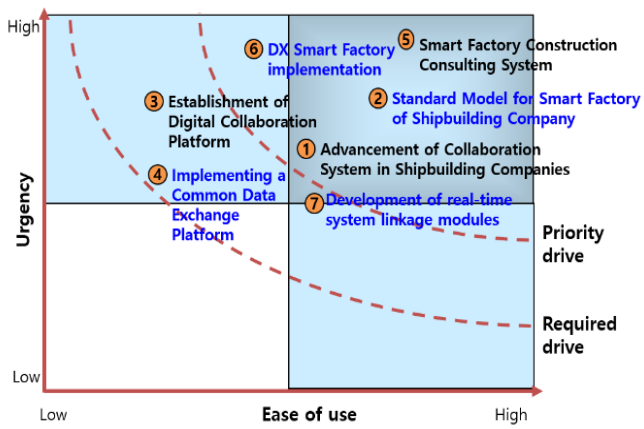

Fig. 6 Task priority

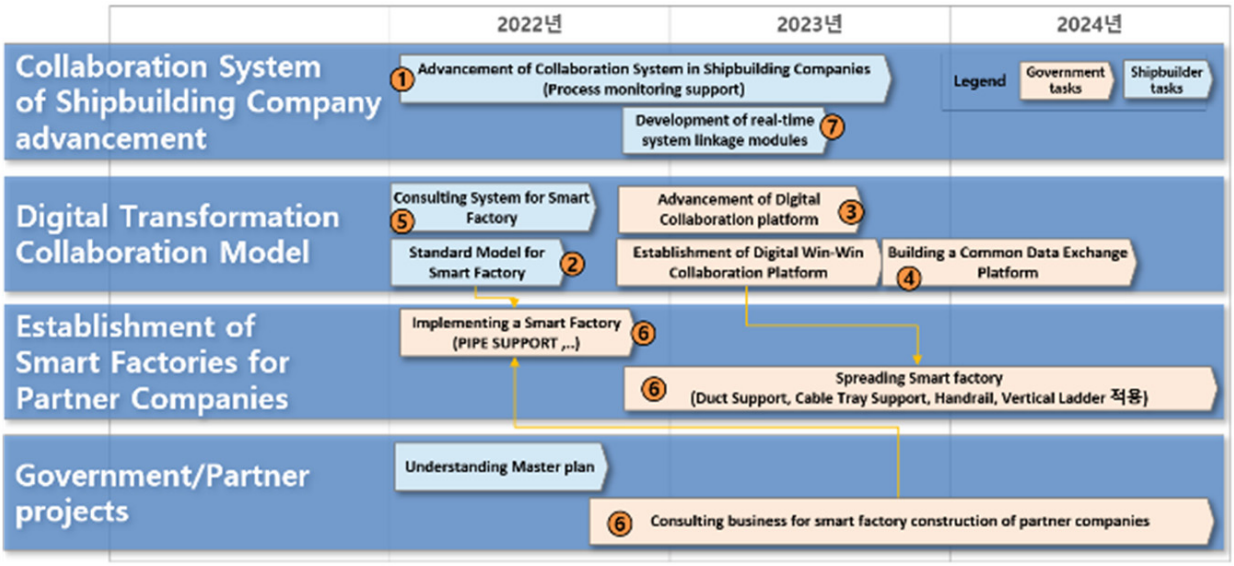

Fig. 7 Road map for digital transformation-based collaboration

transformation-based collaborative cooperation have been established based on business items and priorities, as shown in Fig. 7. This roadmap was developed through extensive consultations with experts related to HO Company over several months.

The key tasks and priorities for promoting collaborative cooperation based on digital transformation in the shipbuilding and marine engineering industries are as follows:

(1) Enhancing shipbuilding company collaboration systems: Improve systems to enable smooth information exchange with partner smart factory systems.

(2) Establishing collaborative cooperation models: Develop a digital transformation-based smart factory construction consulting system, establish a smart factory standard model, enhance the digital collaborative cooperation platform, and create a shared data exchange platform.

(3) Implementation and deployment of smart factory systems by partner companies: Promote the implementation of smart factory systems in partner company fields.

(4) Promotion of Government-Agency-Led Cooperative Projects: Promote support for smart factory construction, pursue agreements on digital transformation-based collaborative cooperation master plans, and provide consulting support to partner companies.

These tasks should be prioritized based on urgency and ease of implementation and can be performed through collaboration between government agencies and shipbuilding companies/partner companies.

5. Conclusion

Digital transformation is a global phenomenon and is widely recognized as a crucial strategy. In South Korea, both the government and businesses are actively promoting digital transformation to enhance competitiveness across various industries. Major shipbuilding companies in the maritime industry have already embarked on their digital transformation journey, achieving remarkable results through various applications in both smart yards and vessels since 2019. The smart yard system shown in Fig. 8 enables digital management of

Fig. 8 Case of smart yard development (Digital twin-based digital production center system)

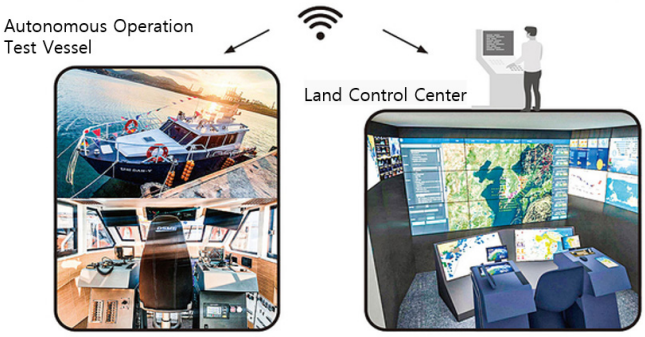

Fig. 9 Case of smart vessel development (Autonomous vessel navigation system)

production based on a digital twin, and the development of autonomous navigation smart vessel systems shown in Fig. 9 effectively showcases the outcomes of these efforts. Given the high dependence of the shipbuilding and maritime industry on partnerships, the digital transformation of partner companies is expected to strengthen the value chain of South Korea's maritime industry. Therefore, major shipbuilding companies and government agencies should collaborate and support the advancement of digital transformation.

In this study, we provided a broad overview of the content of technology interfaces between partner and shipbuilding companies based on digital transformation. The findings of this research are currently under consideration for potential government projects, in consultation with government agencies such as Gyeongnam Techno Park (TP), Busan TP, and the Research Institute of Medium & Small Shipbuilding. The significance of this study lies in its insights into the digital transformation-based collaborative cooperation in the complex collaborative structure of the shipbuilding and maritime industry. The research results can serve as a reference model for digital transformation-based collaborative cooperation in other ETO industries. Future research will focus on the establishment of an information exchange platform, a fundamental component of digital transformation-based collaborative cooperation systems.

Conflict of Interest

Young-Hun Kim serves a journal publication committee member of the Journal of Ocean Engineering and Technology, but he had no role in the decision to publish this article. No potential conflict of interest relevant to this article was reported.

Funding

This research was funded and conducted under the Competency Development Program for Industry Specialists of the Korean Ministry of Trade, Industry and Energy (MOTIE), operated by Korean Institute for Advancement of Technology (KIAT) (No. P0012646, HRD program for Global Advanced Engineer Education Program for Future Ocean Structures).

References

Martin, A. (2008). Digital literacy and the “digital society”. In C. Lankshear, & M. Knobel (Eds.), *Digital literacies: Concepts, policies and practices 30*, 151-176. Peter Lang.

White, M. (2012). Digital workplaces: Vision and reality. *Business information review, 29*(4), 205−214.

Kreutzer, R. T. (2014). Digital Darwinism and the need for a digital transformation. In *International Conference on Business Strategy and Organizational Behaviour (BizStrategy). Proceedings* (p. 38). Global Science and Technology Forum.

Westerman, G., Bonnet, D., & McAfee, A. (2014). The nine elements of digital transformation. *MIT Sloan Management Review, 55*(3), 1−6.

Morakanyane, R., Grace, A. A., & O'reilly, P. (2017). Conceptualizing digital transformation in business organizations: A systematic review of literature. *BLED 2017 Proceedings,* 21. https://aisel.aisnet.org/bled2017/21

Schwab, K. (2017). *The fourth industrial revolution*. Crown Business.

Udovita, P. V. M. V. D. (2020). Conceptual review on dimensions of digital transformation in modern era. *International Journal of Scientific and Research Publications, 10*(2), 520−529. https://doi.org/10.29322/IJSRP.10.02.2020.p9873

Vial, G. (2019). Understanding digital transformation: A review and a research agenda. *Journal of Strategic Information Systems, 28*(2), 118−144. https://doi.org/10.1016/j.jsis.2019.01.003Get rights and content.

Oh, J. T., & Kim, E. H. (2022). 기업의 디지털 전환 경쟁우위 요소에 관한 고찰: 포터의 다이아몬드 모델을 기반으로 [A study on the competitive factors of digital transformation in enterprises: Based on Poter's diamond model]. *Korean Management Consulting Review, 22*(3), 207−224.

Kim, C. H. (2022). The study on the digital transformation process of mid-sized companies. *Journal of Industrial Convergence, 20*(1), 23−33. https://doi.org/10.22678/JIC.2022.20.1.023

Lee, S. J., Choi, Y., Ra, J., & Kho, H. S. (2022). An exploratory study on digital transformation services. *Journal of Information Technology and Architecture, 19*(2), 73−91. https://doi.org/10.22865/jita.2022.19.2.73

Author ORCIDs

Author name	ORCID
So, Seung-Uk	0009-0004-9462-8946
Han, Myeong-Ki	0009-0001-3007-6749
Kim, Young-Hun	0000-0002-3072-6852
Park, Jun-Soo	0000-0001-6409-5721

Journal of Ocean Engineering and Technology 37(5), 198-204, October, 2023
https://doi.org/10.26748/KSOE.2023.019

pISSN 1225-0767
eISSN 2287-6715

Original Research Article

Estimating Hydrodynamic Coefficients of Real Ships Using AIS Data and Support Vector Regression

Hoang Thien Vu[1], Jongyeol Park[2] and Hyeon Kyu Yoon[2]

[1]*Graduate Student, Department of Smart Environmental Energy Engineering, Changwon National University, Changwon, Korea*
[2]*Professor, Department of Naval Architecture and Marine Engineering, Changwon National University, Changwon, Korea*

KEYWORDS: AIS data, Real ship, Hydrodynamic coefficient, Support vector regression, Parameter identification

ABSTRACT: *In response to the complexity and time demands of conventional methods for estimating the hydrodynamic coefficients, this study aims to revolutionize ship maneuvering analysis by utilizing automatic identification system (AIS) data and the Support Vector Regression (SVR) algorithm. The AIS data were collected and processed to remove outliers and impute missing values. The rate of turn (ROT), speed over ground (SOG), course over ground (COG) and heading (HDG) in AIS data were used to calculate the rudder angle and ship velocity components, which were then used as training data for a regression model. The accuracy and efficiency of the algorithm were validated by comparing SVR-based estimated hydrodynamic coefficients and the original hydrodynamic coefficients of the Mariner class vessel. The validated SVR algorithm was then applied to estimate the hydrodynamic coefficients for real ships using AIS data. The turning circle test was simulated from calculated hydrodynamic coefficients and compared with the AIS data. The research results demonstrate the effectiveness of the SVR model in accurately estimating the hydrodynamic coefficients from the AIS data. In conclusion, this study proposes the viability of employing SVR model and AIS data for accurately estimating the hydrodynamic coefficients. It offers a practical approach to ship maneuvering prediction and control in the maritime industry.*

1. Introduction

Estimating the hydrodynamic coefficients is crucial for understanding and analyzing the behavior of ships under various operating conditions. Traditionally, obtaining these coefficients requires extensive model tests or complex numerical simulations, which can be time-consuming, expensive, and limited to specific scenarios. On the other hand, with the advent of system identification (SI) and the advances in machine learning algorithms, it has become possible to estimate these coefficients using AIS data and SVR method. AIS data provides real-time information on the position, speed, course, and other relevant parameters of ships, making it a valuable resource for studying the dynamics of ships. SVR is a powerful machine learning technique that can capture complex relationships between input data and hydrodynamic coefficients.

Previous studies have explored various approaches for estimating the hydrodynamic coefficients using the support vector machine (SVM) algorithm. Luo and Zou (2009) employed the least square-SVM (LS-SVM) algorithm to estimate the hydrodynamic coefficients for the Mariner class vessel based on the turning circle simulation results.

Building on this work, Luo (2016) extended the research to KVLCC2, estimating hydrodynamic coefficients from free running model test results using LS-SVM. In another study, Liu et al. (2019) used the ε-SVM approach to estimate the hydrodynamic coefficients of the Mariner class vessel, employing combined simulation results from the turning circle test and zigzag test as training data. Mou et al. (2013) used the ridge regression algorithm to calculate the optimal value of the K and T indices in the Nomoto model using AIS data. Then, the rudder angle was estimated using the optimal values of the K and T indices and from the AIS data. Inazu et al. (2020) described the ship velocity obtained from AIS data into two components according to the ship heading: heading-normal and heading-parallel directions. The surge velocity and sway velocity were calculated using AIS data.

In this study, the linear-SVR algorithm was validated. This was achieved by simulating the turning circle test from the hydrodynamic coefficients of the Mariner class vessel. The linear-SVR algorithm was used to estimate the hydrodynamic coefficients based on the simulation results. The estimated coefficients were then compared with the original coefficients to validate the performance of the algorithm. Once the algorithm is validated, the hydrodynamic coefficient estimation of Silverway ship in AIS data is carried out, and the estimated coefficients are compared with the corresponding AIS data for further analysis and evaluation.

Received 23 June 2023, revised 9 August 2023, accepted 17 September 2023
Corresponding author Hyeon Kyu Yoon: +82-55-213-3683, hkyoon@changwon.ac.kr
This paper was presented at 20th Asian Conference on Maritime System and Safety Research (Vu et al., 2023).

2. Data Collection and Processing

The AIS data was collected through an open-source platform from the automatic identification system at the National University of Singapore. In this study, the data from October 2022 was selected as the study data. This dataset contains substantial information, including more than 7,371,647 data lines relating to more than 22,000 ships and marine vehicles. The AIS data is filtered based on the Maritime Mobile Service Identity (MMSI) number, so that data should be of good quality, with few errors or little missing data. For the purpose of this study, data associated with the MMSI number 636017059 was chosen. The principal dimensions of the ship are described in Table 1.

Table 1 Principal dimensions of Silverway ship

Item	Value
Length (m)	277.00
Breadth (m)	48.00
Depth (m)	23.10
Draft (m)	17.17
Displacement (t)	183261.00
Ship speed (m/s)	4.94

Fig. 1 shows the actual trajectory of the Silverway ship. To facilitate the estimation of the hydrodynamic coefficients, a small trajectory segment has been selected. This trajectory was a segment where the ship turned in a circle to starboard before reaching the mooring area. The selected trajectory segment is shown in Fig. 2.

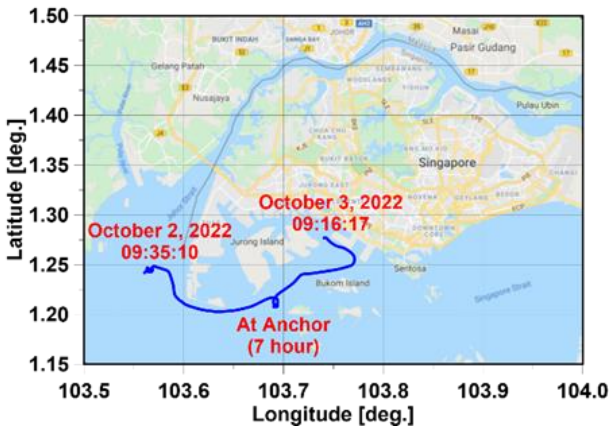

Fig. 1 Ship trajectory in the geographic coordinate system

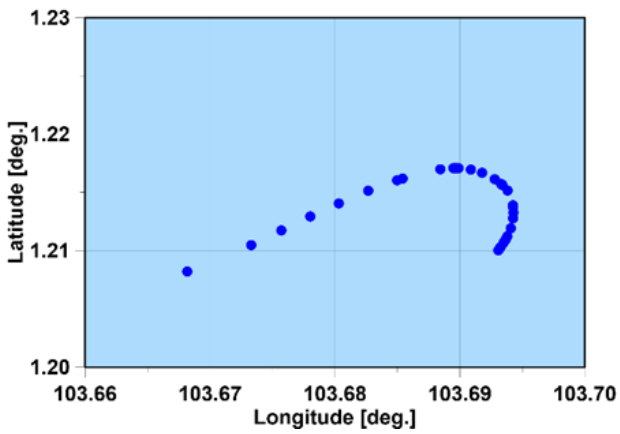

Fig. 2 Selected trajectory segment

AIS data includes data such as longitude, latitude, speed over ground (SOG), rate of turn (ROT), course over ground (COG) and heading angle (HDG). These are the data needed to initialize the training data. First, the conversion process involved converting the geographic coordinates of longitude and latitude in the World Geodetic 1984 (WGS84) system into the X and Y coordinates in the Universal Transverse Mercator (UTM) coordinate system. Second, Mou et al. (2013) calculated the rudder angle using AIS data. The rudder angle was calculated from ROT and HDG using Nomoto's model and Ridge regression method. The Nomoto's model can be expressed as Eq. (1).

$$T\dot{r} + r = K\delta \tag{1}$$

where $\dot{r}$ is the yaw angular acceleration, and r is the yaw rate. δ is the rudder angle. T is the time constant, and K is the proportionality constant.

Finally, Inazu et al. (2020) described the velocity and direction vectors of the ship. The surge and sway velocities are determined by SOG, COG and HDG as expressed in Eq. (2). The results of X and Y coordinates, rudder angle, surge velocity and sway velocity are shown in Figs. 3–6, respectively.

$$\begin{aligned} u &= SOG\cos(COG - HDG) \\ v &= SOG\sin(COG - HDG) \end{aligned} \tag{2}$$

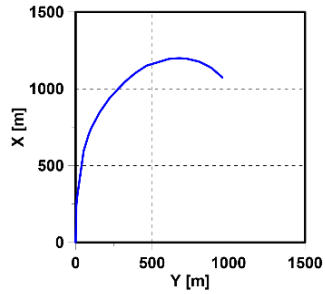

Fig. 3 Ship trajectory in the ship coordinate system

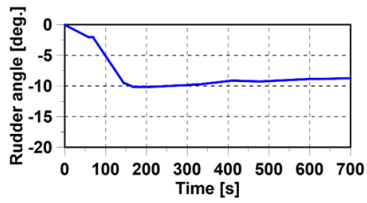

Fig. 4 Rudder angle result

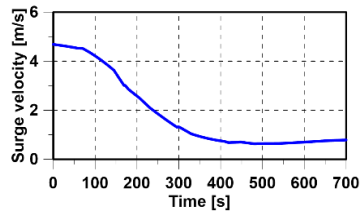

Fig. 5 Surge velocity result

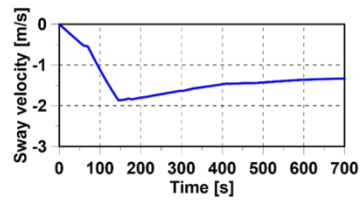

Fig. 6 Sway velocity result

The data measurement time in AIS data ranges from a few seconds to several tens of seconds because it depends on the speed and course alteration of a ship. Therefore, the linear interpolation method was applied to interpolate the missing points based on the time variable. The interval time selected for interpolation is 1 second to synchronize with the interval time in the hydrodynamic coefficient estimation algorithm and ship maneuvering simulation.

3. Methodology

3.1 Equation of Ship Maneuvering Motion

In ship maneuvering, the coordinate system fixed to the earth and the fixed coordinate system of the hull are applied. The Earth-fixed coordinate system $(O_0x_0y_0)$ has the origin as the position of the center of gravity of a ship at time t_0. The body-fixed coordinate system (Oxy) is assumed to be at the midship. The x_0-axis is set in the direction of the initial course of the ship, the y_0-axis points to the left, and the z_0-axis points up. While the x-axis points toward the bow, the y-axis points to starboard, and the z-axis points downwards. The angles between the directions of velocity V and the x-axis are defined as the drift angle β. The angles between the directions of the x_0-axis and x-axis are defined as the heading angles ψ. The coordinate systems in ship maneuvering are shown in Fig. 7.

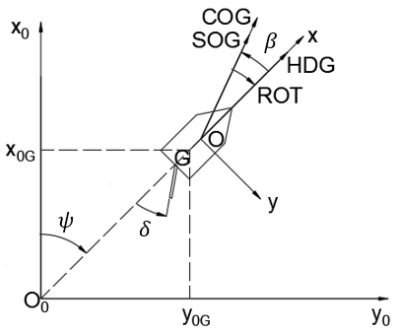

Fig. 7 Coordinate system in ship maneuvering

Abkowitz maneuver model in 3DOF is considered to describe the forces and moment acting on the ship. These motions are expressed as non-dimensional in Eq. (3).

$$\begin{aligned}&(m' - X'_{\dot{u}})\dot{u}' = f'_1\\&(m' - X'_{\dot{u}})\dot{v}' + (m'x'_G - Y'_{\dot{r}})\dot{r}' = f'_2\\&(m'x'_G - Y'_{\dot{r}})\dot{v}' + (I'_z - N'_{\dot{r}})\dot{r}' = f'_3\end{aligned} \tag{3}$$

where the superscript represents non-dimensional variables; m' is the ship mass; x'_G is the longitudinal center of gravity in the body-fixed coordinate system; I'_z is the inertia moment about the z-axis; $\dot{u}', \dot{v}'$ and $\dot{r}'$ are the accelerations in the x-axis, y-axis, and z-axis, respectively; $X'_{\dot{u}}$, $Y'_{\dot{v}}, Y'_{\dot{r}}, N'_{\dot{v}}$, and $N'_{\dot{r}}$ are the acceleration derivatives; f'_1 and f'_2 are forces in the x-axis and y-axis, respectively, and f'_3 is the moment about the z-axis. These forces and moment are displayed as functions of the kinematic parameters and rudder angle by applying the Taylor-series expansion extended to a third-order function, as expressed in Eq. (4).

$$\begin{aligned}f'_1 &= X'_u u' + X'_{uu}u'^2 + X'_{uuu}u'^3 + X'_{vv}v'^2 + X'_{\delta\delta}\delta^2\\&\quad + X'_{u\delta\delta}u'\delta + X'_{rv}r'v' + X'_{v\delta}v'\delta + X'_{v\delta u}v'\delta u'\\f'_2 &= Y'_v v' + Y'_r r' + Y'_{vvv}v'^3 + Y'_{vvr}v'^2 r'\\&\quad + Y'_{vu}v'u' + Y'_{ru}r'u' + Y'_\delta\delta + Y'_{\delta\delta\delta}\delta^3\\&\quad + Y'_{u\delta}u'\delta + Y'_{uu\delta}u'^2\delta + Y'_{v\delta\delta}v'\delta^2 + Y'_{vv\delta}v'^2\delta\\&\quad + Y'_0 + Y'_{0u}u' + Y'_{0uu}u'^2\\f'_3 &= N'_v v' + N'_r r' + N'_{vvv}v'^3 + N'_{vvr}v'^2 r'\\&\quad + N'_{vu}v'u' + N'_{ru}r'u' + N'_\delta\delta + N'_{\delta\delta\delta}\delta^3\\&\quad + N'_{u\delta}u'\delta + N'_{uu\delta}u'^2\delta + N'_{v\delta\delta}v'\delta^2 + N'_{vv\delta}v'^2\delta\\&\quad + N'_0 + N'_{0u}u' + N'_{0uu}u'^2\end{aligned} \tag{4}$$

where the non-dimensional variables are also defined as:

$$\begin{aligned}&m' = \frac{m}{0.5\rho L^3} \quad x'_G = \frac{x_G}{L} \quad I'_z = \frac{I_z}{0.5\rho L^5}\\&u' = \frac{u}{U} \quad v' = \frac{v}{U} \quad r' = \frac{Lr}{U} \quad \delta' = \delta\\&\dot{u}' = \frac{\dot{u}}{(U^2/L)} \quad \dot{v}' = \frac{\dot{v}}{(U^2/L)} \quad \dot{r}' = \frac{\dot{r}}{(U^2/L^2)}\\&X'_{\dot{u}} = \frac{X_{\dot{u}}}{0.5\rho L^3} \quad Y'_{\dot{v}} = \frac{Y_{\dot{v}}}{0.5\rho L^3} \quad Y'_{\dot{r}} = \frac{Y_{\dot{r}}}{0.5\rho L^4}\\&N'_{\dot{v}} = \frac{N_{\dot{v}}}{0.5\rho L^4} \quad N'_{\dot{r}} = \frac{N_{\dot{r}}}{0.5\rho L^5}\end{aligned}$$

3.2 Reconstruction of Ship Maneuvering Model

For the purpose of parameter identification, Eq. (3) is rewritten as Eq. (5). In Eq. (5), $S = (I'_z - N'_{\dot{r}})(m' - Y'_{\dot{v}}) - (m'x'_G - Y'_{\dot{r}})(m'x'_G - N'_{\dot{v}})$. Euler's stepping method was applied to calculate the value of the function at each point using a finite difference approximation of the derivative. h, k, and $k+1$ are the sampling interval and the indices of the two successive samplings, respectively. The acceleration terms of the motion equation can be described as Eq. (6).

$$\begin{aligned}&\dot{u}' = f'_1/(m' - X'_{\dot{u}})\\&\dot{v}' = [(I'_z - N'_{\dot{r}})f'_2 - (m'x'_G - Y'_{\dot{r}})f'_3]/S\\&\dot{r}' = [(m' - Y'_{\dot{v}})f'_3 - (m'x'_G - N'_{\dot{v}})f'_2]/S\end{aligned} \tag{5}$$

$$\begin{aligned}&\dot{u}(k) = [u(k+1) - u(k)]/h\\&\dot{v}(k) = [v(k+1) - v(k)]/h\\&\dot{r}(k) = [r(k+1) - r(k)]/h\end{aligned} \tag{6}$$

By combining Eqs. (5) and (6), the symbol vectors can be expressed as Eq. (7). Symbol vectors include variable vectors of *X*, *Y*, and *Z*, and coefficient vectors of *A*, *B*, and *C*. Variable vectors *X*, *Y*, and *Z* are the non-dimensional hydrodynamic derivatives of surge, sway, and yaw motions, respectively. The coefficient and variable vectors are expressed as Eq. (8) and Eq. (9), respectively.

$$\begin{aligned}&\Delta u(k+1) - \Delta u(k) = AX\\&\Delta v(k+1) - \Delta v(k) = BY\\&\Delta r(k+1) - \Delta r(k) = CZ\end{aligned} \tag{7}$$

$$\begin{aligned}&A = [a_1 \quad a_2 \quad \cdots \quad a_{10}]_{1\times 10}\\&B = [b_1 \quad b_2 \quad \cdots \quad b_{15}]_{1\times 15}\\&C = [c_1 \quad c_2 \quad \cdots \quad c_{15}]_{1\times 15}\end{aligned} \tag{8}$$

$$\begin{aligned}X &= [u(k)U(k), u^2(k), u^3(k)/U(k), v^2(k), r^2(k)L^2,\\&\quad \Delta\delta^2(k)U^2(k), \Delta u(k)\Delta\delta^2(k)U(k), \Delta v(k)\Delta r(k)L,\\&\quad \Delta v(k)\Delta\delta(k)U(k), \Delta v(k)\Delta\delta(k)\Delta u(k)]^T_{10\times 1}\\Y &= N = [\Delta v(k)U(k), \Delta r(k)U(k)L, \Delta v^3(k)/U(k),\\&\quad \Delta v^2(k)\Delta r(k)L/U(k), \Delta v(k)\Delta u(k), \Delta r(k)\Delta u(k),\\&\quad \Delta\delta(k)U^2(k), \Delta\delta^3(k)U^2(k), \Delta u(k)\Delta\delta(k)U(k),\\&\quad \Delta u^2(k)\Delta\delta(k), \Delta v(k)\Delta\delta^2(k)U(k), \Delta v^2(k)\Delta\delta(k),\\&\quad U^2(k), \Delta u(k)U(k), \Delta u^2(k)]^T_{15\times 1}\end{aligned} \tag{9}$$

For example, the longitudinal hydrodynamic coefficient X'_u is defined using Eq. (10). This equation was also applied to determine the other hydrodynamic coefficients of the surge equation.

$$a_1 = \frac{h}{L(m' - X'_{\dot{u}})} X'_u \Rightarrow X'_u = \frac{a_1 L(m' - X'_{\dot{u}})}{h} \tag{10}$$

The same method is used to estimate the hydrodynamic coefficients of sway and yaw equations. A series of equations and matrices need to be solved to determine the hydrodynamic coefficients of sway and yaw. For example, the hydrodynamic coefficients Y'_v and N'_v are obtained by solving Eq. (11). The other hydrodynamic coefficients of the sway and yaw equation are also obtained similarly.

$$\begin{bmatrix} \frac{h(I'_z - N'_{\dot{r}})}{SL} & -\frac{h(m'x'_G - Y'_{\dot{r}})}{SL} \\ -\frac{h(m'x'_G - N'_{\dot{v}})}{SL^2} & \frac{h(m' - Y'_{\dot{v}})}{SL^2} \end{bmatrix} \begin{bmatrix} Y'_v \\ N'_v \end{bmatrix} = \begin{bmatrix} b_1 \\ c_1 \end{bmatrix} \tag{11}$$

The five acceleration derivatives $X'_{\dot{u}}$, $Y'_{\dot{v}}$, $Y'_{\dot{r}}$, $N'_{\dot{v}}$, and $N'_{\dot{r}}$ of the KVLCC2 are well documented in the literature and are used widely as benchmark values for estimating the hydrodynamic coefficients of other ships of the same type and size ratio (Ho et al., 2021). This study assumed five derivatives of the acceleration of KVLCC2 to estimate the hydrodynamic coefficients of the Silverway ship. The values of these coefficients were: $X'_{\dot{u}} = -0.001135$, $Y'_{\dot{v}} = -0.014508$, $Y'_{\dot{r}} = -0.001209$, $N'_{\dot{v}} = -0.000588$, and $N'_{\dot{r}} = -0.000564$.

3.3 Support Vector Regression

SVR has a general approximation function for a multi-input/single-output (MISO) system:

$$\begin{aligned} &f(x_i) = w^T \Phi(x_i) + b \\ &(x_i \in \mathbb{R}^M, \Phi(x_i) \in \mathbb{R}^N, w \in \mathbb{R}^N) \end{aligned} \tag{12}$$

where $f(x_i)$ is the scalar output; w is the weight matrix; b is the bias; x_i is the input vector; $\mathbb{R}^n$ is the n-dimensional feature space, and $\Phi(x_i)$ is a linear or non-linear and refers to the high-dimensional feature space $\mathbb{R}^N$ $(N \gg M)$. In SVR, the regression issue is viewed as an optimization problem in the primal formula subject to an objective function and constraint formula, as expressed in Eqs. (13) and (14), respectively.

$$J(w, \xi_i, \xi_i^*) = \frac{1}{2} w^T w + C \sum_{i=1}^{N} (\xi_i + \xi_i^*) \tag{13}$$

$$\left.\begin{aligned} y_i - [w^T \Phi(x_i) + b] \le \varepsilon + \xi_i \ \ \forall i \\ [w^T \Phi(x_i) + b] - y_i \le \varepsilon + \xi_i^* \ \ \forall i \\ \xi_i, \xi_i^* \ge 0 \ \ \forall i \end{aligned}\right\} \tag{14}$$

where C is called the regularization parameter. This parameter is always positive, which is designed to control the trade-off between empirical error and model complexity. ξ and ξ^* are the slack variables. It defines the upper limit of regression errors until the constraints are still satisfied. In Eq. (14), y and ε are the desired output and an insensitivity factor, respectively. The loss quantification is determined by the distance between the boundary ε and the observed value y shown in Eq. (15).

$$L_e = \begin{cases} 0 & if\ |f(x) - y| \le \varepsilon \\ |f(x) - y| - \varepsilon & otherwise \end{cases} \tag{15}$$

By using the Karush-Kuhn-Tucker (KKT) theorem and Lagrange dual formulation, Lagrange multiples α_n and α_n^* are included for each observation $\Phi(x_n)$. This can obtain the dual formula Eq. (16) such that it is minimized and subject to the constraint formula Eq. (17).

$$\begin{aligned} Q(\alpha, \alpha^*) = \frac{1}{2} \sum_{i=1}^{N} \sum_{j=1}^{N} (\alpha_i - \alpha_i^*)(\alpha_j - \alpha_j^*) \Phi^T(x_i) \Phi(x_j) \\ + \varepsilon \sum_{i=1}^{N} (\alpha_i + \alpha_i^*) - \sum_{i=1}^{N} y_i (\alpha_i - \alpha_i^*) \end{aligned} \tag{16}$$

$$\begin{aligned} &\sum_{i=1}^{N} (\alpha_i - \alpha_i^*) = 0 \\ &0 \le \alpha_i \le C \ \ \forall i \\ &0 \le \alpha_i^* \le C \ \ \forall i \end{aligned} \tag{17}$$

The optimal hyperplane can be obtained as Eq. (18) to predict new values depending only on the support vectors:

$$f(x_j) = \sum_{i=1}^{N} (\alpha_i - \alpha_i^*) [\Phi^T(x_i) \Phi(x_j)] + b \tag{18}$$

The w and b parameters can be described entirely as a linear combination using a linear kernel:

$$w = \sum_{i=1}^{N} (\alpha_i - \alpha_i^*)\, x_i^T \tag{19}$$

$$b = \overline{y_j - \sum_{i=1}^{N} (\alpha_i - \alpha_i^*) x_i^T x_j - \varepsilon sign(\alpha_i - \alpha_i^*)} \tag{20}$$

where the dash on top of Eq. (20) and N refer to the mean value and the total number of support vectors.

4. Result

4.1 Algorithm Validation

Validating the accuracy and performance of the SVR algorithm is done by estimating the hydrodynamic coefficients of the Mariner class vessel. Fossen (1994) described these coefficients in the Abkowitz model. These coefficients were applied to simulate the turning circle test at a rudder angle of 10°. The simulation results were used as training data for the SVR model. Luo and Zou (2009) and Luo (2016) referred to the multicollinearity and parameter drift phenomenon. The hydrodynamic coefficients may be inaccurate or worse, even if the simulation results match well with the target results. A proposed solution to reduce these two phenomena is to add Gaussian noise to the training data. Applying the SVR algorithm and Gaussian noise, the hydrodynamic coefficients are estimated and compared with the original hydrodynamic coefficients. The ship parameters and simulated conditions are described in Table 2. The results of hydrodynamic coefficients are shown in Tables 3–5.

The turning circle test was simulated from the estimated hydrodynamic coefficients and compared with the original simulation results in Fig. 8. The deviations between the estimated hydrodynamic coefficients and the original hydrodynamic coefficients are very low. Therefore, they matched the training data and the regression model well.

In addition, the SVR algorithm is well-validated. In addition, the SVR algorithm is well-validated. Of the 40 hydrodynamic coefficients for the surge, sway and yaw equation, the $Y'_{v\delta\delta}, Y'_{0uu}, N'_{vvv}, N'_{vv\delta}$ and N'_{0u} coefficients were 10% higher. Although this difference was relatively large, the values of these coefficients were small so they are acceptable.

Table 2 Parameters and test condition of the Mariner class vessel

Item	Symbol	Value
Length between perpendiculars (m)	L_{pp}	160.93
Design speed (m/s)	U_o	7.97
Non-dimensional mass of ship (-)	m'	798E-05
Non-dimensional moment of inertia (-)	I_z'	39.2E-05
Non-dimensional longitudinal coordinate of	x_G'	–0.023
Maximum rudder angle (°)	-	10
Turning rate of rudder (°/s)	-	5
Total simulation time (s)	-	1000

Table 3 Hydrodynamic coefficients for the surge equation (Mariner class vessel)

Hydrodynamic	Original	Estimated	Deviation (%)
X'_u	–1.84E-03	–1.84E-03	0.00
X'_{uu}	–1.10E-03	–1.09E-03	–0.91
X'_{uuu}	–2.15E-03	–2.12E-03	–1.40
X'_{vv}	–8.99E-03	–8.99E-03	0.00
X'_{rr}	1.80E-04	1.80E-04	0.00
$X'_{\delta\delta}$	–9.50E-04	–9.50E-04	0.00
$X'_{u\delta\delta}$	–1.90E-03	–1.90E-03	0.00
X'_{rv}	7.98E-03	7.98E-03	0.00
$X'_{v\delta}$	9.30E-04	9.30E-04	0.00
$X'_{uv\delta}$	9.30E-04	9.30E-04	0.00

Table 4 Hydrodynamic coefficients for the sway equation (Mariner class vessel)

Hydrodynamic	Original	Estimated	Deviation (%)
Y'_v	–1.16E-02	–1.16E-02	0.00
Y'_r	–4.99E-03	–4.98E-03	–0.20
Y'_{vvv}	–8.08E-02	–8.23E-02	1.86
Y'_{vvr}	1.54E-01	1.53E-01	–0.65
Y'_{vu}	–1.16E-02	–1.17E-02	0.86
Y'_{ru}	–4.99E-03	–5.05E-03	1.20
Y'_δ	2.78E-03	2.78E-03	0.00
$Y'_{\delta\delta\delta}$	–9.00E-04	–9.00E-04	0.00
$Y'_{u\delta}$	5.56E-03	5.53E-03	–0.54
$Y'_{uu\delta}$	2.78E-03	2.71E-03	–2.52
$Y'_{v\delta\delta}$	–4.00E-05	–3.00E-05	–25.00
$Y'_{vv\delta}$	1.19E-02	1.15E-02	–3.36
Y'_0	–4.00E-05	–4.00E-05	0.00
Y'_{0u}	–8.00E-05	–8.00E-05	0.00
Y'_{0uu}	–4.00E-05	–2.00E-05	–50.00

Table 5 Hydrodynamic coefficients for the yaw equation (Mariner class vessel)

Hydrodynamic	Original	Estimated	Deviation (%)
N'_v	–2.64E-03	–2.65E-03	0.38
N'_r	–1.66E-03	–1.67E-03	0.60
N'_{vvv}	1.64E-02	1.82E-02	10.98
N'_{vvr}	–5.48E-02	–5.37E-02	–2.01
N'_{vu}	–2.64E-03	–2.50E-03	–5.30
N'_{ru}	–1.66E-03	–1.59E-03	–4.22
N'_δ	–1.39E-03	–1.39E-03	0.00
$N'_{\delta\delta\delta}$	4.50E-04	4.50E-04	0.00
$N'_{u\delta}$	–2.78E-03	–2.74E-03	–1.44
$N'_{uu\delta}$	–1.39E-03	–1.31E-03	–5.76
$N'_{v\delta\delta}$	1.30E-04	1.20E-04	–7.69
$N'_{vv\delta}$	–4.89E-03	–4.36E-03	–10.84
N'_0	3.00E-05	3.00E-05	0.00
N'_{0u}	6.00E-05	5.00E-05	–16.67
N'_{0uu}	3.00E-05	3.00E-05	0.00

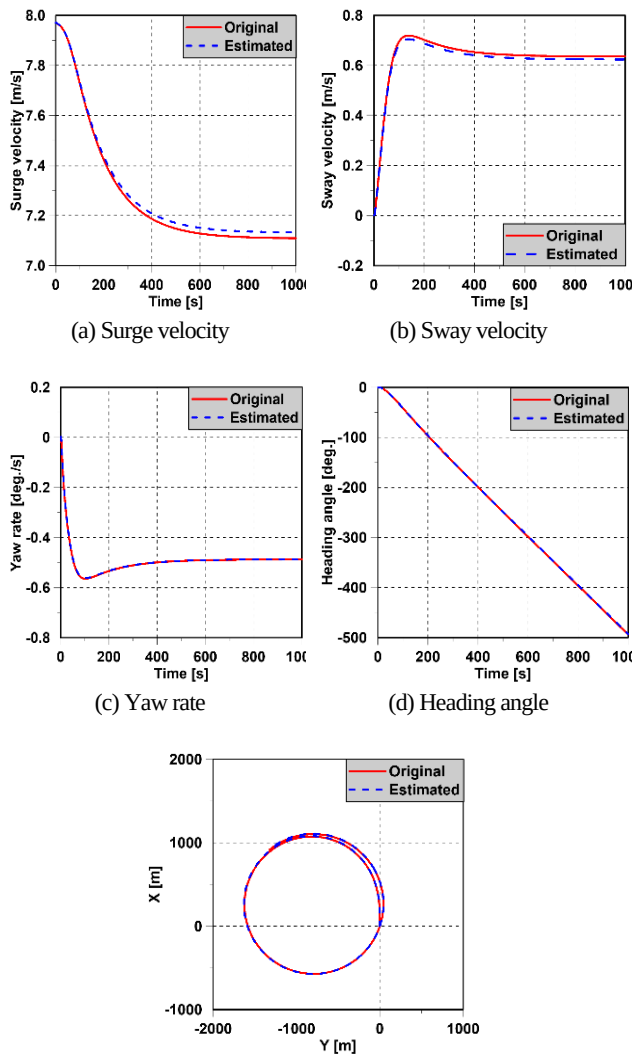

(a) Surge velocity (b) Sway velocity

(c) Yaw rate (d) Heading angle

(e) 10° port turning trajectory

Fig. 8 Comparison of the simulation motions (Mariner class vessel)

4.2 Hydrodynamic Coefficients of Silverway Ship in AIS Data

After validating the SVR algorithm, the hydrodynamic coefficients of the Silverway ship in AIS data are estimated. In this case, Gaussian noise is not considered because Luo (2016) suggested that this method is unsuitable for AIS data. Ship parameters and simulated conditions are shown in Table 6. This simulation condition is established based on the calculation results of the rudder angle from the AIS data. The time required for the rudder angle to change from 0° to approximately 10° was approximately 163 seconds. Therefore, the maximum rudder angle derivative is defined as 0.06°/s.

The result of the hydrodynamic coefficients for the surge, sway and yaw equations are shown in Tables 7 and 8. AIS data typically represents real-world ship movements and provides a reference for evaluating the accuracy and validity of the simulation results. When comparing the simulation results with AIS data, the goal was that the simulated trajectories closely match the observed ship movements. Therefore, the turning circle test was simulated from estimated hydrodynamic coefficients and compared with the AIS data in Fig. 9. Generally, the simulation results from the estimated hydrodynamic coefficients were in good agreement with the AIS data. Therefore, the estimated hydrodynamic coefficients are reliable. Moreover, the SVR algorithm is also successfully applied to AIS data.

Table 6 Parameters and test condition of Silverway

Item	Symbol	Value
Length (m)	L	277
Design speed (m/s)	U_o	4.68
Non-dimensional mass of ship (-)	m'	1.68E-02
Non-dimensional moment of inertia (-)	I_z'	9.65E-14
Non-dimensional longitudinal coordinate of	x_G'	–0.035
Maximum rudder angle (°)	-	10
Turning rate of rudder (°/s)	-	0.06
Total simulation time (s)	-	700

Table 7 Hydrodynamic coefficients for surge equation (Silverway)

Hydrodynamic	Estimated	Hydrodynamic	Estimated
X'_u	–1.01E-03	$X'_{\delta\delta}$	–2.95E-03
X'_{uu}	1.87E-03	$X'_{u\delta\delta}$	–1.10E-04
X'_{uuu}	–5.00E-04	X'_{rv}	6.45E-03
X'_{vv}	–2.47E-02	$X'_{v\delta}$	–8.09E-03
X'_{rr}	8.30E-04	$X'_{uv\delta}$	–3.87E-03

Table 8 Hydrodynamic coefficients for the sway and yaw equation (Silverway)

Hydrodynamic	Estimated	Hydrodynamic	Estimated
Y'_v	–9.40E-04	N'_v	–5.00E-04
Y'_r	7.50E-04	N'_r	–1.40E-04
Y'_{vvv}	–8.00E-04	N'_{vvv}	4.40E-04
Y'_{vvr}	8.40E-04	N'_{vvr}	–2.50E-04
Y'_{vu}	3.20E-03	N'_{vu}	1.00E-05
Y'_{ru}	–2.85E-03	N'_{ru}	–1.90E-04
Y'_δ	6.20E-04	N'_δ	1.00E-05
$Y'_{\delta\delta\delta}$	7.00E-05	$N'_{\delta\delta\delta}$	5.00E-05
$Y'_{u\delta}$	1.09E-03	$N'_{u\delta}$	–1.60E-04
$Y'_{uu\delta}$	–5.00E-05	$N'_{uu\delta}$	–1.20E-04
$Y'_{v\delta\delta}$	9.00E-05	$N'_{v\delta\delta}$	1.30E-04
$Y'_{vv\delta}$	–6.00E-05	$N'_{vv\delta}$	2.60E-04
Y'_0	–6.28E-03	N'_0	–2.30E-04
Y'_{0u}	–6.33E-03	N'_{0u}	–1.50E-04
Y'_{0uu}	–3.36E-03	N'_{0uu}	–4.00E-05

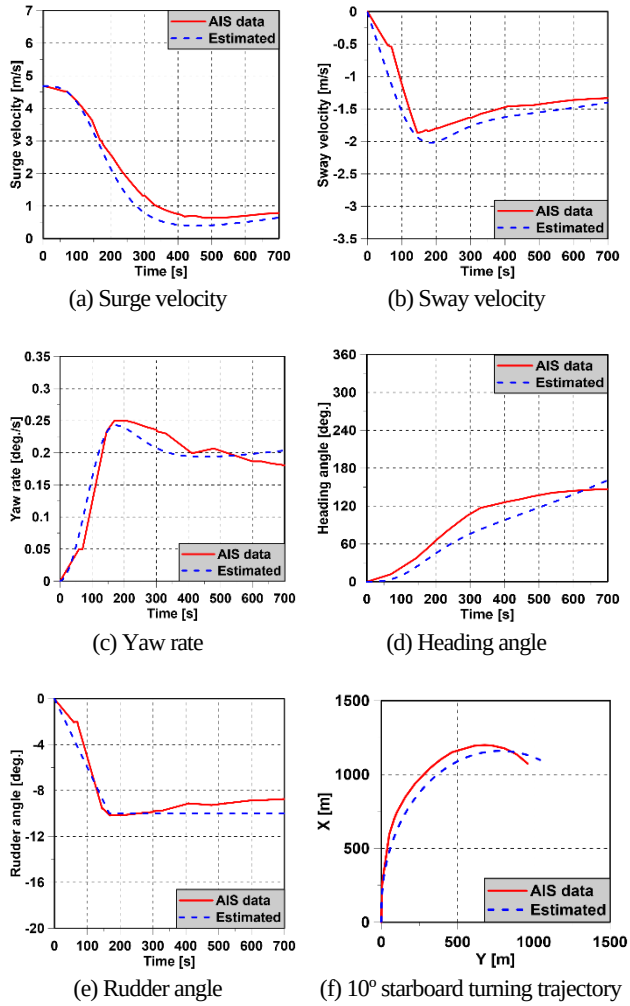

(a) Surge velocity (b) Sway velocity (c) Yaw rate (d) Heading angle (e) Rudder angle (f) 10° starboard turning trajectory

Fig. 9 Comparison of the simulation motions (Silverway)

5. Conclusions

In conclusion, this study aimed to estimate the hydrodynamic coefficients of Silverway ship in AIS data using the Linear SVR model. The study used the simulation results of the maneuvers of the Mariner class vessel to validate the accuracy and suitability of the estimated hydrodynamic coefficients.

First, the collection and conversion of AIS data into a usable form have been successfully accomplished for the purpose of hydrodynamic coefficient estimation. The transformed AIS data provides valuable information on vessel identification, position, speed, and course, which is essential for further analysis and modeling in ship maneuvering studies.

Secondly, the SVR algorithm is validated by estimating hydrodynamic coefficients using the Mariner class vessel simulation results. When applying the method of adding Gaussian noise to reduce the

multicollinearity and parameter drift phenomena, the estimated hydrodynamic coefficients matched well with the original coefficients. This demonstrated the accuracy and efficiency of the SVR algorithm. In addition, it confirmed the suitability of adding Gaussian noise to the results of ship maneuvering simulations.

Finally, the hydrodynamic coefficients of Silverway ship in AIS data were estimated using the validated SVR algorithm. The results show that the estimated hydrodynamic coefficients and the simulated movements are in good agreement with the AIS data. Therefore, it is possible to apply the SVR model to AIS data.

Conflict of Interest

Hyeon Kyu Yoon serves as a journal publication committee member of the Journal of Ocean Engineering and Technology, but he had no role in the decision to publish this article. No potential conflict of interest relevant to this article was reported.

Funding

This research was supported by the “Development of Autonomous Ship Technology (PJT201313, Development of Autonomous Navigation System with Intelligent Route Planning Function)” funded by the Ministry of Oceans and Fisheries (MOF, Korea).

References

Fossen, T. I. (1994). *Guidance and Control of Ocean Vehicle*s. A John Wiley and Sons, Ltd., Publication.

Ho, Y., Song, L., Liu, Z., & Yao, J. (2021). Identification of ship hydrodynamic derivatives based on LS-SVM with wavelet threshold denoising. *Journal of Marine Science and Engineering (JMSE)*, *9*(12), 1356. https://doi.org/10.3390/jmse9121356

Inazu, D., Ikeya, T., Iseki, T., & Waseda, T. (2020). Extracting clearer tsunami currents from shipborne automatic identification system data using ship yaw and equation of ship response. *Earth, Planets and Space Journal*, *72*, 41. https://doi.org/10.1186/s40623-020-01165-7

Liu, B., Jin, Y., Magee, A. R., Yiew, L. J., & Zhang, S. (2019). System identification of abkowitz model for ship maneuvering motion based on ε-support vector regression. *The ASME 2019 38th International Conference on Ocean, Offshore & Arctic Engineering (OMAE2019)*, OMAE2019-96699. https://doi.org/10.1115/OMAE2019-96699

Luo, W. L., & Zou, Z. J. (2009). Parametric identification of ship maneuvering models by using support vector machines. *Journal of Ship Research*, *53*(1), 19–30, https://doi.org/10.5957/jsr.2009.53.1.19

Luo, W. L. (2016). Parameter identifiability of ship maneuvering modeling using system identification. *Mathematical Problems in Engineering Journal*, *2016*, 8909170. https://doi.org/10.1155/2016/8909170

Mou, J. M., Tang, G. H., Rong, H., & Yue, X. (2013). Predict manoeuvring indices using AIS data by ridge regression. *Scientific Journals of Maritime University of Szczecin*, *36*(108), 137–142. https://bibliotekanauki.pl/articles/359863.pdf

Vu, H. T., Park, J., & Yoon, H. K. (2023) An Application of Support Vector Machine to Estimate Hydrodynamic Coefficient using AIS Data. In *20th Asian Conference on Maritime System and Safety Research. ACMSSR*.

Author ORCID

Author name	ORCID
Vu, Hoang Thien	0000-0001-8147-0597
Park, Jongyeol	0000-0003-4931-1339
Yoon, Hyeon Kyu	0000-0001-6639-0927

Journal of Ocean Engineering and Technology 37(5), 205-214, October, 2023
https://doi.org/10.26748/KSOE.2023.022
pISSN 1225-0767
eISSN 2287-6715

Original Research Article

Study on Stiffened-Plate Structure Response in Marine Nuclear Reactor Operation Environment

Han Koo Jeong[1], Soo Hyoung Kim[2] and Seon Pyoung Hwang[3]

[1]Professor, Department of Naval Architecture and Ocean Engineering, Kunsan National University, Gunsan, Korea
[2]Principal Researcher, Innovative SMR Development Division, Korea Atomic Energy Research Institute, Daejeon, Korea
[3]Graduate Student, Naval Architecture and Ocean Engineering, Kunsan National University, Gunsan, Korea

KEYWORDS: Finite element analysis, Marine nuclear reactor operation, Material property variation, Neutron irradiation, Stiffened plated structure, Structural Responses

ABSTRACT: *As the regulations on greenhouse gas emissions at sea become strict, efforts are being made to minimize environmental pollutants emitted from fossil fuels used by ships. Considering the large sizes of ships in conjunction with securing stable supplies of environment-friendly energy, interest in nuclear energy to power ships has been increasing. In this study, the neutron irradiation that occurs during the nuclear reactor operation and its effect on the structural responses of the stiffened-plate structures are investigated. This is done by changing the material properties of DH36 steel according to the research findings on the neutron-irradiated steels and then performing the structural response analyses of the structures using analytical and finite-element numerical solutions. Results reveal the influence of neutron irradiation on the structural responses of the structures. It is shown that both the strength and stiffness of the structures are affected by the neutron-irradiation phenomenon as their maximum flexural stress and deflection are increased with the increase in the amount of neutron irradiation. This implies that strength and stiffness need to be considered in the design of ships equipped with marine nuclear reactors.*

Nomenclature

a_{mn}	General coefficient
b	Breadth of a rectangular grillage plate
E	Elastic modulus
I_r	Moment of inertia of longitudinal stiffeners
I_s	Moment of inertia of transverse stiffeners
l	Length of a rectangular grillage plate
m, n	Wave numbers
P	Load per unit area on a rectangular grillage plate
r	Number of longitudianl stiffeners
s	Number of transverse stiffeners
w	Deflection of a rectangular grillage plate
ν	Poisson's ratio
σ_{allow}	Allowable stress

1. Introduction

With the increasing importance of ocean environments, the International Maritime Organization (IMO) is strengthening regulations on greenhouse gas emissions at sea, such as by adopting the 2023 IMO Greenhouse Gas Strategy to achieve carbon neutrality in international shipping by 2050. To achieve this, technologies are being actively developed to minimize environmental pollutants emitted from ships using fossil fuels, alongside efforts to use eco-friendly renewable energy to power ships. However, the stability of renewable energy supply is limited, and the generation costs are high. Considering the increasing size of super-large ships, large amounts of energy are needed. Consequently, there is a growing interest in nuclear energy as an alternative energy source for ship operations.

While ships powered by fossil fuels have established systematic design rules based on abundant design and operating experience, for ships using nuclear energy for propulsion, it is difficult to find domestically driven design examples. Therefore, it is necessary to prioritize research on developing technology that converges nuclear and shipbuilding industries for future ship design using shipboard reactors.

Most studies on applying nuclear propulsion systems to ships deal

Received 31 July 2023, revised 13 August 2023, accepted 14 August 2023
Corresponding author Han Koo Jeong: +82-63-469-1853, hkjeong@kunsan.ac.kr

with the selection of ship types that can increase the efficiency of reactor installation using economic analysis, or concepts related to the placement of nuclear propulsion systems within the hull based on risk assessment. Gravina et al. (2013) proposed the concept of a modular vessel composed of a propulsion module with a reactor and a cargo hold module for cargo loading, and conducted research on its application to large container ships. Gil et al. (2014) performed an economic analysis for various dedicated cargo ships, selected container ships as the target ships for reactor installation, and investigated the optimal placement of the reactor system in the engine room compartment within the hull. In similar research based on risk assessment associated with reactor operation, Hirdaris et al. (2014) conducted a conceptual design study applying a small modular reactor (SMR) to a Suezmax tanker. Meanwhile, research on marine nuclear power generation using reactors has also been conducted. Lee et al. (2015) investigated structural platforms at sea where reactors are installed, and extensively researched the types, sizes, and placement methods of the reactors to be applied to them, as well as the cooling system and other components.

It is evident that the focus of the selected literature differs from the focus of this study—the influence of the operating environment of the reactor on the surrounding structures within a vessel once installed inside the vessel. Therefore, from the perspective of the structural design of the vessel, we first analyzed the operating environment of the reactor installed on the ship as part of the development of convergence technology between the nuclear and shipbuilding industries. This study focused on changes in material properties of the hull structural steel due to neutron irradiation—which is not considered in conventional fossil fuel-based ship design—and its impact on the responses of internal structural components where the reactor is installed.

In nuclear operating environments, steel is exposed to neutron energy, creating defects such as those resulting from the generation of knock-on atoms from the lattice atoms that make up the steel structural material. The generated knock-on atoms move within the lattice, causing other atoms to be knocked out and producing a chain reaction that leads to the creation of numerous knock-on atoms (Knaster et al., 2016). This ultimately changes the mechanical properties of the steel, leading to phenomena revealed in related research such as radiation hardening and embrittlement (Hong, 2012). The tensile strength of steel exposed to continuous neutron irradiation during reactor operation has been found to increase, while the maximum absorbed energy and fracture toughness are reduced, as proved by Charpy notch impact tests. These characteristics of the neutron-irradiated steel are connected to a reduction in the elastic modulus and Poisson's ratio (Ahn et al., 2002). Therefore, the structures inside the containment of the hull where the reactor is installed will be affected by such changes in steel properties due to neutron energy. Consequently, they will show different structural responses compared to similar structures of a fossil-fuel-based propulsion system inside the hull. This is an important consideration for structural designers.

We used DH36 high-strength steel—a representative shipbuilding and marine steel for stiffened-plate structures—as an example of the material constituting the structure around the reactor of the ship exposed to neutron irradiation. The extent of the changes in the properties of the DH36 steel irradiated with neutrons was determined using experimental data and theoretical estimates of neutron-irradiated steel used in terrestrial reactor facilities (Straalsund and Day, 1973). Through this, we derived scenarios with varying properties of DH36 steel such as elastic modulus, Poisson's ratio, and allowable stress values. The structural response analysis of the configured DH36 steel-based stiffened plate was performed using the grillage-structure theory and finite-element analysis methods, calculating the load-bearing capacity, strength, deflection values, etc., against transverse loads assuming the support load of the reactor of the ship. Through this, we quantitatively analyzed the impact of neutron irradiation occurring in the reactor operating environment on the structural responses of the hull structure.

2. Material Property Variation of Hull Steel due to the Neutron-Irradiation Phenomenon

According to studies on neutron-irradiated steel of terrestrial nuclear power plants, the stress-strain curve of irradiated steel shows a different correlation from that of non-irradiated steel (Jhung et al.,

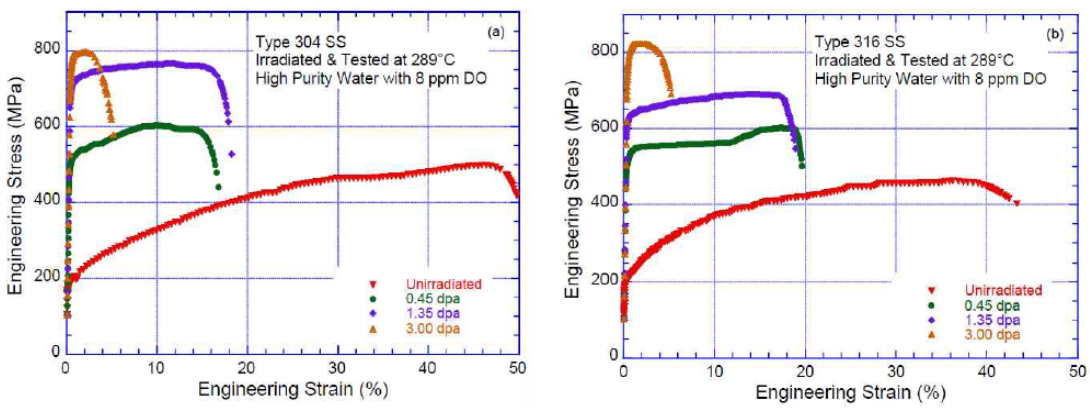

(a) (b)

Fig. 1 Stress-strain curves of neutron-irradiated stainless steel (Jhung et al., 2013): (a) Type 304 SS and (b) Type 316 SS

2013). Fig. 1 shows the nominal stress–nominal strain curves of Type 304 and Type 316 stainless steel subjected to various neutron-irradiation amounts ranging from 0.45 to 3 dpa (displacements per atom). As the neutron irradiation increases, the tensile strength and yield stress of the steel increase, while the ductility decreases. The hardening and embrittlement of steel due to neutron irradiation becomes more evident when comparing the nominal stress–nominal strain curves of non-irradiated and irradiated steel. Although not shown in Fig. 1, studies report that the yield stress of irradiated steel at about five dpa is up to five times higher than that of non-irradiated steel (Jhung et al., 2013).

Straalsund and Day (1973) used ultrasonic techniques to measure the changes in elastic modulus and Poisson's ratio of neutron-irradiated Type 304 stainless steel, and theoretically predicted the rate of change in these material properties as upper and lower bounds. In their theoretical predictions, they calculated the reduction rates of the elastic modulus and Poisson's ratio as functions of void volume, ranging from a minimum of 1% to a maximum of 10%. The experimentally determined and theoretically estimated changes in the elastic modulus and Poisson's ratio for neutron-irradiated Type 304 stainless steel closely matched. This implies that as the neutron irradiation increases, the void volume fraction increases, while the elastic modulus and Poisson's ratio decrease. The authors concluded that applying these results is feasible for structural steel with different crystal structures (body-centered cubic (BCC) and face-centered cubic (FCC)), where the void volume changes due to neutron irradiation. Additionally, Hong (2012) found that the increase in tensile strength and embrittlement phenomenon was stronger in the neutron-exposed BCC and FCC crystalline structured steel than in the non-irradiated identical steel, by simultaneously comparing the nominal stress–nominal strain curves of the irradiated two types of steel.

In this study, the stiffened-plate structure inside the hull containment structure used as an example was assumed to be located outside the reactor pressure vessel and subjected to a relatively low level of neutron irradiation, corresponding to the initial stage of void volume fraction. Based on the research results of Straalsund and Day (1973) and other preceding studies on neutron-irradiated steel (Ahn et al., 2002; Hong, 2012; Jhung et al., 2013), we investigated the rates of change of the elastic modulus, Poisson's ratio, and allowable stress of DH36 steel as the material property variation scenarios, as shown in Table 1.

Where, MPC_0 represents the properties of non-irradiated DH36 steel with a density of 7,850 kg/m³ (Korean Register, 2020; RMRS, 2018), and MPC_1 to MPC_6 show the changes in material properties at void volume fractions ranging from 1% to 3%. The reduction rates of the elastic modulus were 2%, 4%, and 6%, and those of Poisson's ratio were 0.4%, 0.7%, and 1%, respectively. The changes in the allowable stress of neutron-irradiated DH36 steel were only considered for MPC_4 to MPC_6; these were increased by 25%, 50%, and 100%, respectively.

Table 1 Material property variation scenarios of DH36 HTS steel

% Void volume	Elastic modulus (GPa)		Poisson's ratio		Allowable stress (MPa)	
	E	% change	ν	% change	σ_{allow}	% change
0% (MPC_0)	200	0	0.290	0.0	355.0	0
1% (MPC_1)	196	-2	0.289	-0.4	355.0	0
2% (MPC_2)	192	-4	0.288	-0.7	355.0	0
3% (MPC_3)	188	-6	0.287	-1.0	355.0	0
1% (MPC_4)	196	-2	0.289	-0.4	443.8	+25
2% (MPC_5)	192	-4	0.288	-0.7	532.5	+50
3% (MPC_6)	188	-6	0.287	-1.0	710.0	+100

3. Stiffened-Plate Structures and Their Analytical and Numerical Solutions

The details of the stiffened-plate structures inside the hull containment structure, previously mentioned as the example, were determined by referring to the stiffened plate used in related studies (Kõrgesaar et al., 2018; Nam, 2019). The referenced stiffening plate meets the buckling requirements of FSICR (2008) and IACS (2016) and is composed of flat bars, web frames, and stringers. Based on the above, two stiffened-plate structures named Case A and Case B were considered, both of which commonly employ multiple Tee-section steel stiffeners in the transverse and longitudinal directions. Regarding their differences, the stiffened-plate structure of Case A had the same dimensions for both transverse and longitudinal stiffeners, while the stiffened-plate structure of Case B had different dimensions for the transverse and longitudinal stiffeners. The specifications of the two stiffened-plate structures are shown in Table 2; the dimensions of the stiffeners are denoted in the order of web thickness × web height × flange thickness × flange width.

Table 2 Structural details of Cases A and B stiffened-plate structures with 3×7 stiffeners

Specifications	Stiffened-plate structures	
	Case A	Case B
Frame spacing trans. (mm)	625	625
Frame spacing long. (mm)	1,000	1,000
No. of trans. stiffeners	7	7
No. of long. stiffeners	3	3
Plate thickness (mm)	13	13
Trans. stiffener dimensions (mm)	9×227×11×50	9×227×11×50
Long. stiffener dimensions (mm)	9×227×11×50	10×365×12×55
Frame weight (kg/m)	20.15	24.75
Panel weight (kg/m^2)	102.05	102.05
Total weight (t)	2.91	3.11

3.1 Analytical Solutions for Laterally Loaded Flat Grillage Plates

As shown in Fig. 2, we consider a simply supported stiffened-plate structure with s evenly spaced stiffeners in the length direction l, and r evenly spaced stiffeners in the width direction b. The moment of inertia for the longitudinal stiffeners is I_r, and that for the transverse stiffeners is I_s. If the deflection in the x, y plane of the stiffened-plate structure caused by the bending load is denoted by w, the deflection curve of the stiffened-plate structure can be obtained using the following equation.

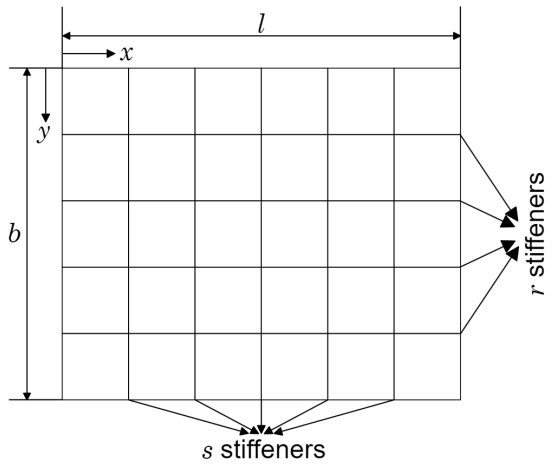

Fig. 2 $r \times s$ multi-stiffener grillage (Clarkson, 1965)

$$w = \sum_{m=1}^{\infty}\sum_{n=1}^{\infty} a_{mn} Sin\frac{m\pi x}{l} Sin\frac{n\pi y}{b} \tag{1}$$

The above equation can be solved by calculating the bending deformation energy of the stiffener system and equating it to the work done by the load. The deformation energy of a single longitudinal stiffener can be expressed as follows.

$$\int_0^l \frac{EI_r}{2}\left(\frac{\partial^2 w}{\partial x^2}\right)^2 dx = \frac{\pi^4 EI_r}{4l^3}\sum_{m=1}^{\infty}\sum_{n=1}^{\infty} a_{mn}^2 m^4 Sin^2\frac{n\pi y}{b} \tag{2}$$

In Eq. (2), the value of y corresponds to a specific stiffener, and the corresponding equation for the p-th stiffener is expressed as Eq. (3).

$$y_p = \frac{pb}{r+1} \tag{3}$$

Therefore, the deformation energy is expressed as Eq. (4).

$$\frac{\pi^4 EI_r}{4l^3}\sum_{m=1}^{\infty}\sum_{n=1}^{\infty} a_{mn}^2 m^4 Sin^2\frac{n\pi p}{r+1} \tag{4}$$

By using Eq. (4), the total deformation energy for all the stiffeners placed in the same direction is,

$$\frac{\pi^4 EI_r}{4l^3}\sum_{p=1}^{r}\sum_{m=1}^{\infty}\sum_{n=1}^{\infty} a_{mn}^2 m^4 Sin^2\frac{n\pi p}{r+1} \tag{5}$$

The bending deformation energy for all the stiffeners placed in the direction orthogonal to the stiffeners represented in Eq. (5) can be similarly expressed as Eq. (6).

$$\frac{\pi^4 EI_s}{4b^3}\sum_{p=1}^{s}\sum_{m=1}^{\infty}\sum_{n=1}^{\infty} a_{mn}^2 n^4 Sin^2\frac{m\pi p}{s+1} \tag{6}$$

Therefore, the total deformation energy for all longitudinal and transverse stiffeners installed on the stiffened plate can be calculated using Eq. (7).

$$\frac{\pi^4 EI_r}{4l^3}\sum_{p=1}^{r}\sum_{m=1}^{\infty}\sum_{n=1}^{\infty} a_{mn}^2 m^4 Sin^2\frac{n\pi p}{r+1} + \frac{\pi^4 EI_s}{4b^3}\sum_{p=1}^{s}\sum_{m=1}^{\infty}\sum_{n=1}^{\infty} a_{mn}^2 n^4 Sin^2\frac{m\pi p}{s+1} \tag{7}$$

If the load per unit area applied to the stiffened plate is P, the work done by this load is expressed as Eq. (8).

$$\int_0^l\int_0^b \frac{1}{2}Pwdxdy = \int_0^l\int_0^b \frac{1}{2}p\sum_{m=1}^{\infty}\sum_{n=1}^{\infty} a_{mn} Sin\frac{m\pi x}{l} Sin\frac{n\pi y}{b}dxdy \tag{8}$$

The general coefficient a_{mn} can be found by equating the general terms of Eq. (7) and Eq. (8) as in Eq. (9).

$$a_{mn} = \frac{4\int_0^l\int_0^b PSin\frac{m\pi x}{l}Sin\frac{n\pi y}{b}dx\,dy}{\frac{\pi^4 EI_r}{l^3}\left[m^4(r+1)+\frac{I_s}{I_r}\frac{l^3}{b^3}n^4(s+1)\right]} \tag{9}$$

Since no assumptions have been made regarding the equation for the applied load P, the coefficient a_{mn} obtained from Eq. (9) can be used in any distributed load acting on a simply supported symmetric stiffened-plate structure. As most load distributions of interest are uniformly distributed loads, if a stiffened plate with a symmetrical distribution load is considered, the coefficient a_{mn} can be obtained using Eq. (10).

$$a_{mn} = \frac{16\,p\,l^4 b/EI_r}{\pi^6 mn\left[m^4(r+1)+\frac{I_s}{I_r}\frac{l^3}{b^3}n^4(s+1)\right]} \tag{10}$$

Therefore, the final equation regarding the deflection deformation of the stiffened plate under bending load is Eq. (11).

$$w = \sum_{m=1}^{\infty}\sum_{n=1}^{\infty} \frac{16\,p\,l^4 b / EI_r}{\pi^6 mn[m^4(r+1) + \frac{I_s}{I_r}\frac{l^3}{b^3}n^4(s+1)]} \times Sin\frac{m\pi x}{l} Sin\frac{n\pi y}{b} \tag{11}$$

From Eq. (11), the bending moment equations for the p-th longitudinal stiffener and the q-th transverse stiffener can be obtained as follows.

For the bending moment for the p-th longitudinal stiffener,

$$M = -EI_r\frac{\partial^2 w}{\partial x^2} = \sum_{m=1}^{\infty}\sum_{n=1}^{\infty} \frac{16\,p\,l^2 b}{\pi^4 \frac{n}{m}[m^4(r+1) + \frac{I_s}{I_r}\frac{l^3}{b^3}n^4(s+1)]} \times Sin\frac{m\pi x}{l} Sin\frac{n\pi p}{r+1} \tag{12}$$

For the bending moment for the q-th transverse stiffener,

$$M = -EI_s\frac{\partial^2 w}{\partial y^2} = \sum_{m=1}^{\infty}\sum_{n=1}^{\infty} \frac{16\,p\,b^2 l}{\pi^4 \frac{m}{n}[n^4(s+1) + \frac{I_t}{I_s}\frac{b^3}{l^3}m^4(r+1)]} \times Sin\frac{m\pi q}{s+1} Sin\frac{n\pi y}{b} \tag{13}$$

Finally, using the bending stress equation, the tensile and compressive stresses for the p-th longitudinal stiffener and the q-th transverse stiffener can be determined individually (Clarkson, 1965).

3.2 Finite-Element Solutions for Laterally Loaded Stiffened Plates

We developed finite-element models based on the specifications of Cases A and B stiffened-plate structures shown in Table 2. The geometries of these stiffened-plate structures, the dimensions of the stiffeners, and the applied boundary and load conditions are shown in Figs. 3 and 4.

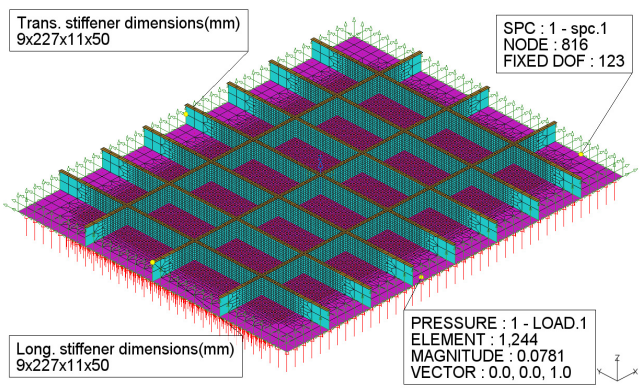

Fig. 3 3×7 Case A stiffened-plate structure

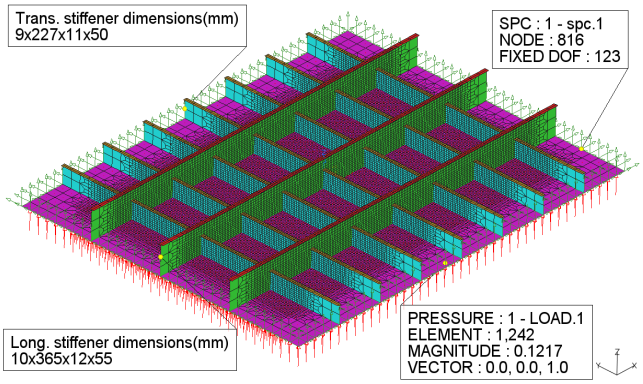

Fig. 4 3×7 Case B stiffened-plate structure

Patran and Nastran programs of MSC—general-purpose finite-element analysis packages—were used to develop the finite-element models. MSC Nastran is a structural analysis and multi-disciplinary integrated solver, and MSC Patran is a pre- and post-software for finite-element analysis that supports the entire process of finite-element modeling, from mesh division to setting analysis conditions and post-processing results.

QUAD4 elements with four nodes per element were used to develop the finite-element models 2D shell elements widely used in the analysis of quadrilateral membrane-bending planar structures and provided in Patran. The mesh density was increased to 25 mm for the central part of the structure, where maximum deformation was expected, whereas the remainder was divided into elements of 125 mm; this was based on the element size used in previous research (Kõrgesaar et al., 2018) on stiffened plates when developing a finite-element model. In the finite-element model of Case A stiffened-plate structure, 39,664 QUAD4 elements were used, whereas in the finite-element model of Case B stiffened-plate structure with relatively larger longitudinal stiffeners, 42,406 QUAD4 elements were used. The load was applied perpendicularly to the plate, allowing the longitudinal and transverse stiffening systems to support the plate vertically, and simple support was implemented by constraining displacements in the *x*-, *y*-, and *z*-axis directions (*UX, UY, UZ*) along the sides of the stiffened-plate structure.

4. Structural Response Analysis of Stiffened-Plate Structures in the Reactor Operation Environment

4.1 Structural Response Analysis of Stiffened-Plate Structures Using the Analytical Solutions Considering the Neutron-Irradiation Phenomenon

The grillage-structure theory summarized in the previous section was implemented in Fortran programming language. The bending load applied to the stiffened-plate structures was gradually increased until the allowable stress value of DH36 steel was met. First, the calculated results for the neutron non-irradiated Cases A and B stiffened-plate structures are shown in Table 3. The stiffened-plate structure of Case A supported a bending load of up to 78.1 kPa, at which point the

Table 3 Structural responses of Cases A and B stiffened-plate structures without the neutron-irradiation phenomenon

Structural responses	Stiffened-plate structures	
	Case A	Case B
σ_{max} (MPa)	354.84	355.08
δ_{max} (mm)	14.13	14.35
P (Applied load, kPa)	78.10	121.70

maximum deflection was 14.13 mm, and the maximum bending stress was 354.84 MPa. The Case B stiffened-plate structure supported a bending load of up to 121.7 kPa, at which point the maximum deflection was 14.35 mm, and the maximum bending stress was 355.08 MPa.

For the Case A stiffened-plate structure, in which the changes in the material properties of the steel were considered (Table 4), the elastic modulus and Poisson's ratio decreased, and the changes in allowable stress were not considered. The stiffened plates in the MPC_1 to MPC_3 scenarios supported loads up to 78.1 kPa, with no change in maximum bending stress at 354.84 MPa, but the maximum deflection increased to 14.62 mm, 14.72 mm, and 15.04 mm, respectively. Next, in the MPC_4 to MPC_6 scenarios, where the allowable stress was further increased by 25%, 50%, and 100% in the MPC_1 to MPC_3 scenarios, the stiffened plates were able to support loads in the order of 97.67 kPa, 117.2 kPa, and 156.27 kPa, and the maximum bending stress increased in the order of 443.75 MPa, 532.48 MPa, and 709.99 MPa. The maximum deflection also increased in the order of 18.04 mm, 22.09 mm, and 30.09 mm.

Table 4 Structural responses of Case A stiffened-plate structure considering the material property variation scenarios of DH36 HTS steel

Case A stiffened-plate structure						
MPC	1	2	3	4	5	6
σ_{max} (MPa)	354.84	354.84	354.84	443.75	532.48	709.99
δ_{max} (mm)	14.62	14.72	15.04	18.04	22.09	30.09
P (kPa)	78.10	78.10	78.10	97.67	117.20	156.27
δ_{max}/P (mm/kPa)	0.1872	0.1885	0.1926	0.1847	0.1885	0.1926

Table 5 Structural responses of Case B stiffened-plate structure considering the material property variation scenarios of DH36 HTS steel

Case B stiffened-plate structure						
MPC	1	2	3	4	5	6
σ_{max} (MPa)	355.08	355.08	355.08	443.75	532.50	709.98
δ_{max} (mm)	14.64	14.95	15.26	18.30	22.42	30.52
P (kPa)	121.70	121.70	121.70	152.09	182.51	243.34
δ_{max}/P (mm/kPa)	0.1203	0.1228	0.1254	0.1203	0.1228	0.1254

Subsequently, for the stiffened-plate structure of Case B considering variations in steel material properties (Table 5), the maximum bending load of the stiffened plate was the same (121.7 kPa) in scenarios MPC_1 to MPC_3, and the maximum bending stress did not change (355.08 MPa); however, the maximum deflection increased to 14.64 mm, 14.95 mm, and 15.26 mm, respectively. On the other hand, for the stiffened plate under scenarios MPC_4 to MPC_6, the maximum support bending load increased in the order of 152.09 kPa, 182.51 kPa, and 243.34 kPa, and the maximum bending stress increased in the order of 443.75 MPa, 532.5 MPa, and 709.98 MPa, while the maximum deflection increased in the order of 18.3 mm, 22.42 mm, and 30.52 mm.

For the above two types of stiffened-plate structures, regarding the ratio of deflection per applied load, the ratio in scenarios MPC_1 to MPC_3 was nearly equaled that in scenarios MPC_4 to MPC_6 as the analysis was performed based on the allowable stress value of the steel.

4.2 Structural Response Analysis of Stiffened-Plate Structures Using the FE Numerical Solutions Considering the Neutron-Irradiation Phenomenon

This section summarizes the structural response analysis results based on the allowable stress of DH36 steel using the finite-element models for Cases A and B stiffened-plate structures. By comparing with the results obtained using the grillage-structure theory for the same stiffened-plate structures, the accuracy of the developed finite-element models can be confirmed, and the structural deformation of the stiffened plates can be simulated. The deformation of Cases A and B stiffened-plate structures under bending loads is shown in Figs. 5 and 6, respectively.

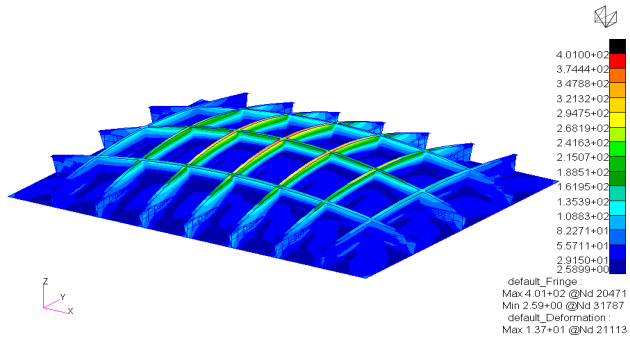

Fig. 5 Structural deformation of Case A stiffened-plate structure

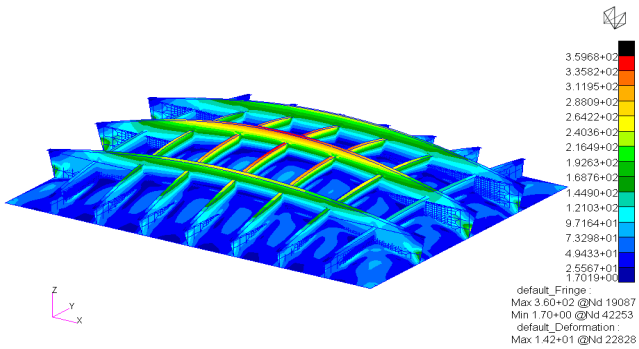

Fig. 6 Structural deformation of Case B stiffened-plated structure

The analysis results for Case A stiffened-plate structure are summarized as follows. Owing to the characteristics of the simply supported boundary conditions of the stiffened plate, the maximum deflection and maximum bending stress occurred at the central point of the stiffened plate, not only in scenario MPC_0 where the material properties were not changed but also in scenarios MPC_1 to MPC_6. From the analysis of the scenario without material property changes, a maximum deflection of 13.69 mm and a maximum bending stress of 365.40 MPa were obtained at a bending load of 78.1 kPa. For scenarios MPC_1 to MPC_3 with changes to material properties of the stiffened plate, under a bending load of 78.1 kPa, the maximum bending stress remained the same at 365.40 MPa, but the maximum deflection gradually increased to 13.97 mm, 14.26 mm, and 14.57 mm. For scenarios MPC_4 to MPC_6, bending loads of 97.67 kPa, 117.2 kPa, and 156.27 kPa were applied to the stiffened plate; the maximum bending stresses were 456.96 MPa, 548.33 MPa, and 731.11 MPa, and the maximum deflections were 17.47 mm, 21.41 mm, and 29.15 mm, respectively.

Figs. 7 and 8 compare the maximum deflection and maximum bending stress obtained using the grillage-structure theory and finite-element model for Case A stiffened-plate structure. The maximum deflection shows a 3.3% error and the maximum bending stress shows a 3% error, confirming the accuracy of the developed finite-element model as the above two solutions closely match.

The analysis results for Case B stiffened-plate structure showed a similar trend to the analysis results for Case A stiffened-plate structure. The analysis results, not considering changes in material properties, as well as the analysis results for scenarios MPC_1 to MPC_6 with changes in material properties, revealed that the maximum deflection and maximum bending stress occurred at the central point of the stiffened plate owing to the characteristics of the simple support boundary condition. In results of the analysis not considering changes in material properties, the stiffened plate showed a maximum deflection of 14.19 mm and maximum bending stress of 348.91 MPa under a bending load of 121.7 kPa. In the analysis results for scenarios MPC_1 to MPC_3 applying changes to the material properties of the stiffened plate, a bending load of 121.7 kPa was applied, and all had the same maximum bending stress of 348.9 MPa, but the maximum deflection progressively increased to 14.48 mm, 14.78 mm, and 15.1 mm. For the scenarios MPC_4 to MPC_6, where

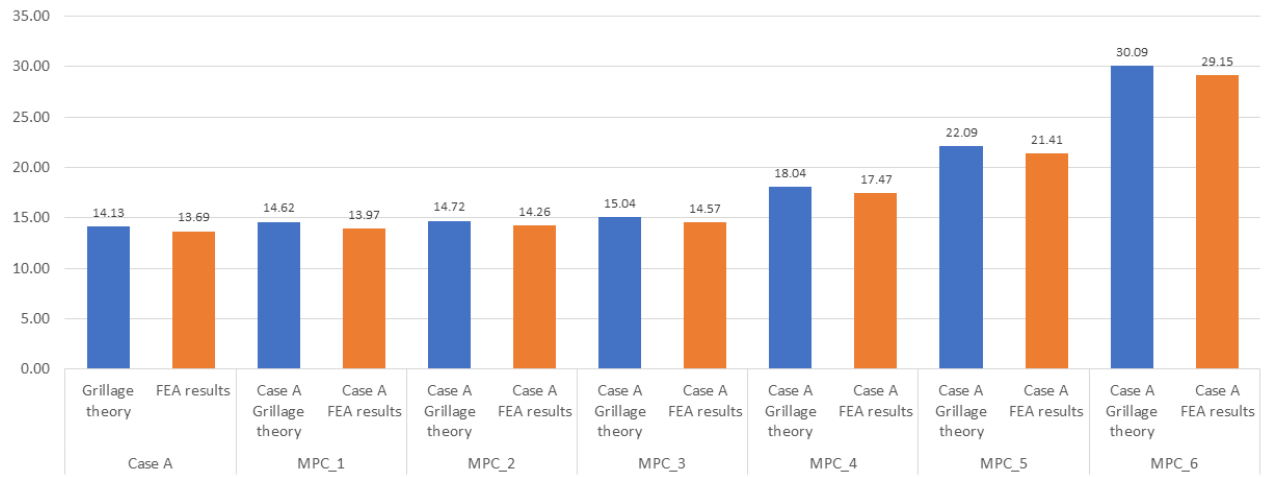

Fig. 7 Comparison of maximum deflections between the analytical and numerical solutions of Case A stiffened-plate structure

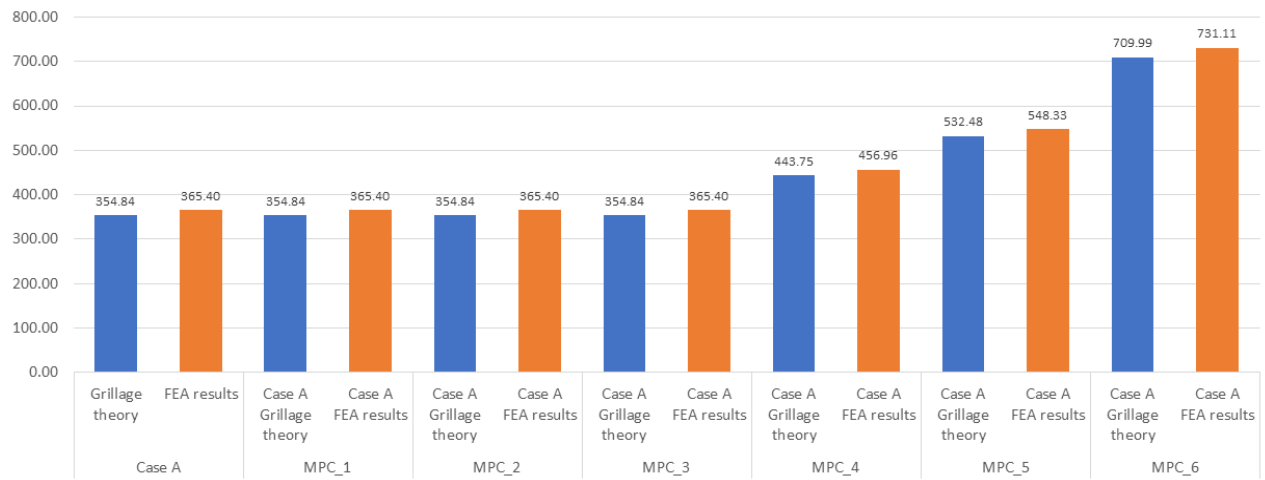

Fig. 8 Comparison of maximum flexural stresses between the analytical and numerical solutions of Case A stiffened-plate structure

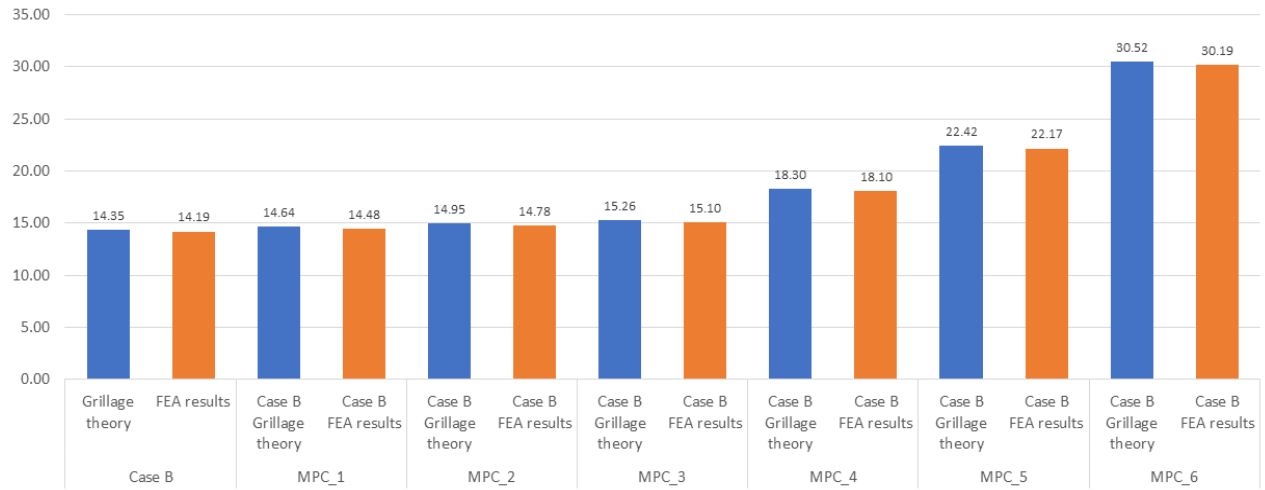

Fig. 9 Comparison of maximum deflections between the analytical and numerical solutions of Case B stiffened-plate structure

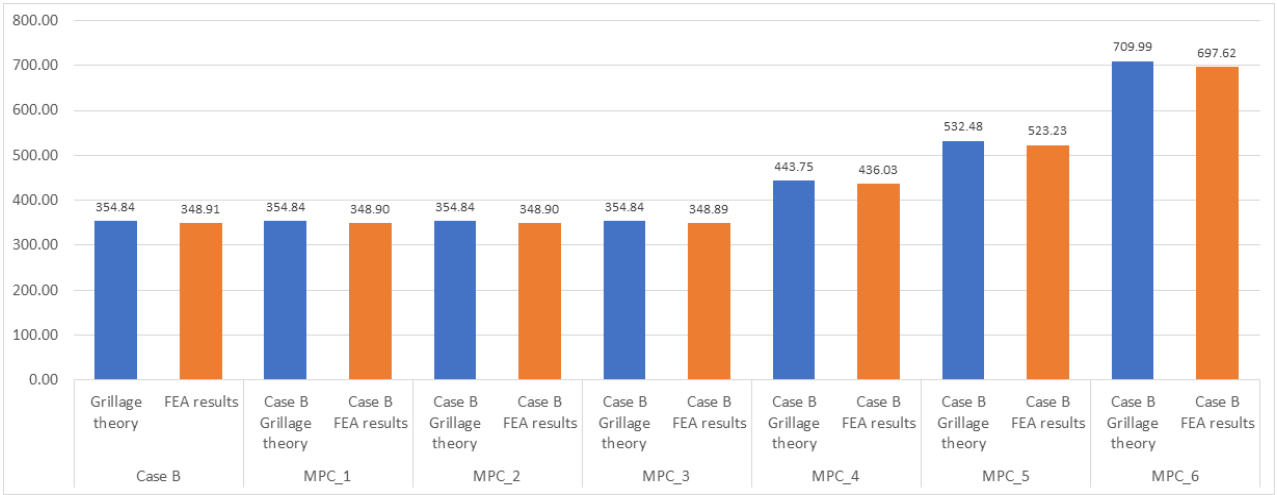

Fig. 10 Comparison of maximum flexural stresses between the analytical and numerical solutions of Case B stiffened-plate structure

the allowable stress of DH36 steel material increased by 25%, 50%, and 100% respectively, bending loads of 152.09 kPa, 182.51 kPa, and 243.34 kPa were applied to the stiffened plate; the maximum bending stresses and maximum deflections were 436.03 MPa, 523.23 MPa, and 697.62 MPa, and 18.10 mm, 22.17 mm, and 30.19 mm, respectively.

Figs. 9 and 10 compare the maximum deflection and maximum bending stress obtained for Case B stiffened-plate structure using the grillage-structure theory and finite-element modeling, respectively. The maximum deflection shows an error of 1% and the maximum bending stress shows an error of 1.7%, demonstrating relatively low errors compared to Case A stiffened-plate structure. Therefore, the above two solutions closely match, confirming the accuracy of the developed finite-element model.

5. Conclusions

We conducted a structural response analysis of stiffened-plate structures, a typical hull structure subject to lateral pressure loads, considering changes in material properties of steel used in shipbuilding and marine applications affected by neutron irradiation in the operating environment of nuclear reactors for ships.

In the operating environment of nuclear reactors installed on ships, the material properties of steel exposed to neutron energy change, and we confirmed that the structural responses of stiffened-plate structures in Cases A and B, which consider these changes, differ from those of the identical stiffened-plate structure in ships using conventional fossil fuels. This proves that neutron irradiation affects the steel hull structure of ships and marine applications in terms of strength and stiffness, although there are differences in the extent. The accumulation of neutron irradiation signifies an increase in the changes in the material properties of steel. This was represented by scenarios MPC_1 to MPC_6 in the analysis of this study, considering variations in material properties such as elastic modulus, Poisson's ratio, and allowable stress, based on the experimental and theoretical research on the neutron-irradiated steel.

We analyzed the structural response of the stiffened-plate structure using theoretical grillage-structure theory and analytical finite-element modeling within the static and elastic range. The impact of neutron

irradiation on the stiffened-plate structure was determined in terms of load-bearing capacity, strength, and stiffness.

The results of the analysis of the stiffened-plate structure under the same bending load indicated that, as the steel-based stiffened-plate structure got exposed to neutron energy, the maximum deflection proportionally increased, thereby weakening the structural stiffness. For scenarios MPC_4 to MPC_6 with property changes, as the allowable stress of the steel increased, the maximum deflection and the bending load-bearing capacity of the stiffened-plate structure also increased. Therefore, when designing the structures surrounding the hull containment structure where the ship reactor is installed, both strength and stiffness must be considered, and the amount of neutron energy received by the steel is an important consideration.

Ship reactors are typically protected by primary and secondary shielding systems, and the containment structure protects the reactor and serves as a secondary shield. The stiffened-plate structure used as an example in this study was assumed to be located inside the containment structure, thus it was not directly exposed to radiation from the reactor. However, these structures are still in an environment exposed to indirect radiation; therefore, we believe the analysis results for changes in steel properties of stiffened-plate structures under relatively low levels of neutron-irradiation scenarios apply.

The results of this study can be used in the structural design of ships considering the future installation of reactors. Furthermore, the results can be used to formulate the hull design rules from classification societies for ships that adopt nuclear propulsion systems.

A summary of future research plans is as follows. In this study, owing to limited data on the specifications of reactors for ships, the load generated from the weight of the reactor was simply assumed to be the lateral bending load. To supplement this, it is necessary to calculate the specifications for the reactor system and select the target ship to install the reactor, and then carry out structural analysis based on accurate load information calculated therefrom. For the operation of a reactor, a cooling system must be considered. Unlike land-based nuclear power plants, an efficient cooling system must be placed within the confined space of the hull of the ship. Therefore, further structural models must be developed using finite-element modeling for the hull compartment where the reactor and cooling systems are installed, based on the stiffened-plate structures used as examples in this paper. Additionally, structural analysis considering the additional load generated by the cooling system is needed. It is also necessary to understand the effect of neutron irradiation on the welds of the steel structure of the hull. Ships contain a considerable number of welds; these welds sustain the initial residual stress caused by welding, as well as the stress and strain expected during ship operation. Therefore, research on the welds of neutron-irradiated steel is necessary to ensure the structural safety of ships equipped with nuclear reactors.

Conflict of Interest

No potential conflict of interest relevant to this article was reported.

Funding

This work was supported by the National Research Foundation of Korea (NRF) grant funded by the Korea government (Ministry of Science and ICT) (No. 2019M2D1A1072954). Additionally, this work was supported by the Kunsan National University's financial support for Faculty Member in the year 2021.

References

Ahn, S. B., Kim, Y. S., & Kim, J.K. (2002). Tensile behavior characteristics of CANDU pressure tube material degraded by neutron irradiations. *Transactions of the Korean Society of Mechanical Engineers A, 26*(1), 188−195. https://doi.org/10.3795/ksme-a.2002.26.1.188

Clarkson, J. (1965). *The elastic analysis of flat grillages: With particular reference to ship structures.* Cambridge University Press.

Finnish-Swedish Ice Class Rules (FSICRS). (2008). The structural design and engine output required of ships for navigation in ice. *Guidance for ships for navigation in ice.*

Gil, Y., Yoo, S., Kim, Y., Oh, J., Byun, Y., Woo, I., Kim, J., & Choi, S. (2014, May 29−30). Concept design and risk assessment of nuclear propulsion ship. In *Proceedings of the Transactions of the Korean Nuclear Society Spring Meeting, Jeju, Korea.*

Gravina, J., Blake, J. I. R., Shenoi, R. A., Turnock, S., & Hirdaris, S. (2013). Concepts for a modular nuclear powered containership. *7th International Conference on Ships and Shipping Research, Naples, Italy.* http://eprints.soton.ac.uk/id/eprint/351357

Hirdaris, S. E., Cheng, Y. F., Shallcross, P., Bonafoux, J., Carlson, D., Prince, B., & Sarris, G. A. (2014). Considerations on the potential use of nuclear small modular reactor (SMR) technology for merchant marine propulsion. *Ocean Engineering, 79*, 101−130. https://doi.org/10.1016/j.oceaneng.2013.10.015

Hong, J. H. (2012). *Nuclear materials*. Hans House.

International Association of Classification Societies (IACS). (2016). *Requirements concerning polar class.*

Jhung, M. J., Park, J. S., Ko, H. O., & Kim, S. J. (2013). Aging mechanism and operating experience of reactor vessel internals (KINS/RR-1009). Daejeon: Korea Institute of Nuclear Safety.

Korean Register. (2020). *Guidance for Ships for Navigation in Ice*.

Knaster, J., Moeslang, A., & Muroga, T. (2016). Materials research for fusion. *Nature Physics, 12*(5), 424−434. https://doi.org/10.1038/nphys3735

Kõrgesaar, M., Kujala, P., & Romanoff, J. (2018). Load carrying capacity of ice-strengthened frames under idealized ice load and boundary conditions. *Marine Structures, 58*, 18−30. https://doi.org/10.1016/j.marstruc.2017.10.011

Lee, K.H., Kim, M.G., Lee, J.I., & Lee, P.S. (2015). Recent advances in ocean nuclear power plants. *energies*, *8*(10), 11470−11492. https://doi.org/10.3390/en81011470

Nam, W. (2019). Numerical analysis of iceberg impact interaction with ship stiffened plates considering low-temperature characteristics

of steel. *Journal of Ocean Engineering and Technology, 33*(5), 411−420. https://doi.org/10.26748/KSOE.2019.046

Russian Maritime Register Shipping (RMRS). (2018). *Rules for the classification and construction of nuclear ships and floating facilities.*

Straalsund, J. L., & Day, C. K. (1973). Effect of neutron irradiation on the elastic constants of type-304 stainless steel. *Nuclear Technology, 20*(1), 27−34. https://doi.org/10.13182/NT73-2

Author ORCIDs

Author name	ORCID
Jeong, Han Koo	0000-0002-9926-0982
Kim, Soo Hyoung	0000-0002-9780-4536
Hwang, Seon Pyoung	0009-0000-7433-5151

KSOE

Journal of Ocean Engineering and Technology 37(5), 215-224, October, 2023
https://doi.org/10.26748/KSOE.2023.028

pISSN 1225-0767
eISSN 2287-6715

Original Research Article

Anti-icing Method of Heated Walkway in Ice Class Ships: Efficiency Verification of CNT-based Surface Heating Element Method Through Numerical Analysis

Woo-Jin Park[1], Dong-Su Park[1], Mun-Beom Shin[2] and Young-Kyo Seo[3]

[1]*Graduate Student, Department of Convergence Study on the Ocean Science and Technology, Korea Maritime and Ocean University, Busan, Korea*
[2]*Graduate Student, Department of Ocean Engineering, Korea Maritime and Ocean University, Busan, Korea*
[3]*Professor, Department of Ocean Engineering, Korea Maritime and Ocean University, Busan, Korea*

KEYWORDS: Anti-icing, Surface heating element, Heating coil, Heated walkway, CFD, Heat transfer

ABSTRACT: *While melting glaciers due to global warming have facilitated the development of polar routes, Arctic vessels require reliable anti-icing methods to prevent hull icing. Currently, the existing anti-icing method, i.e., the heating coil method, has disadvantages, such as disconnection and power inefficiency. Therefore, a carbon nanotube-based surface heating element method was developed to address these limitations. In this study, the numerical analysis of the surface heating element method was performed using ANSYS. The numerical analysis included conjugate heat transfer and computational fluid dynamics to consider the conduction solids and the effects of wind speed and temperature in cold environments. The numerical analysis method of the surface heating element method was validated by comparing the experimental results of the heating coil method with the numerical analysis results (under the –30 ℃ conditions). The surface heating element method demonstrated significantly higher efficiency, ranging from 56.65–80.17%, depending on the conditions compared to the heating coil method. Moreover, even under extreme environmental conditions (–45 ℃), the surface heating element method satisfied anti-icing requirements. The surface heating element method is more efficient and economical than the heating coil method. However, proper heat flux calculation for environmental conditions is required to prevent excessive design.*

Nomenclature

h	Heat transfer coefficient (W/m^2·K)
h_{stat}	Static enthalpy (J/kg)
h_{tot}	Specific total enthalpy (J/kg)
k	Turbulence kinetic energy per unit mass (W/kg)
p	Pressure (Pa, N/m^2)
T	Temperature (K)
V	Volume (m^3)
ρ	Density (kg/m^3)
μ_t	Turbulent viscosity (m^2/s)
S_E	Energy source
S_M	Momentum source
U	Vector of velocity $U_{x,y,z}$
u	Velocity component in turbulent flow
λ	Thermal conductivity (W/m·K)
τ	Molecular stress tensor
$p\ \gamma_t$	Turbulent Prantl number ($C_p\mu_t/\lambda_t$)

1. Introduction

The decline in Arctic glaciers caused by global warming has made the development of shipping routes by countries adjacent to the Arctic more feasible, resulting in a growing demand for ice-class ships for developing maritime energy and resources in the Arctic. Ships navigating the Arctic ocean are exposed to extreme environments characterized by high wind speeds and low atmospheric temperatures. Therefore, sea spray and atmospheric moisture generated during navigation leading to icing on the external surfaces and deck equipment of the ship. As shown in Fig. 1, water droplets coming into contact with the external chilled surfaces of the ship in these extreme conditions cause icing. The rate of icing and ice density vary depending on external conditions (Rashid, 2016).

The formed ice poses risks to human safety while also negatively impacting the working conditions and equipment performance on deck passages, workspaces, and superstructures. Hence, the International Maritime Organization (IMO) has established international regulatory

Received 17 August 2023, revised 5 September 2023, accepted 11 September 2023
Corresponding author Young-Kyo Seo: +82-51-410-4683, yseo@kmou.ac.kr

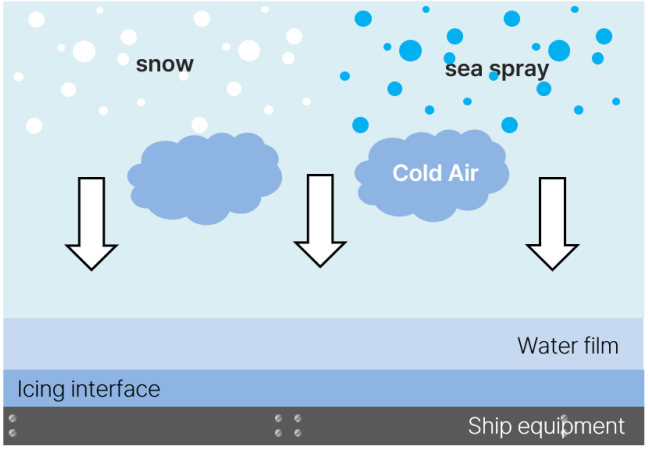

Fig. 1 Schematic of sea spray icing on ice class ships in cold region

requirements for ice-class criteria and winterization notation, aiming to ensure the safety of ships and protection in extreme environments, considering the anticipated operating conditions and risks that ships may encounter in polar waters (IMO, 2015). Classification societies from various countries also define low-temperature designs and anti-icing treatments. The Norwegian Classification Society (Det Norske Veritas, DNV) broadly categorizes winterization technologies for ship equipment into Categories Ⅰ and Ⅱ. Category Ⅰ covers issues related to anti-icing designs for navigation, steering and propulsion, anchoring, life-saving, and escape routes, while Category Ⅱ focuses on winterization design technologies related to decks and superstructures, helidecks, handrails, and cargo deck areas (DNV, 2005).

In South Korea, development projects, such as 'Development of Safe Navigation Technologies in Polar Routes and Evaluation Methods for Extreme Low-Temperature Ice Performance for Ice-Class Ships (KRISO, 2013)' and 'Development of Evaluation Technologies for Low-Temperature Design and Anti-Icing Treatment (Winterization) (Ministry of Knowledge Economy, 2012)' have been implemented, utilizing heating coils as the method to prevent icing on ice-class ships. However, issues with the efficiency of power consumption required to maintain this method and the lack of stability due to partial circuit disconnection have recently led to the research and development of the surface heating element method based on carbon nanotubes (CNT).

The CNT-based surface heating element method offers the advantages of improved energy consumption efficiency, durability, and flexibility, making it applicable to a broader range of equipment (B.P. Technology Transaction, 2017). However, there is a lack of quantitative research evaluating the anti-icing performance of the surface heating element method compared to the conventional heating coil method.

In this study, numerical analyses were conducted by referencing the heated walkway—a ship equipment application that employs the CNT-based surface heating element method developed by Yu et al. (2022)—to verify its efficiency against the conventional heating coil method. Calibration was performed based on numerical analysis results at ambient temperature using the heating coil method developed by Lee et al. (2012). Parameters such as heat flux were determined, with the results validated based on the results of the conducted laboratory experiments and numerical analysis. This study was verified that the heat flux derived from the surface heating element method is more efficient compared to that of the existing heating coil method.

2. CNT-based Surface Heating Element Method

2.1 Overview of the Surface Heating Element Method

The existing methods using heating coils suffer from energy loss issues, such as heat generated by the heating coils being transferred by convective air currents, reducing efficiency over time, and failing to maintain stable temperatures. Furthermore, the heating coil can disconnect or deform owing to rapid temperature rise or high temperature, significantly compromising its performance (B.P. Technology Transaction, 2017).

In contrast, the surface heating element method involves installing metal electrodes at both ends of a thin, conductive, carbon-based surface heating element, and then insulating it. A rated voltage is then applied to the metal electrodes, inducing heat across the entire surface. Nano heating elements are new heat-generating materials that contain a mix of various metallic compounds of tin oxide and various minerals crushed into nano-sized particles. This method is 50~60% more efficient than existing nichrome wire methods, offers a faster response time, can heat from low temperatures to above 500 °C, and is flexible in design and application, allowing for a wide range of shapes and materials. It has the advantages of excellent fire resistance, moisture resistance, and wear resistance. Moreover, it maintains its efficiency over the long term (B.P. Technology Transaction, 2017).

Specifically, the CNT-based surface heating element method utilizes the electrical properties of carbon, converting electrical energy to thermal energy through resistance. This method is easy to manufacture, allows for convenient temperature control, and offers uniform heat distribution, reducing temperature variations. Fig. 2 illustrates the thermal diffusion and emission characteristics of conventional heating coil methods and surface heating element

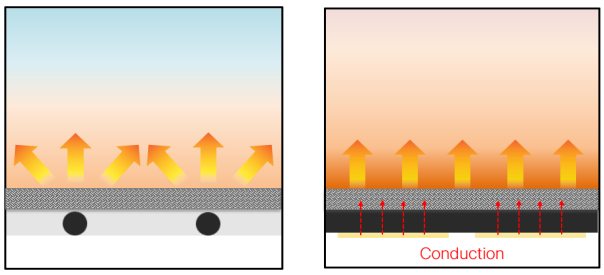

(a) (b)

Fig. 2 Comparison of the thermal diffusion of different heating methods: (a) Heating coil and (b) Surface heating element

methods, highlighting the advantages of the latter in terms of heat distribution and energy consumption efficiency.

The surface heating element method applied in this study is shown in Fig. 2(b). Using a multi-layer structure, it aims for thermal diffusion and distribution, considering conduction up to the top layer, achieving a uniform temperature distribution and offering thermal advantages, such as higher heat energy diffusion and efficiency compared to the heating coil method shown in Fig. 2(a).

2.2 Heated Walkways for Polar Route Vessels

In this study, the surface heating element method were applied to the heated walkway prototype developed by Yu et al. (2022). The design ensures that the anti-icing performance is maintained even in extreme environmental conditions of −62 °C for the vessels operating in Arctic ocean. The purpose of the heated walkway is to prevent safety incidents in advance by preventing icing on the upper decks of ships navigating icy waters, thereby ensuring safe operation for workers and equipment.

The CNT-based surface heating element method designed for this heated walkway is illustrated in Fig. 3. It is composed of a CNT-based heating film at the center. For anti-icing, the upper layer includes a steel plate and a heat-dissipating silicone pad considering the conduction phenomena. The sides and bottom are designed with insulating foam silicone pads, VIP insulating materials, and aluminum side and bottom covers to minimize heat loss and ensure product stability (Yu et al., 2022).

To evaluate the performance of the heated walkway prototype using the CNT-based heating film, winterization performance tests were conducted in ambient and low-temperature environments at the Korea Research Institute of Ship & Ocean Engineering (KRISO) polar environment testing facility. The performance through computational fluid dynamics(CFD)-based numerical analyses were also simulated. Additionally, the efficiency of the surface heating element method was verified by comparing and validating the temperature distribution results of the heated walkways and heated stairs in ambient and low-temperature experiments with numerical analysis results (Park et al., 2023).

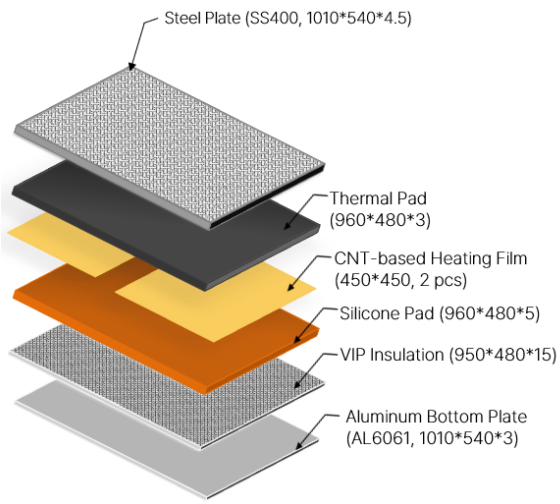

Fig. 3 Schematic of the surface heating element in the walkway

3. Numerical Analysis Methods and Process

3.1 Governing Equations

To numerically simulate the CNT-based surface heating element method used for anti-icing, thermal heat flow was considered based on wind speed and temperature conditions in extreme environments. The analysis considered conjugate heat transfer for considering conduction phenomena through the heat source (heat flux) in the heating film to the upper solid layers of the heated walkway, as shown in Fig. 3. For this analysis, the CFX tool in the ANSYS was used and the unsteady Reynolds-averaged Navier–Stokes equation as the governing equation was applied. The continuity equation and momentum equation are defined as Eqs. (1) and (2), respectively.

$$\text{Continuity Equation: } \frac{\partial \rho}{\partial t} + \frac{\partial}{\partial x_j}(\rho U_j) = 0 \tag{1}$$

Momentum Equation:

$$\frac{\partial \rho U_i}{\partial t} + \frac{\partial}{\partial x_j}(\rho U_i U_j) = -\frac{\partial p}{\partial x_i} + \frac{\partial}{\partial x_j}(\tau_{ij} - \rho\overline{u_i u_j}) + S_M \tag{2}$$

In Eq. (2), τ represents the molecular stress tensor, which includes normal and shear components. S_M signifies the momentum term, representing the force acting per unit volume on the fluid. Additionally, $\rho\overline{u_i u_j}$ denotes Reynolds stresses, which refer to the turbulent flow term added to the molecular diffusion flow (ANSYS Inc., 2017). Another turbulence model, the k–ω shear stress transport (SST) model, was used to accurately represent the heat transfer phenomena on the surface of the heating element (Lee et al., 2012). Through this, the Reynolds-averaged energy equation is defined in Eq. (3), where S_E refers to the energy source term (ANSYS Inc., 2017).

$$\frac{\partial \rho h_{tot}}{\partial t} - \frac{\partial \rho}{\partial t} + \frac{\partial}{\partial x_j}(\rho U_j h_{tot}) = \frac{\partial}{\partial x_j}(\lambda \frac{\partial T}{\partial x_j} + \frac{\mu_t}{pr_t}\frac{\partial h}{\partial x_j}) + \frac{\partial}{\partial x_j}[U_i(\tau_{ij} - \rho\overline{u_i u_j})] + S_E \tag{3}$$

where λ, h_{tot}, h_{stat}, and k represent the thermal conductivity coefficient, total enthalpy, and turbulent kinetic energy, respectively, as defined in Eqs. (4)–(5) (ANSYS Inc., 2017).

$$h_{tot} = h_{stat} + \frac{1}{2}U_i^2 + k \tag{4}$$

$$k = \frac{1}{2}\overline{u_i^2} \tag{5}$$

Furthermore, considering the multi-layered structural characteristics between the materials of the heated walkway, the heat transfer

phenomena between solids, known as conduction (Q_{conv}, solid–solid interface) were considered, which is defined in Eq. (6) (ANSYS Inc., 2017).

$$Q_{conv} = h A_p (T_g - T_p) \tag{6}$$

where h denotes the heat transfer coefficient, A_p represents the contact area between parts, and T_p and T_g indicate the temperatures between solids based on the conduction phenomenon.

3.2 Numerical Analysis Method and Boundary Conditions

The laboratory tests setup at KRISO were used for the numerical analysis and modeled the internal structural components, including a cold chamber and wind generation device (air inlet), identical to those used by Lee et al. (2012). The schematic is shown in Fig. 4(a). For the numerical analysis involving the surface heating element, the heating coil model from Lee et al. (2012) with the surface heating element was replaced. The schematic is as shown in Fig. 4(b). Any desks that did not directly impact the heat transfer phenomena in the heated walkway were considered fully insulated.

Additionally, in the design and performance testing of the prototype, the side structural components (plates and brackets) of the surface heating element and aluminum cover at the bottom were designed to be fully insulated, setting the boundary conditions as fully insulated. Each part and model generated within the CFX tool are shown in Fig. 5(a). The air inlet, corresponding to the wind generation device, is represented by the green area. To improve the accuracy and time-efficiency of the analysis, a volumetric growth ratio of 1.2 was applied to the grid in areas closely related to the boundaries, based on a criterion of 0.1E−3 m (Kim et al., 2011). The mesh of the entire model, including the cold chamber, is shown in Fig. 5(b). It consists of approximately 860,000 elements and 240,000 nodes.

In this numerical analysis, the heat flux applied as a thermal boundary condition was identical to that used in the heating coil method by Lee et al. (2012). The heat flux is shown in Table 1; it is a converted value based on the power specifications used in the laboratory experiments and numerical analysis of the original heating

Table 1 Heat flux of the heating cable (Lee et al., 2012)

Heating cable product	Nominal electric power output (W/m at 10 ℃)	Heat flux (W/m^2)
10XTV_CT	33	970.00
15XTV_CT	49	1441.17
20XTV_CT	65	1911.76

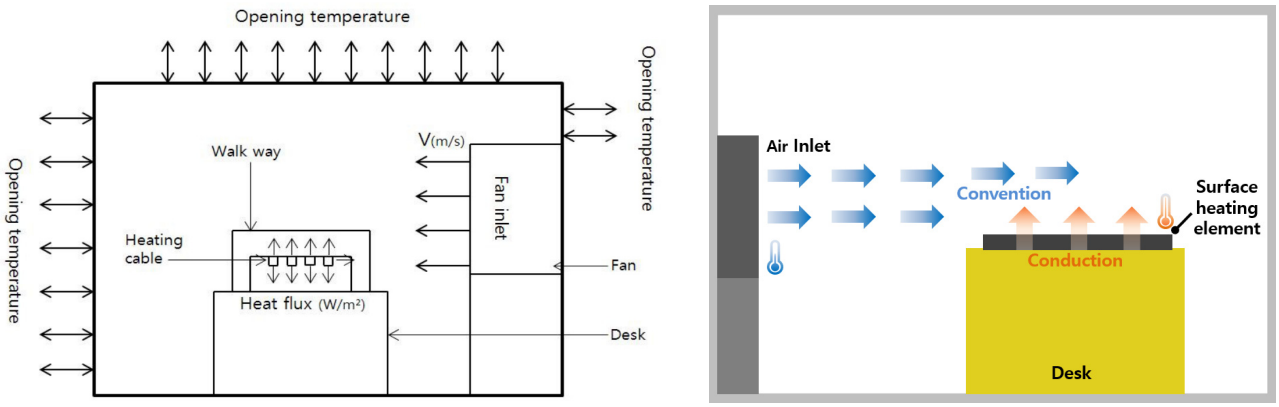

(a) (b)

Fig. 4 Conceptual diagram of numerical analysis: (a) heating coil (Lee et al., 2012) and (b) surface heating element

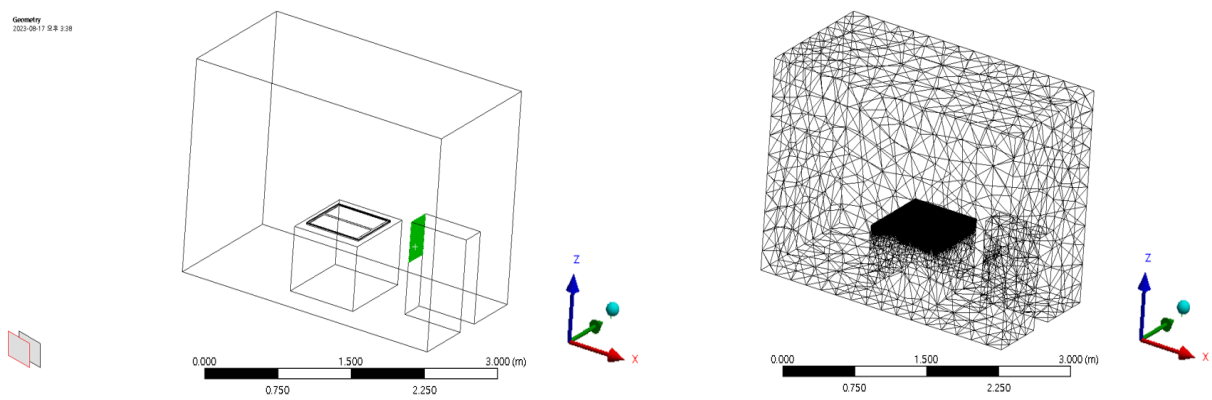

(a) (b)

Fig. 5 Modeling in ANSYS CFX: (a) geometry and (b) mesh

Table 2 Properties of air (20 to −45 ℃) (Vargaftic, 1972)

Temperature (℃)	Density (kg/m^3)	Specific heat capacity (J/kg·K)	Thermal conductivity (W/m·K)	Expansion coefficient (1/K)	Dynamic viscosity (kg/m·s)
20	1.204	1.006	0.026	0.0034	1.83E-5
10	1.246	1.005	0.025	0.0036	1.78E-5
0	1.292	1.005	0.024	0.0037	1.73E-5
-15	1.341	1.005	0.023	0.0039	1.66E-5
-30	1.394	1.005	0.022	0.0041	1.58E-5
-45	1.547	1.005	0.021	0.0044	1.50E-5

coil method. Lee et al. (2012) showed the average temperature results based on wind speed and heating coil conditions in their research. By comparing these laboratory experimental and numerical analysis results, a reliability in the proposed model and numerical analysis methods was established, indicated by an average temperature difference of ±1−3 ℃.

In this numerical analysis, the heat flux was applied as a thermal boundary condition to the areas of the two silicone pads that are in direct contact with the heating film. The applied heat flux represents the thermal energy per unit area, and by multiplying it by the area of the heating film, the thermal energy (W) can be calculated.

Previous numerical results from studies using the heating coil method indicated that the air flow generated by the wind generation device caused substantial and rapid heat transfer phenomena owing to vortex formation and high wind speeds, depending on the shape of the heated walkway. Because the overall temperature distribution could appear asymmetric or irregular, the two-equation SST model, a turbulence model, was applied (Lee et al., 2012).

3.3 Applied Physical Properties for Numerical Analysis

As the properties of air change with temperature, the density and thermal properties of air at low temperatures, as listed in Table 2, were applied. This was necessary to account for the temperature-dependent properties of air, considering the turbulent flow caused by the high wind speed from the wind generation device and the potential laminar flow due to the shape of the heated walkway (Jung and Seo, 2015).

Moreover, in the heated walkway method, solid-to-solid heat conduction occurs through a CNT-based heating film located at the center. To account for this, the material-specific density and thermal properties, such as specific heat and thermal conductivity, were applied, as listed in Table 3, while the patterned steel plate used the standard properties of SS400 (Park et al., 2023).

The insulation design on the sides and bottom of the heated walkway does not affect the primary outcome of the numerical analysis, which is the average temperature on the surface of the surface heating element. Therefore, additional structures, like the aluminum cover (AL6061), side structures, and bolts, were not considered in the numerical modeling. The CNT-based heating film was manufactured to have a thickness within 1 mm using compression equipment and was not considered in the modeling; instead, it was applied to the numerical analysis as a thermal boundary condition based on the contact area between materials.

Table 3 Material properties of the surface heating element (Park et al., 2023)

Material	Density (kg/m^3)	Specific heat capacity (J/kg·K)	Thermal conductivity (W/m·K)
Steel (SS400)	7850	480	60.5
Thermal pad (3T)	2100	1000	2.25
Silicone pad (5T)	650	1400	0.570
VIP insulation	210	850	0.0043

4. Verification of Numerical Analysis Techniques

To validate the reliability of the numerical analysis techniques employed in this study, we referred to the study of Lee et al. (2012), which applied the heating coil method in ambient and low-temperature environments, and the laboratory experimental results from KRISO (2012).

The cases for verifying the numerical analysis technique using the surface heating element method are listed in Table 4. These are cases that Lee et al. (2012) investigated by comparing laboratory experiments and numerical analysis results for heated walkways that utilized the heating coil method. The results of the cases showed an average temperature difference of ±1−3 ℃ depending on air temperature conditions, thus ensuring the reliability of the proposed model and numerical analysis technique.

In this study, numerical analysis techniques were verified by comparing it to the laboratory experimental and numerical analysis results of heated walkways using the heating coil method by Lee et al.

Table 4 Case conditions of numerical analysis (Lee et al., 2012)

Case	Wind speed (m/s)	Interval (mm)	Heat flux (W/m^2)
Case 2−5	2	65	1441.17
Case 2−7		110	970
Case 4−5	5	65	1441.17
Case 4−7		110	970

Table 5 Numerical analysis of average temperature in the heating coil: Case 2, 4 (air temperature: 10 ℃)

Wind speed (m/s)					2				
Case No.	2-1	2-2	2-3	2-4	2-5	2-6	2-7	2-8	2-9
Interval (mm)		33			65			110	
Heat flux (W/m^2)	970.00	1441.17	1911.76	970.00	1441.17	1911.76	970.00	1441.17	1911.76
Heating coil temperature (℃)	62.2	87.7	112	40.8	56.2	56.8	37.7	51.1	73.6
Wind speed (m/s)					5				
Case No.	4-1	4-2	4-3	4-4	4-5	4-6	4-7	4-8	4-9
Interval (mm)		33			65			110	
Heat flux (W/m^2)	970.00	1441.17	1911.76	970.00	1441.17	1911.76	970.00	1441.17	1911.76
Heating coil temperature (℃)	44.6	61.4	80.1	30.4	40.0	51.2	29.6	39.0	52.6

Table 6 Numerical analysis of average temperature in the surface heating element: Case 2, 4 (air temperature: 10 ℃)

Wind speed (m/s)					2				
Case No.	2-1	2-2	2-3	2-4	2-5	2-6	2-7	2-8	2-9
Average temperature (℃)	62.19	87.68	112.2	40.78	56.15	56.77	37.66	51.19	73.55
Heat flux (W/m^2)	420.2	624.7	821.8	249.2	373.3	379	223	333.7	1911.76
Efficiency (%)	56.68	56.65	57.01	74.31	74.10	80.17	77.01	76.85	73.6
Wind speed (m/s)					5				
Case No.	4-1	4-2	4-3	4-4	4-5	4-6	4-7	4-8	4-9
Average temperature (℃)	44.78	61.30	80.11	30.27	40.11	51.22	29.68	39.08	52.69
Heat flux (W/m^2)	407.5	605	827	238.8	354.8	485.4	232	343	504.5
Efficiency (%)	57.99	58.02	56.74	75.38	75.38	74.61	76.08	76.20	73.61

(2012), as shown in Table 5. Table 5 presents the average temperature results of numerical analysis using the heating coil method at an ambient temperature of 10 ℃, where cases are determined based on external wind speed, coil interval, and heat flux.

Table 6 provides the numerical analysis results for the surface heating element method, corresponding to the average temperature results of the cases derived in Table 5. The heat flux for the surface heating element method was identified to have an average temperature difference within a maximum range of 0.2 ℃ when compared to the heating coil method.

The numerical analysis for the surface heating element method applied the same boundary conditions for wind speed and air temperature as those in the laboratory experiments and numerical analyses in the existing heating coil method. The heat flux derived for the surface heating element method was significantly lower than that for the heating coil method.

Furthermore, by comparing the differences in heat flux magnitudes applied in the heating coil and surface heating element methods, the efficiency of the surface heating element method was found depending to the coil interval and heat flux to be between 80.17% and 56.65% at an external wind speed of 2 m/s and between 76.20% and 56.74% at 5 m/s.

Next, additional verification was conducted by applying the heat flux derived at an ambient temperature of 10 ℃ for the surface heating element method in Table 6 to the cases in Table 4 and compared the average temperature results of numerical analysis to the laboratory experiments and numerical analysis of the heating coil method. This is detailed in Tables 7–10. Compared to the ±1–3 ℃ average temperature difference observed in the numerical analysis of the heating coil method based on air temperature conditions, the surface heating element method showed a smaller average temperature difference of ±0.8–2 ℃ compared to the laboratory experimental results. This confirms that the numerical analysis model and techniques proposed in this study are reliable.

Table 7 Numerical analysis and experimental results: Case 2-5

Air temperature (℃)	Results		
	Heating coil (Interval: 65 mm)		Surface heating element
	Experiments (KRISO, 2012)	Numerical analysis (Lee et al., 2012)	Present study (Numerical analysis)
10	53.2	56.2	56.15
0	46.3	48.7	46.13
-10	37.2	37.1	36.99
-20	27.8	26.9	26.99
-30	18.2	16.7	17.79

Table 8 Numerical analysis and experimental results: Case 2-7

Air temperature (℃)	Results		
	Heating coil (Interval: 110mm)		Surface heating element
	Experiments (KRISO, 2012)	Numerical analysis (Lee et al., 2012)	Present study (Numerical analysis)
10	36.4	37.7	37.66
0	26.7	28.2	27.53
-10	17.0	19.0	17.53
-20	10.5	9.5	10.53
-30	-2.0	-0.4	-1.98

Table 9 Numerical analysis and experimental results: Case 4-5

Air temperature (℃)	Results		
	Heating coil (Interval: 65mm)		Surface heating element
	Experiments (KRISO, 2012)	Numerical analysis (Lee et al., 2012)	Present study (Numerical analysis)
10	37.8	40.0	40.11
0	28.7	31.7	30.08
-10	21.2	21.5	21.09
-20	11.3	10.7	11.08
-30	2.1	0.54	1.89

Table 10 Numerical analysis and experimental results: Case 4-7

Air temperature (℃)	Results		
	Heating coil (Interval: 110mm)		Surface heating element
	Experiments (KRISO, 2012)	Numerical analysis (Lee et al., 2012)	Present study (Numerical analysis)
10	27.2	29.6	29.68
0	20.5	19.8	20.67
-10	10.0	9.9	10.17
-20	0.0	0.1	0.175
-30	-10	-9.7	-10.23

5. Numerical Analysis Results and Discussion

Building on the validation of numerical techniques in Chapter 4, the numerical analyses of the CNT-based surface heating element method under the same analysis conditions as Lee et al. (2012) were conducted. Fig. 6 displays a subset of these numerical analysis results. Among the numerical analysis results, Fig. 6(a) shows the temperature distribution at the top surface of the heated walkway and the air flow field in the air inlet of the wind generation device. Fig. 6(b) reveals that the surface temperature of the surface heating element method relatively drops owing to the influence of thermal heat flow, especially near the wind generation device affected by the external wind speed conditions.

To represent the thermal energy efficiency of the surface heating element method, Tables 11–13 present the average temperature results of the heated walkways under the lowest air temperature condition of −30 ℃ based on the heat flux conditions of the heating coil method. These results indicate that under extreme air temperature conditions, some cases fail to meet the anti-icing requirements, showing negative average temperatures on the heated walkway. Therefore, it suggests that heated walkways using the existing heating coil method require more thermal energy and heat flux to satisfy anti-icing technology requirements.

To demonstrate the performance of the CNT-based surface heating element method, the external environmental conditions and heat flux of the heating coil were applied, which failed to meet the anti-icing technology requirements in the previous heating coil method, to the numerical analysis. Then, the average temperature results of the heated walkway accordingly were displayed. Fig. 7 shows that at the lowest air temperature of −30 ℃, the results ranged from 34.97 ℃ at 7 m/s to 129.2 ℃ at 1 m/s, depending on the wind speed generated by the wind generation device. The average temperature results, derived from applying the minimum heat flux of the coil to the CNT-based heating film, were higher than the results for the case applying the maximum heat flux of the coil. Although the smallest heat source value from the heating coil method was used, the surface heating element method

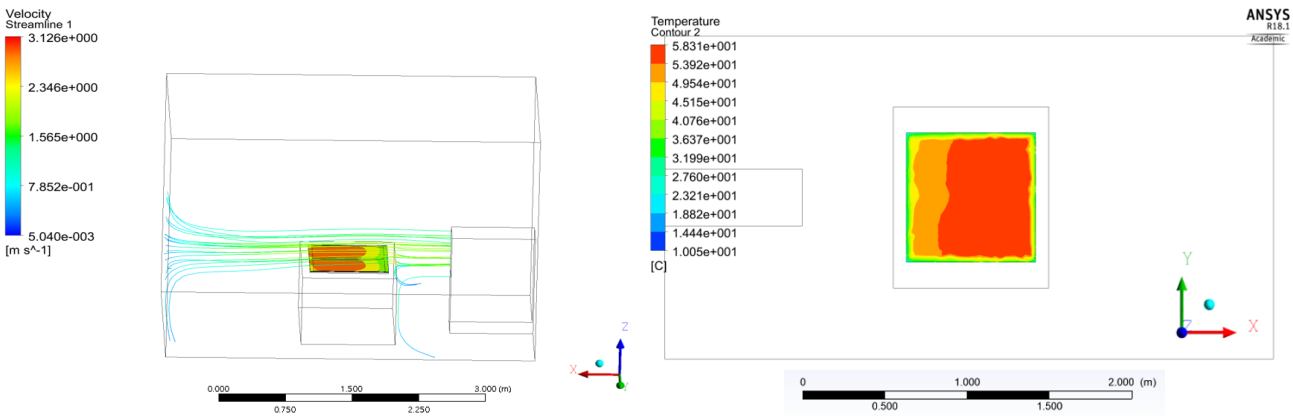

(a) (b)

Fig. 6 Contour cut of numerical analysis results: (a) 3D view and (b) XY plane

Table 11 Numerical analysis of the average temperature at −30 ℃, 33 W/m (Lee et al., 2012)

Interval (mm)	Wind speed (m/s)				
	1	2	3	5	7
33	31.4	24.0	15.5	5	-0.9
65	15.8	1.6	-3.5	-9.4	-12.6
110	9.1	-0.4	-3.9	-9.7	-13.0

Table 12 Numerical analysis of the average temperature at −30 ℃, 49 W/m (Lee et al., 2012)

Interval (mm)	Wind speed (m/s)				
	1	2	3	5	7
33	68.3	49.9	37.7	22.2	13.3
65	28.34	16.7	9.9	0.5	-2.2
110	22.4	13.9	8.5	1.0	-4.7

Table 13 Numerical analysis of the average temperature at −30 ℃, 65 W/m (Lee et al., 2012)

Interval (mm)	Wind speed (m/s)				
	1	2	3	5	7
33	98.8	76.1	59.9	39.2	27.3
65	49.5	39.5	28.2	15.6	6.1
110	46.9	31.2	23.3	11.8	4.2

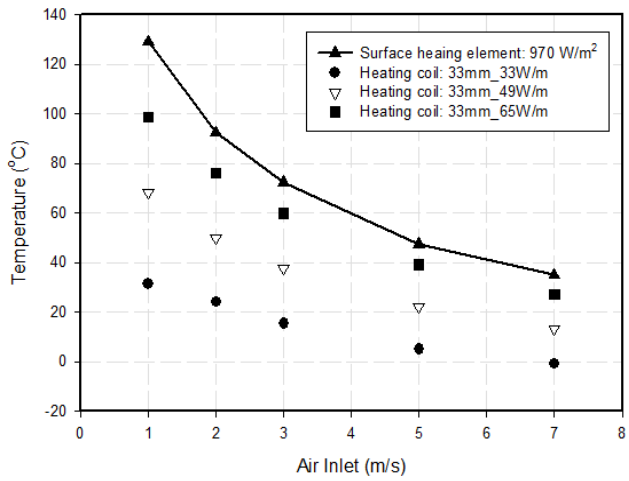

Fig. 7 Comparison of the average temperature of the heating coil and surface heating element on each air inlet (−30 ℃)

exceeded the anti-icing technology requirements even under extreme external environmental conditions.

Park et al. (2023) state that current ice-class ships require winterization technology at lower air temperatures than those of extreme conditions applied in the existing heating coil method. Table 14 shows the average temperature results of the heated walkway under the external wind speed conditions, applying the heat flux of the existing heating coil method at an air temperature of −45 ℃. Fig. 8

Table 14 Numerical analysis of the average temperature at −45 ℃ (surface heating element)

Heat flux (W/m^2)	Wind speed (m/s)				
	1	2	3	5	7
970	114.5	77.48	57.33	32.49	19.97
1441.17	189.6	137.3	107.4	70.20	51.53
1911.76	265.2	196.8	157.6	107.9	83.05

displays the temperature distribution at the top of the heated walkway under the strongest wind speed condition of 7 m/s from analysis conditions of Table 14. Although the average temperature of the heated walkway was lower than that under the previous −30 ℃ ambient condition, the heated walkway maintained the positive temperature, thus satisfying the anti-icing conditions.

However, applying the same heat source from the existing heating coil method to the surface heating element method seems excessive and inefficient from an energy efficiency standpoint. To address this, it seems necessary to derive and apply the optimal heat flux needed to maintain room temperature under varying external environmental conditions for anti-icing, similar to those shown in Table 6 derived to validate the numerical analysis technique in Chapter 4.

6. Conclusions

In this study, the conventional heating coil method with the surface heating element method for the anti-icing and winterization design of heated walkways located on the upper deck of ice-class ships were compared and analyzed. The analysis was performed through heat transfer and computational fluid dynamics numerical analysis. The findings can be summarized as follows.

(1) The numerical analysis of the CNT-based surface heating element method considered forced convection from a wind generation device and turbulence characteristics in forced specimens. Various factors, such as numerical analysis tools, turbulence models, and heat transfer characteristics, were applied.

(2) To validate the efficiency of the surface heating element method in contrast to the conventional heating coil method, the heated walkway—a CNT-based surface heating element for shipping equipment developed by Yu et al. (2022) was referenced—for our numerical analysis. The parameters were determined based on the numerical analysis results of Lee et al. (2012) under positive temperature conditions and validated through laboratory experiments results and additional numerical analysis.

(3) The average temperature results of the heated walkways for verification demonstrated that the surface heating element method yielded results similar to laboratory experiment outcomes than the conventional heating coil method, with the efficiency derived from the difference in heat flux between the two methods. The surface heating element method displayed high efficiency, ranging from a minimum of 56.65% to a maximum of 80.17%, depending on the coil interval and

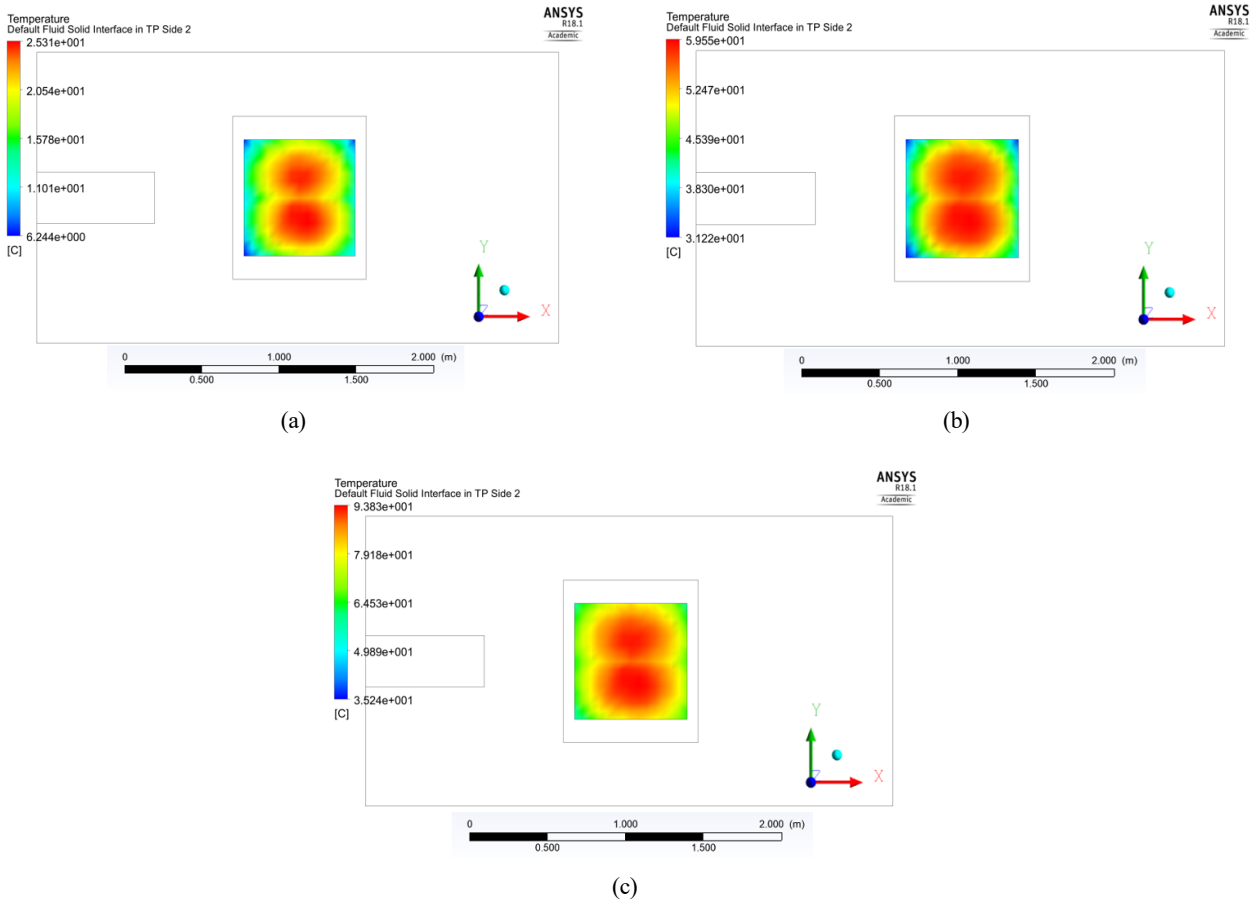

Fig. 8 Temperature distribution of numerical analysis results (case conditions: −45 ℃, 7 m/s): (a) 970 W/m^2, (b) 1441.17 W/m^2, and (c) 1911.76 W/m^2

heat flux conditions of the heating coil method.

(4) The surface heating element method was applied in the numerical analysis as a substitute in certain cases where the conventional heating coil method failed to meet anti-icing conditions. The average temperature of the heated walkways satisfied the minimum anti-icing condition of 34.97 °C when the same heat flux was applied. Additionally, the heated walkways maintained positive temperature for anti-icing even in conditions as low as −45 °C, which is lower than the conventional air temperature conditions.

(5) In this study, the numerical analyses were conducted using a CNT-based surface heating element method verified against the conventional heating coil method. The findings suggest the need to derive and apply the optimal heat flux for heating films in various external environmental conditions to achieve a more economical and efficient design than the conventional heating coil method.

Conflict of Interest

The authors declare that they have no conflict of interests.

Funding

This research was conducted with the support of the Ministry of Education and the National Research Foundation of Korea as part of Leading University Industry-University Cooperation 3.0 (LINC 3.0).

References

ANSYS Inc. (2017). *ANSYS CFX-Solver theory guide (Release 18.1)*. ANSYS Inc.

B. P. Technology Transaction. (2017). *Surface heating element (center on CNT)*. Interesting Media, Inc.

Det Norske Veritas (DNV). (2005). *DNV rules for classification of ships*. DNV.

International Maritime Organization (IMO). (2015). *International code of safety for ships operating in polar waters (Polar code)*. A.1024(26).

Jung, Y. J., & Seo, Y. K., (2015). A study on the de-icing performance evaluation and design guide for ice class louver of the vessels operating in cold region. *Journal of the Society of Naval Architects of Korea*, *52*(4), 323−329. https://doi.org/10.3744/SNAK.2015.52.4.323

Kim, Y. K. Yang, J. S. Kim, K. C., & Ji, H. S. (2011). Numerical study on the performance assessment for defrost and de-icing modes. *Transactions of the Korean Society of Mechanical Engineers B*, *35*(2), 161−168. https://doi.org/10.3795/KSME-B. 2011.35.2.161

Lee, J. C., Seo, Y. K., & Lee, C. J. (2012). A study on the anti-icing

performance evaluating and design uide by Heating Coil for Upper Deck of Icebreaking Vessels. *Journal of the Society of Naval Architects of Korea*, *49*(6), 541−549. https://doi.org/10.3744/SNAK.2012.49.6.541

Korea Research Institute of Ships & Ocean Engineering (KRISO). (2013). *Development of Polar Route Safety Operation Technology and Cryogenic Ice Performance Test Evaluation Techniques for Ice Class Ships* (TRKO201500009099).

Ministry of Knowledge Economy. (2012). *Cold region design specification and winterization*. (PNS133C).

Park, W. J., Park, D. S., Shin, M. B., & Seo, Y. K. (2023). Evaluation of surface heating element performance installed under the walkway through the numerical analysis. In *the 2023 Joint Academic Conference of The Korean Association of Ocean Science and Technology Societies*.

Rashid, T., Khawaja, H. A., & Edvardsen, K., (2016). Review of marine icing and anti-/de-icing systems. *Journal of Marine Engineering & Technology*, *15*(2), 79−87. https://doi.org/10.1080/20464177.2016.1216734

Vargaftic, N. B. (1972). *Handbook Thermophysical Properties of Gases and Liquids*, Nauka Publishing House.

Yu, S. H., Kim, T. S., & Kim, S. H. (2022). Machined surface texture monitoring using acoustic emission signals in micro milling process. *Proceedings of the 10th International Conference of Manufacturing Technology Engineers (ICMTE)*.

Author ORCIDs

Author name	ORCID
Park, Woo-Jin	0000-0002-1323-4442
Park, Dong-Su	0000-0001-6525-1511
Shin, Mun-Beom	0000-0003-2879-3658
Seo, Young-Kyo	0000-0002-8838-113X

Instructions for Authors

General information

To submit a manuscript to the Journal of Ocean Engineering and Technology (JOET), it is advised to first carefully read the aims and the scope section of this journal, as it provides information on the editorial policy and the category of papers it accepts. Unlike many regular journals, JOET usually has no lag in acceptance of a manuscript and its publication. Authors that find a match with the aims and the scope of JOET are encouraged to submit as we publish works from all over the world. JOET adheres completely to guidelines and best practices published by professional organizations, including Principles of Transparency and Best Practice in Scholarly Publishing (joint statement by COPE, DOAJ, WAME, and OASPA (http://doaj.org/bestpractice) if otherwise not described below. As such, JOET would like to keep the principles and policies of those professional organizations during editing and the publication process.

Research and publication ethics

Details on publication ethics are found in http://joet.org/authors/ethics.php. For the policies on research and publication ethics not stated in the Instructions, Guidelines on Good Publication (http://publicationethics.org/) can be applied.

Requirement for membership

One of the authors who submits a paper or papers should be member of the Korean Society of Ocean Engineers (KSOE), except a case that editorial board provides special admission of submission.

Publication type

Article types include scholarly monographs (original research articles), technical articles (technical reports and data), and review articles. The paper should have not been submitted to other academic journal. When part or whole of a manuscript was already published to conference papers, research reports, and dissertations, then the corresponding author should note it clearly in the manuscript.

Copyright

After published to JOET, the copyright of manuscripts should belong to KSOE. A transfer of copyright (publishing agreement) form can be found in submission website (http://www.joet.org).

Manuscript submission

Manuscript should be submitted through the on-line submission website (http://www.joet.org). The date that manuscript was received through on-line website is the official date of receipt. Other correspondences can be sent by an email to the Editor in Chief or secretariat. The manuscript must be accompanied by a signed statement that it has been neither published nor currently submitted for publication elsewhere. The manuscript should be written in English or Korean. Ensure that online submission are in a standard word processing format. Corresponding author must write the manuscript using the JOET template provided in Hangul or MS Word format. Ensure that graphics are high-resolution. Be sure all necessary files have been uploaded/ attached.

Authors' checklist

Please refer to “Authors' Checklist” for details.

Article structure

Manuscript must be edited in the following order: (1) Title, (2) Authors' names and affiliations, (3) Keywords, (4) Abstract, (5) Nomenclature (optional), (6) Introduction, (7) Main body (analyses, tests, results, and discussions), (8) Conclusions, (9) Conflict of interest, (10) Funding (optional), (11) Acknowledgements (optional), (12) References, (13) Appendices (optional), (14) Author’s ORCIDs.

Abstract

A concise and factual abstract is required. The abstract should state briefly the background, purpose and methods of the research, the principal results and conclusions. An abstract should be written in 150-200 words. References are not cited in abstract whenever possible. Also, non-standard or uncommon abbreviations should be avoided, but if essential they must be defined at their first mention in the abstract itself.

Keywords

Immediately after the abstract, provide a maximum of 5 or 6 keywords.

Unit

Use the international system units(SI). If other units are mentioned, please give their equivalent in SI.

Equations

All mathematical equations should be c1early printed/typed using well accepted explanation. Superscripts and subscripts should be typed clearly above or below the base line. Equation numbers should be given in Arabic numerals enclosed in parentheses on the right-hand margin.

Tables

Tables should be numbered consecutively with Arabic numerals. Each table should be fully titled. All tables should be referred to in the texts.

Figures

Figures should be numbered consecutively with Arabic numerals. Each figure should be fully titled. All figures should be referred to in the texts. All the illustrations should be of high quality meeting with the publishing requirement with legible symbols and legends.

Conflict of interest

It should be disclosed here according to the statement in the Research and publication ethics regardless of existence of conflict of interest. If the authors have nothing to disclose, please state: “No potential

conflict of interest relevant to this article was reported."

Funding

Funding to the research should be provided here. Providing a FundRef ID is recommended including the name of the funding agency, country and if available, the number of the grant provided by the funding agency. If the funding agency does not have a FundRef ID, please ask that agency to contact the FundRef registry (e-mail: fundref.registry@crossref.org). Additional detailed policy of FundRef description is available from http://www.crossref.org/fundref/. Example of a funding description is as follows:

The study is supported by the Inha University research fund (FundRef ID: 10.13039/501100002632), and the Korea Health Personnel Licensing Examination Institute research fund (FundRef ID: 10.13039/501100003647).

Acknowledgments

Any persons that contributed to the study or the manuscript, but not meeting the requirements of an authorship could be placed here. For mentioning any persons or any organizations in this section, there should be a written permission from them.

References in text

References in texts follow the APA style. Authors can also see how references appear in manuscript text through the 'Template'.

Reference list

Reference list follows the APA style. Authors can see how references should be given in reference section through the 'Template'.

Appendices

The appendix is an optional section that can contain details and data supplemental to the main text. If there is more than an appendix, they should be identified as A, B, C, etc. Formulae and equations in appendices should be given separate numbering: Eq. (A1), Eq. (A2), etc.; in a subsequent appendix, Eq. (B1) and so on. Similarly for tables and figures: Table A1; Fig. A1, etc.

ORCID (Open Researcher and Contributor ID)

All authors are recommended to provide an ORCID. To obtain an ORCID, authors should register in the ORCID web site: http://orcid.org. Registration is free to every researcher in the world. Example of ORCID description is as follows:

Joonmo Choung: https://orcid.org/0000-0003-1407-9031

Peer review and publication process

The peer review process can be broadly summarized into three groups: author process, review process, and publishing process for accepted submissions. General scheme is presented in Figure 1.

Check-in process for review

If the manuscript does not fit the aims and scope of the Journal or does not adhere to the Instructions to Authors, it may be rejected immediately after receipt and without a review. Before reviewing, all submitted manuscripts are inspected by Similarity Check powered by iThenticate (https://www.crossref.org/services/similarity-check/), a plagiarism-screening tool. If a too high degree of similarity score is found, the Editorial Board will do a more profound content screening.

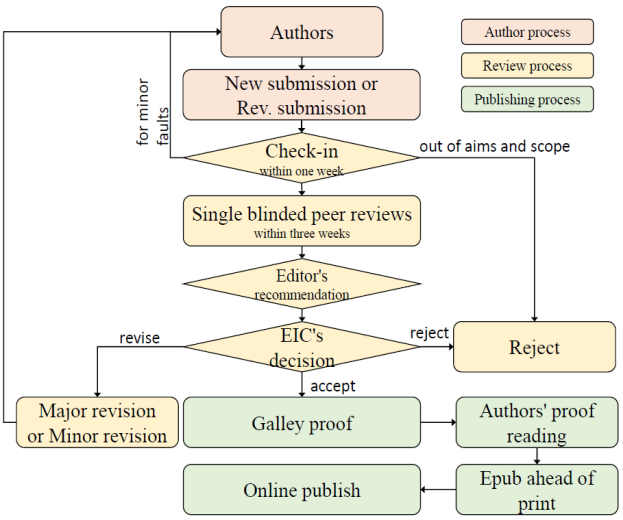

Figure 1 Flow chart of the peer review and publication process of JOET

The criterion for similarity rate for further screening is usually 15%; however, rather than the similarity rate, the Editorial Board focuses on cases where specific sentences or phrases are similar. The settings for Similarity Check screening are as follows: It excludes quotes, bibliography, small matches of 6 words, small sources of 1%, and the Methods section.

Number of reviewers

Reviewers will be selected from the list of reviewers. Manuscripts are then peer reviewed by at least 2 experts in the corresponding field, usually by 2.

Peer review process and the author response to the reviewer comments

JOET adopts single blind review, which means that the authors do not know the identity of the reviews. All papers, including those invited by the Editor, are subject to peer review.

The review period is 4 weeks. Usually the first decision is made within a week after completion of the review. The Editorial Board's decision after the review will be one of followings: Accept, Minor revision, Major revision, or Rejection. The Editorial Board may request the authors to revise the manuscript according to the reviewers' comments. If there are any requests for revision of the manuscript by the reviewers, the authors should do their best to revise the manuscript. If the reviewer's opinion is not acceptable or is believed to misinterpret the data, the author should reasonably indicate that. After revising the manuscript, the author should upload the revised files with a separate response sheet to each item of the reviewer's commentary. The author's revisions should be completed within 3 months after the request. If it is not received by the due date, the Editorial Board will notify the author. To extend the revision period beyond 3 months, the author should negotiate that with the Editorial Board. The manuscript review process can be provided for up two rounds. If the authors wish further review, the Editorial Board may consider it. The Editorial Board will make a final decision on the approval of the submitted manuscript for publication and can request any further corrections, revisions, and deletions of the article text if necessary. Statistical editing is also performed if the data requires professional statistical review by a statistician.

Processing after acceptance

If the manuscript is finally accepted, the galley proof will be sent to the corresponding author after professional manuscript editing and English proofreading. Proofreading should be performed for any misspellings or errors by the authors. Proofreading manuscript for publication is provided to the corresponding author, and the corresponding author must review the proofreading manuscript. Corresponding authors are responsible for the content of the proofreading manuscript and any errors. After final proofreading, the manuscript may appear at the journal homepage as an article in press with a unique DOI number for rapid communication. All published articles will be replaced by the replacement XML file and a final PDF.

Feedback after publication

If the authors or readers find any errors, or contents that should be revised, it can be requested from the Editorial Board. The Editorial Board may consider erratum, corrigendum or a retraction. If there are any revisions to the article, there will be a CrossMark description to announce the final draft. If there is a reader's opinion on the published article with the form of Letter to the editor, it will be forwarded to the authors. The authors can reply to the reader's letter. Letter to the editor and the author's reply may be also published.

How the journal handle complaints and appeals

The policy of JOET is primarily aimed at protecting the authors, reviewers, editors, and the publisher of the journal. If not described below, the process of handling complaints and appeals follows the guidelines of the Committee of Publication Ethics available from: https://publicationethics.org/appeals

- *Who complains or makes an appeal?*

Submitters, authors, reviewers, and readers may register complaints and appeals in a variety of cases as follows: falsification, fabrication, plagiarism, duplicate publication, authorship dispute, conflict of interest, ethical treatment of animals, informed consent, bias or unfair/inappropriate competitive acts, copyright, stolen data, defamation, and legal problem. If any individuals or institutions want to inform the cases, they can send a letter via the contact page on our website: https://www.joet.org/about/contact.php. For the complaints or appeals, concrete data with answers to all factual questions (who, when, where, what, how, why) should be provided.

- *Who is responsible to resolve and handle complaints and appeals?*

The Editorial Board or Editorial Office is responsible for them. A legal consultant or ethics editor may be able to help with the decision making.

- *What may be the consequence of remedy?*

It depends on the type or degree of misconduct. The consequence of resolution will follow the guidelines of the Committee of Publication Ethics (COPE).

Article processing charge

Payment due

Article processing charge (APC) covers the range of publishing services JOET provides. This includes provision of online tools for editors and authors, article production and hosting, and customer services. Upon editorial acceptance of an article for the regular review service and upon submission of an article for the fast review service, the corresponding author will be notified that payment is due.

APC

The APC up to 6 pages is ₩300,000 (or ＄300) and ₩650,000 (or ＄650) for the for the regular and fast review services, respectively. An extra APC of $100 per page is charged for papers longer than 6 pages, No taxes are included in this charge. For the fast review service, an advance fee of ₩250,000 ($250) should be paid on submission.

Payment methods

Credit card payment can be made online using a secure payment form as soon as the manuscript has been editorially accepted. We will we send a receipt by email once payment has been processed. Please note that payment by credit card carries a surcharge of 10% of the total APC.

Invoice payment is due within 7 days of the manuscript receiving editorial acceptance. Receipts are available on request.

JOET Template 2022.08.27

Journal of Ocean Engineering and Technology 00(0), 000-000, December, 2100
https://doi.org/10.26748/KSOE.2100.000

pISSN 1225-0767
eISSN 2287-6715

Original Research Article, Technical Article, Review Article, etc

Title of Article

Firstname Lastname[1], Firstname Lastname[2] and Firstname Lastname[3]

[1]*Professor, Department of OO, OO School, OO University, Busan, Korea*
[2]*Graduate Student, Department of OO, OO University, Seoul, Korea*
[3]*Senior Researcher, Department of OO, OO Engineering. Corp., Seoul, Korea*

KEYWORDS: Lumped mass line model, Explicit method, Steel lazy wave riser (Provide a maximum of 5 or 6 keywords.)

ABSTRACT:

Abstract Construction Guidelines
1) Describe the research background and aims in 1-2 sentences
2) Describe the research/analysis method (method section) in 2-3 sentences.
3) Describe the research/analysis results (results) in 2-3 sentences.
4) Describe the research conclusion in 1-2 sentences.
Abstract Editing Guidelines
1) Review English grammar.
2) Describe in 150-200 words.
3) When using an abbreviation or acronym, write the acronym after full words.
4) Abbreviations (acronyms) used only once should be written in full words only, and no acronyms.
5) References are not included in the abstract.

Nomenclature (Optional)

ITOC	Increment of total operating cost ($/yr)
LHV	Lower heating value (kJ/kg)
Pw	Power (kW)
T	Temperature (K)
V	Volume (m^3)
ρ	Density (kg/m^3)

1. Introduction

The introduction should briefly place the study in a broad context and highlight why it is important. It should define the purpose of the work and its significance. The current state of the research field should be reviewed carefully and key publications cited. Please highlight controversial and diverging hypotheses when necessary. Finally, briefly mention the main aim of the work and highlight the principal conclusions. As far as possible, please keep the introduction comprehensible to scientists outside your particular field of research.

Received 00 February 2100, revised 00 October 2100, accepted 00 October 2100
Corresponding author Firstname Lastname: +82-51-759-0656, e-mail@e-mail.com
It is a recommended paper from the proceedings of 2019 spring symposium of the Korea Marine Robot Technology (KMRTS).

2. General Information for Authors

2.1 Research and Publication Ethics

Authorship should be limited to those who have made a significant contribution to the conception, design, execution, or interpretation of the reported study. All those who have made significant contributions should be listed as co-authors. Where there are others who have participated in certain substantive aspects of the research project, they should be acknowledged or listed as contributors.

The corresponding author should ensure that all appropriate co-authors and no inappropriate co-authors are included on the paper, and that all co-authors have seen and approved the final version of the paper and have agreed to its submission for publication.

Details on publication ethics are found in the journal's website (http://joet.org/authors/ethics.php). For the policies on research and publication ethics not stated in the Instructions, Guidelines on Good Publication (http://publicationethics.org/) can be applied.

2.2 Requirement for Membership

One of the authors who submits a paper or papers should be member of The Korea Society of Ocean Engineers (KSOE), except a case that editorial board provides special admission of submission.

2.3 Publication Type

Article types include scholarly monographs (original research articles), technical articles (technical reports and data), and review articles. The paper should have not been submitted to another academic journal. When part or whole of a manuscript was already published to conference papers, research reports, and dissertations, then the corresponding author should note it clearly in the manuscript.

Example: It is noted that this paper is revised edition based on proceedings of KAOST 2100 in Jeju.

2.4 Copyright

After published to JOET, the copyright of manuscripts should belong to KSOE. A transfer of copyright (publishing agreement) form can be found in submission website (http://www.joet.org).

2.5 Manuscript Submission

Manuscript should be submitted through the on-line submission website (http://www.joet.org). The date that manuscript was received through on-line website is the official date of receipt. Other correspondences can be sent by an email to the Editor in Chief or secretariat. The manuscript must be accompanied by a signed statement that it has been neither published nor currently submitted for publication elsewhere. The manuscript should be written in English or Korean. Ensure that online submission is in a standard word processing format. Corresponding author must write the manuscript using the JOET template provided in Hangul or MS Word format. Ensure that graphics are high-resolution. Be sure all necessary files have been uploaded/ attached.

2.5.1 Authoer's checklist

Authoer's checklist and Transfer of copyright can be found in submission homepage (http:/www.joet.org).

3. Manuscript

Manuscript must be edited in the following order: (1) Title, (2) Authors' names and affiliations, (3) Keywords, (4) Abstract, (5) Nomenclature (optional), (6) Introduction, (7) Main body (analyses, tests, results, and discussions), (8) Conclusions, (9) Conflict of interest, (10) Funding (optional), (11) Acknowledgements (optional), (12) References, (13) Appendices (optional), (14) Author's ORCIDs.

3.1 Unit

Use the international system units (SI). If other units are mentioned, please give their equivalent in SI.

3.2 Equations

All mathematical equations should be clearly printed/typed using well accepted explanation. Superscripts and subscripts should be typed clearly above or below the base line. Equation numbers should be given in Arabic numerals enclosed in parentheses on the right-hand margin. The parameters used in equation must be defined. They should be cited in the text as, for example, Eq. (1), or Eqs. (1)~(3).

$$G_{GEV}(x;\mu,\sigma,\xi)=\begin{cases}\exp[-(1+\xi(x-\mu)/\sigma)^{-1/\xi}] & \xi\neq 0\\ \exp[-\exp(-(x-\mu)/\sigma)] & \xi=0\end{cases} \tag{1}$$

in which μ, σ, and ξ represent the location ("Shift" in figures), scale, and shape parameters, respectively.

3.3 Tables

Tables should be numbered consecutively with Arabic numerals. Each table should be typed on a separate sheet of paper and be fully titled. All tables should be referred to in the texts.

Table 1 Tables should be placed in the main text near to the first time they are cited

Item	Buoyancy riser
Segment length[1)] (m)	370
Outer diameter (m)	1.137
Inner diameter (m)	0.406
Dry weight (kg/m)	697
Bending rigidity ($N\cdot m^2$)	1.66E8
Axial stiffness (N)	7.098E9
Inner flow density ($kg\cdot m^3$)	881
Seabed stiffness ($N/m/m^2$)	6,000

[1)]Tables may have a footer.

3.4 Figures

Figures should be numbered consecutively with Arabic numerals. Each figure should be fully titled. All the illustrations should be of high quality meeting with the publishing requirement with legible symbols and legends. All figures should be referred to in the texts. They should be referred to in the text as, for example, Fig. 1, or Figs. 1–3.

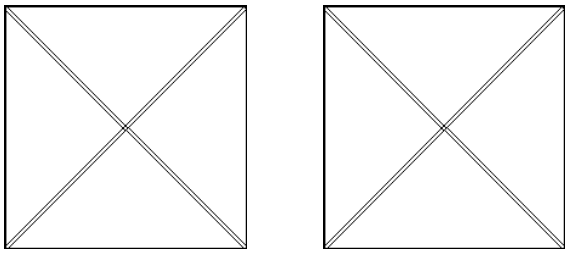

(a) (b)

Fig. 1 Schemes follow the same formatting. If there are multiple panels, they should be listed as: (a) Description of what is contained in the first panel; (b) Description of what is contained in the second panel. Figures should be placed in the main text near to the first time they are cited

3.5 How to Describe the References in Main Texts

- JOET recommends to edit authors' references using MS-Word reference or ZOTERO plug-in
- How to add a new citation and source to a document using MS-Word is found in MS Office web page: https://support.microsoft.com/en-us/office/add-citations-in-a-word-document-ab9322bb-a8d3-47f4-80c8-63c06779f127
- How to add a new citation and source to a document using ZOTERO is found in zotero web page: https://www.zotero.org/

4. Results

This section may be divided by subheadings. It should provide a concise and precise description of the experimental results, their interpretation as well as the experimental conclusions that can be drawn. Tables and figures are recommended to present the results more rapidly and easily. Do not duplicate the content of a table or a figure with in the Results section. Briefly describe the core results related to the conclusion in the text when data are provided in tables or in figures. Supplementary results can be placed in the Appendix.

5. Discussion

Authors should discuss the results and how they can be interpreted in perspective of previous studies and of the working hypotheses. The findings and their implications should be discussed in the broadest context possible. Future research directions may also be highlighted

6. Conclusions

This section can be added to the manuscript.

Conflict of Interest

It should be disclosed here according to the statement in the Research and publication ethics regardless of existence of conflict of interest. If the authors have nothing to disclose, please state: “No potential conflict of interest relevant to this article was reported.”, “The authors declare no potential conflict of interest.”, “The authors declare that they have no conflict of interests.”

Funding (Optional)

Please add: “This research was funded by Name of Funder, grant number XXX” and “The OOO was funded by XXX”. Check carefully that the details given are accurate and use the standard spelling of funding agency names at https://search.crossref.org/funding

Acknowledgments (Optional)

In this section you can acknowledge any support given which is not covered by the author contribution or funding sections. This may include administrative and technical support, or donations in kind (e.g., materials used for experiments). For mentioning any persons or any organizations in this section, there should be a written permission from them.

References

JOET follows the American Psychological Association (APA) style.

- Some samples are found in following web pages: https://apastyle.apa.org/style-grammar-guidelines/references/examples or https://www.ntnu.edu/viko/apa-examples
- JOET recommends editing authors’ references using MS-Word reference or ZOTERO plug-in
- How to add a new citation and source to a document using MS-Word is found in MS Office web page: https://support.microsoft.com/en-us/office/add-citations-in-a-word-document-ab9322bb-a8d3-47f4-80c8-63c06779f127
- How to add a new citation and source to a document using ZOTERO is found in ZOTERO web page: https://www.zotero.org/

Appendix (Optional)

The appendix is an optional section that can contain details and data supplemental to the main text. For example, explanations of experimental details that would disrupt the flow of the main text, but nonetheless remain crucial to understanding and reproducing the research shown; figures of replicates for experiments of which representative data is shown in the main text can be added here if brief, or as Supplementary data. Mathematical proofs of results not central to the paper can be added as an appendix.

All appendix sections must be cited in the main text. In the appendixes, Figures, Tables, etc. should be labeled starting with ‘A’, e.g., Fig. A1, Fig. A2, etc.

Examples:

https://doi.org/10.26748/KSOE.2019.022

https://doi.org/10.26748/KSOE.2018.4.32.2.095

Author ORCIDs

All authors are recommended to provide an ORCID. To obtain an ORCID, authors should register in the ORCID web site: http://orcid.org. Registration is free to every researcher in the world. Example of ORCID description is as follows:

Author name	ORCID
So, Hee	0000-0000-000-00X
Park, Hye-Il	0000-0000-000-00X
Yoo, All	0000-0000-000-00X
Jung, Jewerly	0000-0000-000-00X

Authors' Checklist

The following list will be useful during the final checking of a manuscript prior to sending it to the journal for review. Please submit this checklist to the KSOE when you submit your article.

< Checklist for manuscript preparation >

☐ I checked my manuscript has been 'spell-checked' and 'grammar-checked'.

☐ One author has been designated as the corresponding author with contact details such as
- E-mail address
- Phone numbers

☐ I checked abstract 1) stated briefly the purpose of the research, the principal results and major conclusions, 2) was written in 150–200 words, and 3) did not contain references (but if essential, then cite the author(s) and year(s)).

☐ I provided 5 or 6 keywords.

☐ I checked color figures were clearly marked as being intended for color reproduction on the Web and in print, or to be reproduced in color on the Web and in black-and-white in print.

☐ I checked all table and figure numbered consecutively in accordance with their appearance in the text.

☐ I checked abbreviations were defined at their first mention there and used with consistency throughout the article.

☐ I checked all references mentioned in the Reference list were cited in the text, and vice versa according to the APA style.

☐ I checked I used the international system units (SI) or SI-equivalent engineering units.

< Authorship checklist >

JOET considers individuals who meet all of the following criteria to be authors:

☐ Made a significant intellectual contribution to the theoretical development, system or experimental design, prototype development, and/or the analysis and interpretation of data associated with the work contained in the article.

☐ Contributed to drafting the article or reviewing and/or revising it for intellectual content.

☐ Approved the final version of the article as accepted for publication, including references.

< Checklist for publication ethics >

☐ I checked the work described has not been published previously (except in the form of an abstract or as a part of a published lecture or academic thesis).

☐ I checked when the work described has been published previously in other proceedings without copyright, it has clearly noted in the text.

☐ I checked permission has been obtained for use of copyrighted material from other sources including the Web.

☐ I have processed Plasgiarism Prevention Check through reliable web sites such as www.kci.go.kr, http://www.ithenticate.com/, or https://www.copykiller.org/ for my submission.

☐ I agree that final decision for my final manuscript can be changed according to results of Plasgiarism Prevention Check by JOET administrator.

☐ I checked one author at least is member of the Korean Society of Ocean Engineers.

☐ I agreed all policies related to 'Research and Publication Ethics'

☐ I agreed to transfer copyright to the publisher as part of a journal publishing agreement and this article will not be published elsewhere including electronically in the same form, in English or in any other language, without the written consent of the copyright-holder.

☐ I made a payment for reviewing of the manuscript, and I will make a payment for publication on acceptance of the article.

☐ I have read and agree to the terms of Authors' Checklist.

Title of article	:	
Date of submission	: DD/MM/YYYY	
Corresponding author	:	signature
Email address	:	

※ E-mail this with your signature to ksoehj@ksoe.or.kr

Publishing Agreement

ARTICLE DETAILS

Title of article :

Corresponding author :

E-mail address :

DOI : https://doi.org/10.26748/KSOE.2XXX.XXX

YOUR STATUS

I am one author signing on behalf of all co-authors of the manuscript.

ASSIGNMENT OF COPYRIGHT

I hereby assign to the Korean Society of Ocean Engineers, the copyright in the manuscript identified above and any tables, illustrations or other material submitted for publication as part of the manuscript (the "Article"). This assignment of rights means that I have granted to Korean Society of Ocean Engineers the exclusive right to publish and reproduce the Article, or any part of the Article, in print, electronic and all other media (whether now known or later developed), in any form, in all languages, throughout the world, for the full term of copyright, and the right to license others to do the same, effective when the Article is accepted for publication. This includes the right to enforce the rights granted hereunder against third parties.

SCHOLARLY COMMUNICATION RIGHTS

I understand that no rights in patents, trademarks or other intellectual property rights are transferred to the Journal owner. As the author of the Article, I understand that I shall have: (i) the same rights to reuse the Article as those allowed to third party users of the Article under the CC-BY-NC License, as well as (ii) the right to use the Article in a subsequent compilation of my works or to extend the Article to book length form, to include the Article in a thesis or dissertation, or otherwise to use or re-use portions or excerpts in other works, for both commercial and non-commercial purposes. Except for such uses, I understand that the assignment of copyright to the Journal owner gives the Journal owner the exclusive right to make or sub-license commercial use.

USER RIGHTS

The publisher will apply the Creative Commons Attribution-Noncommercial Works 4.0 International License (CC-BY-NC) to the Article where it publishes the Article in the journal on its online platforms on an Open Access basis.
The CC-BY-NC license allows users to copy and distribute the Article, provided this is not done for commercial purposes and further does not permit distribution of the Article if it is changed or edited in any way, and provided the user gives appropriate credit (with a link to the formal publication through the relevant DOI), provides a link to the license, and that the licensor is not represented as endorsing the use made of the work. The full details of the license are available at http://creativecommons.org/licenses/by-nc/4.0/legalcode.

REVERSION OF RIGHTS

Articles may sometimes be accepted for publication but later rejected in the publication process, even in some cases after public posting in "Articles in Press" form, in which case all rights will revert to the author.

☑ I have read and agree to the terms of the Journal Publishing Agreement.

Corresponding author:

name signature

※ E-mail this with your signature to ksoehj@ksoe.or.kr (Papers will not be published unless this form is signed and returned)

Research and Publication Ethics

Journal of Ocean Engineering and Technology (JOET) adheres to the guidelines published by professional organizations, including Committee on Publication Ethics (COPE; https://publicationethics.org/)

1. Authorship

JOET considers individuals who meet all of the following criteria to be authors:

1) Made a significant intellectual contribution to the theoretical development, system or experimental design, prototype development, and/or the analysis and interpretation of data associated with the work contained in the article.
2) Contributed to drafting the article or reviewing and/or revising it for intellectual content.
3) Approved the final version of the article as accepted for publication, including references.

Contributors who do not meet all of the above criteria may be included in the Acknowledgment section of the article. Omitting an author who contributed to your article or including a person who did not fulfill all of the above requirements is considered a breach of publishing ethics.

Correction of authorship after publication: JOET does not correct authorship after publication unless a mistake has been made by the editorial staff.

2. Originality and Duplicate Publication

All submitted manuscripts should be original and should not be in consideration by other scientific journals for publication. Any part of the accepted manuscript should not be duplicated in any other scientific journal without permission of the Editorial Board, although the figures and tables can be used freely if the original source is verified according to the Creative Commons Attribution License (CC BY-NC). It is mandatory for all authors to resolve any copyright issues when citing a figure or table from other journal that is not open access.

3. Conflict-of-Interest Statement

Conflict of interest exists when an author or the author's institution, reviewer, or editor has financial or personal relationships that inappropriately influence or bias his or her actions. Such relationships are also known as dual commitments, competing interests, or competing loyalties. These relationships vary from being negligible to having a great potential for influencing judgment. Not all relationships represent true conflict of interest. On the other hand, the potential for conflict of interest can exist regardless of whether an individual believes that the relationship affects his or her scientific judgment. Financial relationships such as employment, consultancies, stock ownership, honoraria, and paid expert testimony are the most easily identifiable conflicts of interest and the most likely to undermine the credibility of the journal, the authors, or of the science itself. Conflicts can occur for other reasons as well, such as personal relationships, academic competition, and intellectual passion. If there are any conflicts of interest, authors should disclose them in the manuscript. The conflicts of interest may occur during the research process as well; however, it is important to provide disclosure. If there is a disclosure, editors, reviewers, and reader can approach the manuscript after understanding the situation and the background of the completed research.

4. Management Procedures for the Research and Publication Misconduct

When JOET faces suspected cases of research and publication misconduct such as a redundant (duplicate) publication, plagiarism, fabricated data, changes in authorship, undisclosed conflicts of interest, an ethical problem discovered with the submitted manuscript, a reviewer who has appropriated an author's idea or data, complaints against editors, and other issues, the resolving process will follow the flowchart provided by the Committee on Publication Ethics (http://publicationethics.org/resources/flowcharts). The Editorial Board of JOET will discuss the suspected cases and reach a decision. JOET will not hesitate to publish errata, corrigenda, clarifications, retractions, and apologies when needed.

5. Editorial Responsibilities

The Editorial Board will continuously work to monitor and safeguard publication ethics: guidelines for retracting articles; maintenance of the integrity of the academic record; preclusion of business needs from compromising intellectual and ethical standards; publishing corrections, clarifications, retractions, and apologies when needed; and excluding plagiarism and fraudulent data. The editors maintain the following responsibilities: responsibility and authority to reject and accept articles; avoiding any conflict of interest with respect to articles they reject or accept; promoting publication of corrections or retractions when errors are found; and preservation of the anonymity of reviewers.

6. Hazards and human or animal subjects

If the work involves chemicals, procedures or equipment that have any unusual hazards inherent in their use, the author must clearly identify these in the manuscript. If the work involves the use of animal or human subjects, the author should ensure that the manuscript contains a statement that all procedures were performed in compliance with relevant laws and institutional guidelines and that the appropriate institutional committee(s) has approved them. Authors should include a statement in the manuscript that informed consent was obtained for experimentation with human subjects. The privacy rights of human subjects must always be observed.

Ensure correct use of the terms sex (when reporting biological factors) and gender (identity, psychosocial or cultural factors), and, unless inappropriate, report the sex and/or gender of study participants, the sex of animals or cells, and describe the methods used to determine sex and gender. If the study was done involving an exclusive population, for example in only one sex, authors should justify why, except in obvious cases. Authors should define how they determined race or ethnicity and justify their relevance.

7. Secondary publication

It is possible to republish manuscripts if the manuscripts satisfy the conditions of secondary publication. These are:

- The authors have received approval from the Editorial Board of both journals (the editor concerned with the secondary publication must have access to the primary version).
- The priority for the primary publication is respected by a publication interval negotiated by editors of both journals and the authors.
- The paper for secondary publication is intended for a different group of readers
- The secondary version faithfully reflects the data and interpretations of the primary version.
- The secondary version informs readers, peers, and documenting agencies that the paper has been published in whole or in part elsewhere, for example, with a note that might read, "This article is based on a study first reported in the [journal title, with full reference]"
- The title of the secondary publication should indicate that it is a secondary publication (complete or abridged republication or translation) of a primary publication.

8. Complaints and Appeals

The process of handling complaints and appeals follows the guidelines of the COPE available from: https://publicationethics. org/appeals

9. Post-publication discussions and corrections

The post-publication discussion is available through letter to editor. If any readers have a concern on any articles published, they can submit letter to editor on the articles. If there found any errors or mistakes in the article, it can be corrected through errata, corrigenda, or retraction.

KSOE

The Korean Society of Ocean Engineers